

**INVESTIGATION OF THE MECHANISM AND THERAPEUTIC POTENTIAL OF A
TRANSCRIPTION FACTOR DECOY TARGETING SIGNAL TRANSDUCER AND
ACTIVATOR OF TRANSCRIPTION-3 (STAT3) FOR SQUAMOUS CELL
CARCINOMA OF THE HEAD AND NECK (SCCHN)**

by

Amanda L. Boehm

B.A., Washington and Jefferson College, 2002

Submitted to the Graduate Faculty of
Medicine in partial fulfillment
of the requirements for the degree of
Doctor of Philosophy

UNIVERSITY OF PITTSBURGH

SCHOOL OF MEDICINE

This dissertation was presented

by

Amanda L. Boehm

It was defended on

April 2, 2007

and approved by

Marie DeFrances, M.D., Ph.D.
Department of Pathology

Daniel E. Johnson, Ph.D.
Department of Pharmacology

Alan Wells, M.D., F.A.C.S.
Department of Pathology

Committee Chair: Reza Zarnegar, Ph.D.
Department of Pathology

Dissertation Advisor: Jennifer R. Grandis, M.D.
Departments of Otolaryngology and Pharmacology

Copyright © by Amanda L. Boehm

2007

**INVESTIGATION OF THE MECHANISM AND THERAPEUTIC POTENTIAL OF A
TRANSCRIPTION FACTOR DECOY TARGETING SIGNAL TRANSDUCER AND
ACTIVATOR OF TRANSCRIPTION-3 (STAT3) FOR SQUAMOUS CELL
CARCINOMA OF THE HEAD AND NECK (SCCHN)**

Squamous cell carcinoma of the head and neck (SCCHN) is the 5th most common cancer worldwide. Signal transducer and activator of transcription 3 (STAT3) is overexpressed in SCCHN and associated with decreased survival. A transcription factor decoy was designed to bind to the DNA binding domain of STAT3, abrogating expression of downstream target genes. The antitumor mechanisms of transcription factor decoys, including the STAT3 decoy, are incompletely understood. STAT3 forms heterodimers with STAT1 suggesting that the STAT3 decoy may interact with STAT1. We determined that the STAT1 pathway was functional in SCCHN cell lines. The STAT3 decoy inhibited STAT1-mediated expression of the target gene, IRF-1. Stimulation of the STAT1 pathway with IFN- γ did not mitigate STAT3 decoy-mediated growth inhibition. STAT3 decoy-mediated inhibition of STAT1 signaling did not abrogate its antitumor effects *in vitro*. Studies using STAT3 knockout cells indicated that STAT3 is necessary for decoy-mediated growth inhibition. The STAT3 decoy was then studied in combination with an EGFR inhibitor and/or a Bcl-X_L inhibitor as a therapeutic strategy for SCCHN. Targeting this pathway at several levels—the upstream receptor (EGFR), the intracellular transcription factor (STAT3), and the downstream target gene (Bcl-X_L)—has not been previously investigated. Combined targeting of EGFR and STAT3 using erlotinib and the STAT3 decoy enhanced growth inhibition of SCCHN cells *in vitro*. The STAT3 decoy in combination with gossypol, a Bcl-X_L inhibitor, resulted in enhanced growth inhibition. The triple

combination of all 3 agents enhanced growth inhibition *in vitro*. These results indicate that targeting the EGFR-STAT3-Bcl-X_L pathway at three distinct levels may be a promising treatment strategy for SCCHN.

TABLE OF CONTENTS

FORWARD	XV
LIST OF ABBREVIATIONS	XVII
PREFACE.....	19
1.0 INTRODUCTION.....	20
1.1 GENERAL INTRODUCTION.....	20
1.1.1 Squamous cell carcinoma of the head and neck.....	20
1.2 STAT3.....	20
1.2.1 STAT3 protein structure.....	21
1.2.2 STAT3 pathways and cellular functions.....	22
1.2.3 STAT3 as an oncogene.....	24
1.2.4 STAT3 in disease.....	25
1.2.5 STAT3 in SCCHN.....	27
1.3 STAT3 AS A THERAPEUTIC TARGET IN CANCER.....	27
1.3.1 Inhibiting STAT3 mRNA translation using antisense or siRNA	28
1.3.2 Blocking the SH2 domain to prevent STAT3 activity	31
1.3.3 Blocking the STAT3 DNA binding domain to prevent target gene expression.....	32
1.4 THE STAT3 TRANSCRIPTION FACTOR DECOY.....	33
1.4.1 Transcription factor decoys	33

1.4.2	STAT3 decoy design	36
	The mutant control decoy differs from the mutant control decoy by a single base pair mutation (Figure 3). The mutant control decoy has previously demonstrated no DNA binding activity to STAT3 and does not inhibit STAT3 binding activity in EMSAs after SCCHN cells are treated [53]. In cell proliferation experiments, the mutant control decoy does not significantly decrease cell proliferation compared to an untreated control. Also, STAT3 target gene expression is not decreased by the mutant control decoy either. Therefore, the mutant control decoy serves as a control for all STAT3 decoy experiments.	37
1.4.3	STAT3 decoy in preclinical models	38
1.5	RATIONALE AND HYPOTHESES	39
2.0	STAT1 DOES NOT CONTRIBUTE TO OR MITIGATE THE STAT3 DECOY ANTIPROLIFERATIVE MECHANISMS	41
2.1	INTRODUCTION	41
2.1.1	STAT1	41
2.1.2	STAT1 signaling pathways	41
2.1.3	STAT1 in cancer and SCCHN	43
2.1.4	Rationale and hypotheses	44
2.2	MATERIALS AND METHODS	45
2.2.1	Chemicals and reagents	45
2.2.2	Cell culture	45
2.2.3	Preparation and transfection of STAT3 decoy and mutant control decoy	
	46	
2.2.4	siRNA transfections	47

2.2.5	Western blotting.....	47
2.2.6	Cell counting.....	48
2.2.7	MTT Assay	48
2.2.8	Statistics	48
2.3	RESULTS	49
2.3.1	STAT1 pathway is intact in SCCHN cells	49
2.3.2	SCCHN cell lines express STAT1 and STAT3 and are sensitive to STAT3 decoy-mediated cell death	50
2.3.3	Stimulation of the STAT1 pathway does not mitigate STAT3 decoy- mediated antitumor effects in SCCHN cell lines.....	52
2.3.4	STAT1 siRNA down-regulates STAT1 protein expression and signaling in SCCHN cells.....	54
2.3.5	Downmodulation of STAT1 does not mitigate the antiproliferative effects of the STAT3 decoy	56
2.3.6	Characterization of STAT1 and STAT3 protein expression in STAT3 knockout and wild-type mouse embryonic fibroblast cell lines.....	58
2.3.7	STAT3 is necessary for the antiproliferative effects mediated by the STAT3 decoy	59
2.4	DISCUSSION.....	61
3.0	COMBINING THE STAT3 DECOY WITH AN EGFR AND/OR A BCL-X_L INHIBITOR ENHANCES ANTITUMOR EFFECTS IN PRECLINICAL MODELS OF SCCHN	65
3.1	INTRODUCTION	65
3.1.1	EGFR	65

3.1.1.1	EGFR overexpression and mutation in SCCHN	66
3.1.2	EGFR as a therapeutic target for SCCHN	66
3.1.2.1	Monoclonal antibodies.....	67
3.1.2.2	Targeting EGFR with TKIs.....	69
3.1.2.3	EGFR antisense gene therapy.....	70
3.1.2.4	Immunotoxin conjugates targeting EGFR	70
3.1.3	Bcl-X _L	71
3.1.3.1	Bcl-X _L as a therapeutic target for cancer	71
3.1.3.2	Bcl-X _L targeting strategies	72
3.1.3.3	Antisense and siRNA strategies to target Bcl-X _L	74
3.1.3.4	Small molecule inhibitors of Bcl-X _L	74
3.1.3.5	Gossypol.....	76
3.1.4	Rationale and hypotheses.....	77
3.2	MATERIALS AND METHODS	78
3.2.1	Chemicals and reagents.....	78
3.2.2	Cell culture	78
3.2.3	STAT3 decoy preparation and transfection.....	78
3.2.4	Dose response and cell viability experiments	79
3.2.5	Cell treatments	79
3.2.6	Western blotting of cell line lysates	80
3.2.7	Animals and treatment regimen	80
3.2.8	Statistics	80
3.3	RESULTS	81

3.3.1	SCCHN cell lines have similar IC ₅₀ values for (-)-gossypol but not for erlotinib or the STAT3 decoy.....	81
3.3.2	Combining EGFR and STAT3 inhibitors enhances antiproliferative effects in SCCHN <i>in vitro</i>	82
3.3.3	Targeting EGFR and STAT3 in an <i>in vivo</i> SCCHN preclinical model results in enhanced antitumor effects.....	84
3.3.4	Combining STAT3 and Bcl-X _L inhibitors enhances antiproliferative effects in SCCHN cell lines.....	86
3.3.5	A combination of EGFR, STAT3 and Bcl-X _L inhibitors enhances antiproliferative effects in SCCHN cell lines.....	87
3.3.6	A combination of EGFR, STAT3 and Bcl-X _L inhibitors does not increase induction of apoptosis in an SCCHN cell line.....	90
3.4	DISCUSSION.....	92
4.0	CONCLUSIONS AND FUTURE DIRECTIONS.....	95
4.1	CONCLUSIONS.....	95
4.2	FUTURE DIRECTIONS.....	96
4.2.1	Investigation of other signaling molecules involved in the mechanism of the STAT3 decoy	96
4.2.1.1	Role of STAT5 in the STAT3 decoy mechanism.....	97
4.2.1.2	Role of mTOR in the STAT3 decoy mechanism.....	100
4.2.2	Determining the molecular pathways affected by combined targeting of EGFR and STAT3 <i>in vivo</i>	102
4.2.3	Future studies to investigate the therapeutic potential of EGFR, STAT3, and Bcl-X _L combined targeting for SCCHN.....	103

4.2.4	Limitations of the STAT3 decoy as a treatment for SCCHN and other malignancies	104
4.3	CONCLUDING REMARKS	105
	APPENDIX A	107
	BIBLIOGRAPHY.....	140

LIST OF TABLES

Table 1. Strategies to inhibit STAT3.....	28
Table 2. Transcription factor decoys under investigation.	35
Table 3. Summary of EGFR inhibitors studied for SCCHN.	68
Table 4. Summary of Bcl-X_L targeting strategies.	73
Table 5. IC₅₀ values for inhibitors in SCCHN cell lines.	82

LIST OF FIGURES

Figure 1. STAT3 protein structure.....	22
Figure 2. STAT3 signaling pathway.....	23
Figure 3. STAT3 decoy and mutant control decoy sequence.....	37
Figure 4. STAT1 Signaling Pathways.	42
Figure 5. Time course of IFN-γ stimulation of SCCHN cells.	49
Figure 6. Dose-dependent induction of pSTAT1 by IFN-γ in SCCHN cells.....	50
Figure 7. STAT1 levels do not correlate with SCCHN growth inhibition by the STAT3 decoy.....	51
Figure 8. STAT3 decoy mediated inhibition of the STAT1 pathway or growth inhibition is not abrogated by stimulation with IFN-γ in SCCHN cell lines.....	53
Figure 9. STAT1 siRNA downmodulates total STAT1 protein levels, increases proliferation, and decreases STAT1 signaling.	55
Figure 10. Downmodulation of STAT1 protein does not alter decreased cell viability mediated by the STAT3 decoy in SCCHN cells.	57
Figure 11. Characterization of STAT3 or STAT5 knockout and wild-type MEFs.	59
Figure 12. STAT3 but not STAT5 is necessary for STAT3 decoy-mediated decrease in cell survival.....	61

Figure 13. Combining the STAT3 decoy with erlotinib enhances growth inhibition *in vitro*.
..... 83

Figure 14. The STAT3 decoy inhibits SCCHN cell growth *in vivo*. 85

Figure 15. A combination of the STAT3 decoy with (-)-gossypol inhibits growth of head and neck cancer cells. 87

Figure 16. Combining erlotinib, STAT3 decoy and (-)-gossypol further enhances growth inhibition but not apoptosis in SCCHN cells compared with treatment using either the STAT3 decoy alone or a combination of erlotinib, mutant control decoy, and (-)-gossypol.
..... 89

Figure 17. Combined inhibition of STAT3 with erlotinib and (-)-gossypol does not significantly increase apoptosis *in vitro*...... 91

Figure 18. Prolactin receptor and STAT5b protein expression in SCCHN cell lines...... 98

Figure 19. STAT5b is not necessary for STAT3 decoy-mediated growth inhibition of SCCHN cells. 99

FORWARD

I would like to thank my family first and foremost for their never-ending love, support, understanding, encouragement, and inspiration. Without them, I never could have dreamed that I would be the person I am today. At a young age, my mom and dad taught me that I was special and that any dream I had I could make come true with hard work and perseverance. My mom and dad have sacrificed so much for me to succeed in life and knowing that I have their love and support has always helped me to overcome obstacles and challenges. Thank you, Mom and Dad. I would also like to thank my sister, Stacey, for always pretending to be interested in what I do and for being committed to making me laugh.

I have formed several great friendships with other graduate students—Antonia Nemeč, Robert Tomko, Kelly Quesnelle, and Neil Bholā. Each of them has provided an outlet for my scientific and personal angst. These friendships mean very much to me and I am thankful that I was able to surround myself with such intelligent, creative, and sincere persons. I would also like to thank my close friends and sorority sisters, Kristen Moran, Maegan Joseph, Kristen Lewis, and Jenn Henkel Bruns. They have been my emotional support system and I love them very much. It's wonderful to have friends who know who you really are and who accept and love you for it. These women inspire me because of their constant demonstration of faith, hope and love.

I would like to thank Dr. Jennifer Grandis, who has mentored me through the last few years of my graduate career. I have learned a lot about myself as a person as well as a scientist during my time working with her. I would also like to thank the members of the Grandis laboratory.

Because this is the culmination of twenty-one straight years of school, I would also like to sincerely thank my teachers, professors, and mentors that helped guide me through my education: Harold Ohm, Richard Easton, Alice Lee, Ph.D., Candy DeBerry, Ph.D., William F. Goins, Ph.D., Stephen Phillips, Ph.D., and Janey Whalen, Ph.D. Also, I would like to thank the Office of Graduate Studies at the University of Pittsburgh School of Medicine, in particular Cindy Duffy, who has answered more questions than I can count about scheduling, bills, and other administrative issues that have come up over the past five years.

LIST OF ABBREVIATIONS

EGF	Epidermal growth factor
EGFR	Epidermal growth factor receptor
4E-BP1	Eukaryotic initiation factor 4E binding protein 1
FBS	Fetal bovine serum
FDA	Food and Drug Administration
GFP	Green fluorescent protein
IFNR	Interferon receptor
IFNAR	Interferon-alpha receptor
IFNGR	Interferon-gamma receptor
MMP	Matrix metalloproteinase
mRNA	Messenger RNA
MTT	3-(4, 5-dimethylthiazol-2-yl)-2,5-diphenyltetrazolium bromide)
mTOR	Mammalian target of rapamycin
NF- κ B	Nuclear factor-kappa B
NSCLC	Non-small cell lung cancer
OD	Optical density
ODN	Oligodeoxynucleotide
PBS	Phosphate buffered saline
PDGF	Platelet-derived growth factor
PDGFR	Platelet-derived growth factor receptor
PNA	Peptide nucleic acid
P70S6K	Protein 70S6 kinase
pSTAT	Phospho-STAT
PRL	Prolactin
PRLR	Prolactin receptor
RNAi	RNA inhibition

SCCHN	Squamous cell carcinoma of the head and neck
Ser	Serine
SH2	Src Homology 2
siRNA	Small interfering RNA
STAT	Signal transducer and activator of transcription
TGF- α	Transforming growth factor-alpha
TKI	Tyrosine kinase inhibitor
Tyr	Tyrosine
VEGF	Vascular endothelial growth factor

PREFACE

One chapter of this dissertation has been published and can be found in **APPENDIX A**:

Vivian Wai Yan Lui, Amanda L. Boehm, Priya Koppikar, Rebecca J. Leeman, Daniel Johnson, Michelene Ogagan, Erin Childs, Maria Freilino, and Jennifer Rubin Grandis. 2007. Antiproliferative mechanisms of a transcription factor decoy targeting STAT3: the role of STAT1. *Molecular Pharmacology*. February 26 (Epub ahead of print).

1.0 INTRODUCTION

1.1 GENERAL INTRODUCTION

1.1.1 Squamous cell carcinoma of the head and neck

Squamous cell carcinoma of the head and neck (SCCHN) is an epithelial malignancy affecting the mucosa of the upper aerodigestive tract, including the larynx, oral cavity and pharynx. Alcohol consumption and tobacco use are the most important risk factors for development of SCCHN, with 85% of cases linked to tobacco use [1]. Head and neck cancer is the 5th most common malignancy worldwide. Approximately 40,000 Americans will be diagnosed this year and 13,000 will die from their disease. Current treatments, including surgery, chemotherapy and radiation are effective in only half of all cases, and the survival rate has not significantly improved in the past forty years, providing rationale for the development of novel treatment strategies for SCCHN.

1.2 STAT3

New therapies for the treatment of SCCHN are being designed that target proteins involved in signal transduction pathways that have been shown to be associated with SCCHN

tumorigenesis, such as the Signal Transducers and Activators of Transcription (STATs). There are seven members of the STAT family (STAT1, STAT2, STAT3, STAT4, STAT5a, STAT5b, and STAT6) which play different roles in normal cellular processes such as differentiation, proliferation, apoptosis, and angiogenesis [2]. Aberrant activation of STAT proteins leads to transformation at the molecular level [3, 4]. In particular, STAT3 plays an important role in cell cycle and apoptosis, contributing to transformation in a variety of malignancies through overexpression of target genes.

1.2.1 STAT3 protein structure

The STAT protein family has a specific structure consisting of several highly conserved domains (Figure 1). The N-terminal oligomerization domain is critical for stabilizing STAT dimers bound to DNA. The DNA binding domain directly interacts with DNA, ensuring binding specificity to promoter regions [5, 6]. A helical coil region is located between the oligomerization and DNA binding domains and is involved in forming transcriptional complexes. The dimerization domain contains an SH2 domain that is required for STATs to be recruited to the phosphorylated receptors and for the subsequent formation of dimers [7]. A critical tyrosine residue, Tyr 705, is also found in this region of the STAT3 protein, and its phosphorylation is necessary for activation [4]. The carboxy-terminal transactivation domain is involved in the formation of transcriptional complexes and contains a conserved serine residue whose phosphorylation contributes to maximal transcriptional activity [8]. Splice variants lacking this serine residue function as dominant-negative proteins, blocking the function of the protein [9]. Constitutively phosphorylated serine has been observed in human tumors, including leukemias and lymphomas, indicating that it may play a role in oncogenesis [3]. Studies have

shown that blocking serine kinase signaling pathways to inhibit STAT3 serine phosphorylation resulted in decreased STAT3 signaling and inhibition of Src-mediated transformation [9]. In addition to tyrosine phosphorylation, serine phosphorylation of STAT3 also plays a role in malignant transformation.

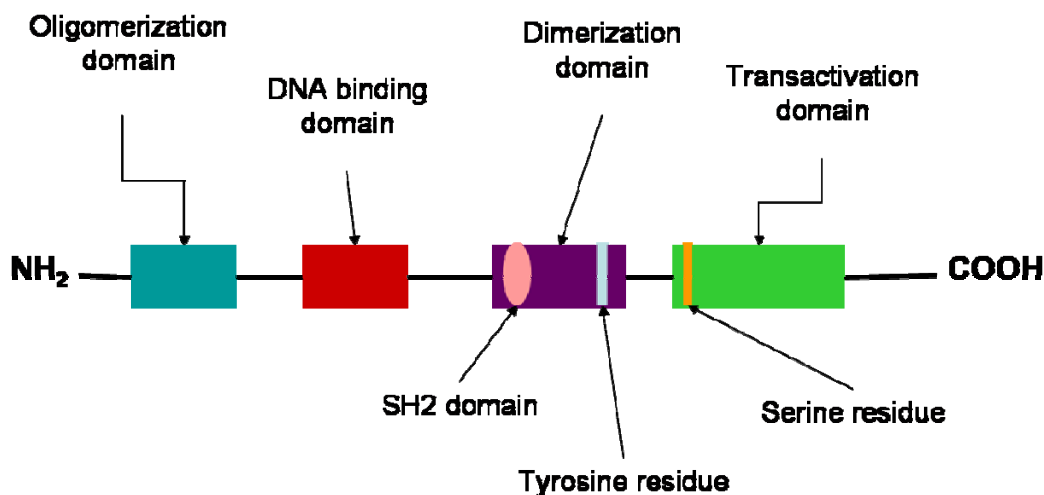


Figure 1. STAT3 protein structure.

STAT proteins consist of four conserved regions: an N-terminal oligomerization domain, a DNA binding domain, a dimerization domain containing an SH2 domain and a tyrosine residue critical for activation, and a C-terminal transactivation domain containing a serine residue that contributes to maximal activation of the STAT protein.

1.2.2 STAT3 pathways and cellular functions

The STAT protein family was initially discovered through studies of IFN receptor signaling [10]. Deletion of STAT3 results in embryonic lethality [11] and studies have shown that it is activated in response to cytokines, growth factors, and other stimuli, indicating that STAT3 participates in a wide variety of cellular processes [10]. STATs are activated by

phosphorylation of tyrosine residues by receptor tyrosine kinases such as Epidermal Growth Factor Receptor (EGFR) [12-14], cytokine receptors such as IL-6/gp130 [15], or non-receptor tyrosine kinases such as Src [16] (Figure 2).

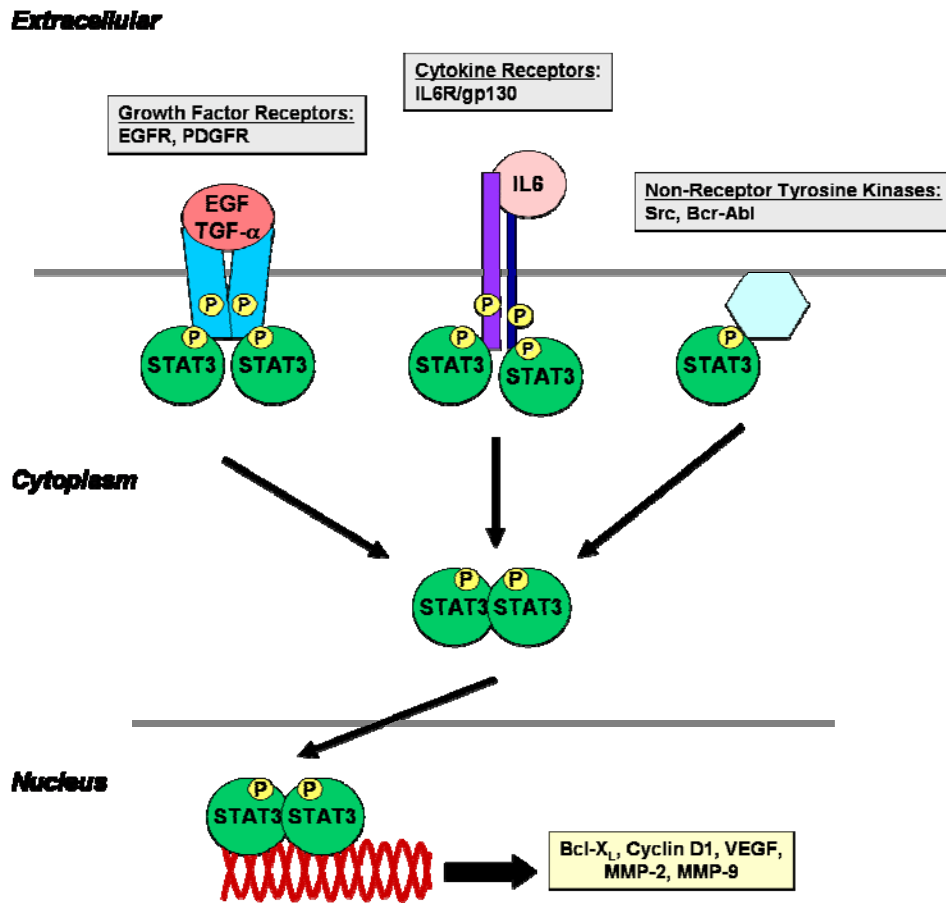


Figure 2. STAT3 signaling pathway.

Activated growth factor receptors, cytokine receptors or non-receptor tyrosine kinases phosphorylate STAT3 at tyrosine 705 located in the dimerization domain of the STAT3 monomer. Phosphorylated STAT3 monomers then dimerize and are translocated into the nucleus where they bind to specific response elements in the promoter region of target genes such as Bcl-XL, Cyclin D1, VEGF, MMP-2 and MMP-9.

Active STATs form homodimers, heterodimers, or multi-protein complexes which translocate into the nucleus where they bind to DNA response elements such as the serum inducible element

of the human *c-fos* gene [17] and transcribe target genes in order to regulate a variety of cellular processes including growth, survival, and differentiation. Studies have identified many STAT3 target genes which are involved in cell cycle regulation (Cyclin D1, Cyclin D3, *c-Myc*, *p21^{waf1}*, *p27*), inhibition of apoptosis (Survivin, *Mcl-1*, and *Bcl-X_L*), angiogenesis (VEGF), migration and invasion (MMP-2 and MMP-9) [18]. The list of STAT3 target genes continues to expand and increase in complexity due to the considerable overlap between STAT3, STAT1, and STAT5 target genes.

1.2.3 STAT3 as an oncogene

Many studies have provided striking evidence that STAT3 is an oncogene. Initial studies suggested that STAT3 activation plays a part in Src-mediated oncogenesis [16, 19]. Subsequently, a constitutively active form of STAT3 (STAT3C) was found to transform fibroblasts in culture that were then able to form tumors in mice—providing genetic evidence that STAT3 plays a part in oncogenesis [20].

To date, no STAT3 mutations have been attributed to constitutive STAT3 activation in either human tumors or cancer cell lines, and it is generally thought that upstream activators (EGFR, Src, or gp130/IL-6R) or negative regulators (SOCS-3, GRIM-19, protein inhibitor of STAT3 (PIAS3)) are mediating constitutively activated STAT3 in cancer [18]. For example, it is generally accepted that IL-6 drives STAT3 activation in multiple myeloma through the gp130/IL-6R [21] and some studies have provided evidence for hypermethylation of the SOCS-1 and SOCS3 genes in various tumor types [22, 23]. Constitutive STAT3 activation has been found in many cancers including multiple myeloma, leukemia, lymphoma, prostate, breast, pancreas, lung, ovary, and head and neck. These studies have shown that inhibition of STAT3

function results in decreased proliferation and increased apoptosis, suggesting that STAT3 contributes to cancer development and progression [2, 3, 24]. The biological significance of increased STAT3 activation in cancer is supported by the correlation of STAT3 over-expression with poor clinical prognosis and decreased survival as well as resistance to chemotherapy [3, 21, 25-27].

1.2.4 STAT3 in disease

STAT3 has been implicated in a variety of blood malignancies and solid tumors, including but not limited to myeloma, lymphoma, astrocytoma, pancreatic cancer, prostate and breast cancer [28, 29]. One of the first reports providing evidence for STAT3 activation in cancer cell growth was in multiple myeloma [21]. A high incidence of STAT3 activation was found in human multiple myeloma cells (elevated DNA binding was observed in all 24 patients), and when IL-6 receptor signaling was inhibited, STAT3 transcription of Bcl-X_L was significantly decreased, inducing apoptosis.

Anaplastic large cell lymphomas (ALCLs), a morphologically and immunophenotypically distinct type of non-Hodgkin lymphoma is caused by chromosomal translocations resulting in the nucleophosmin (*NPM*) gene being fused with the anaplastic lymphoma kinase (*ALK*) gene (*NPM-ALK*) [30]. Studies have shown that human ALCLs have high levels of phospho-STAT3 and that mice engineered to express *NPM-ALK* express constitutively active STAT3 [31, 32].

STAT3 is frequently activated in astrocytomas, the most common type of primary central nervous system tumors, in which STAT3 induces cell proliferation and inhibits apoptosis [33]. While STAT3 activation is necessary for astrocyte differentiation, the role of STAT3 signaling in differentiated astrocytes is unclear. Elevated STAT3 activity in astrocytomas has been reported

[34, 35], and STAT3 knockdown via STAT3 siRNA reduced the expression of target genes such as survivin and Bcl-X_L, as well as increased apoptosis in human astrocytoma cell lines but not in primary astrocytes [33].

STAT3 overexpression has been found in both human pancreatic cancer tissues and cell lines [36-38]. Aberrant STAT3 activation in pancreatic cancer has been postulated to be caused by Src and EGFR signaling, and overexpression of both Src and EGFR has been documented in this disease. STAT3 has been implicated in the malignant transformation of human pancreatic cancer through promotion of cellular proliferation. In addition, cells expressing STAT3 dominant-negative mutants are unable to grow in *in vitro* and *in vivo* models of pancreatic carcinoma. In particular, STAT3 mediated overexpression of VEGF was shown to regulate growth, angiogenesis and metastasis of pancreatic cancer *in vitro* and *in vivo*, again suggesting STAT3 is a therapeutic target for pancreatic cancer [38].

A role for STAT3 in both prostate and breast cancers has also been documented. Studies have shown that aberrant STAT3 activation is due to IL-6 signaling and plays a role in tumorigenesis of prostate cells [39]. In addition, prostate cancer cells expressing constitutively-activated STAT3 were sensitive to STAT3 inhibition, resulting in increased apoptosis [40, 41]. An early experiment identified increased DNA binding of STAT3 in nuclear extracts from human breast cancer tissue [42]. Constitutive activation of STAT3 was detected in a panel of human breast cancer cell lines (five of nine investigated) but not in normal breast epithelial cells, and experiments with an EGFR inhibitor led to the conclusion that STAT3 activation is not necessarily dependent on EGFR activity in human breast carcinoma [43].

1.2.5 STAT3 in SCCHN

The role of STAT3 has been well characterized in SCCHN. Early studies focusing on STAT3 found it was required for EGFR-mediated cell proliferation in SCCHN cell lines where SCCHN cells expressing a dominant-negative mutation did not proliferate and STAT3 antisense oligonucleotides significantly inhibited growth *in vitro* [26]. Further experiments found that STAT3 activation was EGFR-independent in SCCHN *in vitro* [44]. A similar investigation was performed using an *in vivo* SCCHN xenograft model and results indicated that STAT3 antisense oligonucleotides inhibited expression of activated STAT3 and induced apoptosis [45]. Constitutive STAT3 activation was also discovered in SCCHN tumors from patients where a 10.6 fold increase was observed in SCCHN tumors compared to normal mucosa from non-cancer patients [45] and a recent study from Shah *et al.*, found that STAT3 was activated in oral squamous cell carcinoma and may be a risk factor for poor prognosis [46]. These studies give further evidence supporting the hypothesis that STAT3 plays a part in SCCHN and is a potential therapeutic target.

1.3 STAT3 AS A THERAPEUTIC TARGET IN CANCER

Chemotherapeutic agents designed to inhibit tumor growth through induction of apoptosis are frequently rendered ineffective by tumor cells which exhibit aberrant proliferation and resistance to pro-apoptotic stimuli. Therefore, the identification of novel therapeutic targets to kill chemoradiation-resistant tumor cells is essential. Given that STAT3 target genes are involved in cell cycle progression and inhibition of apoptosis, STAT3 has emerged as a

therapeutic target and many strategies to inhibit STAT3 have been investigated in preclinical models. STAT3 targeting strategies include inhibition of upstream signaling molecules, inhibition of mRNA translation, and blocking the SH2 domain or the DNA binding domain of STAT3 (Table 1). To date, no STAT3 inhibitor has been tested in patients with cancer.

Table 1. Strategies to inhibit STAT3.

STAT3 inhibition strategies have focused on inhibiting mRNA translation, blocking the STAT3 SH2 domain, or blocking the STAT3 DNA binding domain using the inhibitors listed below.

Strategy	Inhibitor	References
Inhibition of mRNA translation	Antisense ODN	[30, 45]
	siRNA	[32, 47-49]
Blocking the SH2 domain	Peptide aptamer	[50]
	Phosphotyrosyl peptidomimetic	[51]
	G-quartet ODN	[52]
Blocking the DNA binding domain	Peptide aptamer	[50]
	Transcription factor decoy	[53-56]

1.3.1 Inhibiting STAT3 mRNA translation using antisense or siRNA

One approach to inhibiting STAT3 is the use of antisense oligonucleotides (ODNs). The mechanism by which antisense ODNs elicit mRNA inactivation is well characterized. The single stranded oligonucleotides complementing the sequence of the mRNA target enter the cell and

bind to mRNA, disrupting mRNA transport, splicing, or translation by steric hindrance [57]. In addition, RNase H, a ubiquitously expressed endonuclease is activated by antisense ODNs, resulting in the cleavage of the mRNA, although the exact mechanism of recruitment is incompletely understood. Advances in the efficacy of antisense ODNs have been the result of chemical modifications to the antisense backbone to increase its half-life in the cell by making it more resistant to degradation by nucleases.

A STAT3 antisense gene therapy approach using a modified U6 expression plasmid was applied to an *in vivo* model of SCCHN [45]. This study concluded that liposome-mediated antisense gene therapy blocked STAT3 activation, resulting in increased apoptosis but no inhibition of tumor growth was observed. Chiarle *et al.*, administered a STAT3 antisense oligonucleotide in preclinical models of NPM-ALK lymphoma and observed decreased cell proliferation, increased cleaved PARP, and induction of apoptosis *in vitro*, as well as significantly decreased tumor growth, prolonged survival, and tumor regression *in vivo* [30]. STAT3 antisense oligonucleotides were studied in *in vivo* models of SCCHN and found to block STAT3 activation and induce apoptosis through downmodulation of STAT3 target gene expression as well [45].

RNA interference (RNAi) has been investigated as a therapeutic approach for pathogenesis and is considered to be a more potent inhibitor of mRNA than antisense [57]. Short interfering RNA (siRNA) consists of two strands of nucleotides 19-23 oligomers in length. The siRNA recruits and activates the RNA-silencing complex (RISC) which is a multimeric nuclease that degrades the target mRNA, reducing both RNA and protein expression of a particular gene. siRNA has been investigated extensively in preclinical models, and several studies have chronicled the use of STAT3 siRNA in several types of cancer.

STAT3 RNAi was found to significantly reduce STAT3 protein levels (75-95%) in both normal human astrocytes as well as astrocytoma cell lines 48-72 hrs after transfection [33]. Downmodulation of STAT3 using this approach induced morphological changes and significantly decreased cell viability of several astrocytoma cell lines. Transfection with STAT3 siRNA also induced apoptosis as shown by Hoechst 33258 staining, caspase 3 cleavage, and annexin V staining. In addition, knockdown of STAT3 also down-regulated two antiapoptotic genes: survivin and Bcl-X_L. However, these effects were not consistent throughout the panel of astrocytoma cell lines used—some cell lines were less sensitive to STAT3 knockdown, suggesting that astrocytomas are not uniformly dependent on STAT3.

Recently, short hairpin RNAs transcribed from an RNA polymerase III-based vector under control of the U6 promoter targeting STAT3 were investigated as an antitumor therapy in prostate tumor xenografts in a mouse model [48]. *In vitro* experiments showed downmodulation of STAT3 and phospho-STAT3 levels as well as downmodulation of STAT3 target gene expression (Bcl-2, cyclin D1, and c-Myc). When prostate cancer cell xenografts were injected with STAT3 siRNA, tumor volume was significantly decreased, and both apoptosis and cell cycle arrest were induced.

A similar DNA-vector-based RNAi approach targeting STAT3 was used in both *in vitro* and *in vivo* models of laryngeal tumors using the Hep2 human laryngeal tumor cell line [48, 49]. These studies found that STAT3 siRNA suppressed growth, and induced apoptosis through downmodulation of STAT3 as well as its downstream target genes Bcl-2, Cyclin D1, and survivin, further confirming previously published reports that suggest STAT3 is a rational target for STAT3 overexpressing cancer cells.

1.3.2 Blocking the SH2 domain to prevent STAT3 activity

Using a yeast two-hybrid selection system, a high complexity peptide aptamer library was used to isolate a short peptide, or peptide aptamer, designed to specifically interact with the SH2 domain of STAT3 [50]. STAT3 SH2 domain-binding peptide aptamers were isolated and experiments demonstrated that they bound to STAT3 *in vitro* in NIH3T3 fibroblasts stably transfected with the EGFR gene in order to induce activated STAT3 that could serve as a target for the STAT3 peptide aptamer (Herc cells). Further analysis of their function showed that STAT3-dependent transcription was reduced in a peptide aptamer-dose dependent manner, STAT3 DNA binding was reduced, and STAT3 signaling was downmodulated, specifically through a reduction in STAT3 tyrosine phosphorylation which prevents STAT3 activation. Nonetheless, the peptide aptamers showed no antitumor activity in either murine melanoma or human myeloma cell lines, indicating that these particular peptide aptamers targeting the SH2 domain of STAT3 are not effective in STAT3 overexpressing tumor cells.

Peptidomimetics are small molecules that target specific functional domains of a protein to block its activation. A phosphotyrosyl peptide was designed to inhibit STAT3 by binding to a tyrosine residue in the SH2 domain that is critical for STAT3 dimerization and DNA binding [51]. When the peptide was combined with nuclear extracts containing STAT3, DNA binding was decreased in a dose-dependent manner, and STAT3 dimerization was abrogated. In addition, the phosphotyrosyl peptide decreased transcription of a STAT3-dependent luciferase reporter gene and blocked v-Src-mediated transformation of fibroblasts. These results demonstrated that a peptidomimetic targeting the SH2 domain of STAT3 could block STAT3 activation and suppress signaling, but issues such as delivery of the peptide across the cell membrane and stability of the peptide *in vivo* still remain concerns.

G-quartet oligodeoxynucleotides (ODNs) have also been used to target STAT3 in human cancer. G-rich ODNs can form intra- and inter-molecular structures consisting of four strands of DNA, or G-quartets. G-quartets bind to DNA-binding sites, inhibiting the ability of transcription factors such as STAT3 to bind to promoter regions of target genes. A G-quartet was designed that inhibited IL-6-mediated activation of STAT3 and STAT3-mediated expression of Bcl-X_L and Mcl-1 in a human hepatocarcinoma cell line (HepG2) [52]. The G-quartet not only decreased the DNA binding affinity of STAT3, but also STAT1, probably due to the close sequence homology of the two proteins.

1.3.3 Blocking the STAT3 DNA binding domain to prevent target gene expression

A second peptide aptamer was designed to specifically interact with the DNA binding domain of STAT3 [50]. First, the ability of this 20-amino acid peptide aptamer to interfere with STAT3 function was investigated and the aptamer inhibited DNA binding and transactivation activity of STAT3 in Herc cells. There was no effect on STAT3 phosphorylation. The STAT3 peptide aptamer was next analyzed in human myeloma U266 cells and murine melanoma B16 cells, which both express constitutively active STAT3. After treatment, both cell lines showed a dose-dependent increase in growth inhibition using cell viability assays and increased apoptosis by both TUNEL staining and Western blot analysis of PARP, cleaved caspase 3, and Bcl-X_L.

Another way to target the STAT3 DNA binding domain is to design short double or single-stranded oligonucleotides referred to as transcription factor decoys. STAT3 has been successfully inhibited using a double-stranded STAT3 transcription factor decoy *in vitro* and *in vivo* in preclinical models of SCCHN, skin cancer, and psoriasis and will be discussed in more detail below [53-56]. These studies provide proof-of-principle for a transcription factor decoy

approach to inhibit STAT3 by blocking the DNA binding domain of STAT3, inhibiting target gene expression.

1.4 THE STAT3 TRANSCRIPTION FACTOR DECOY

1.4.1 Transcription factor decoys

Transcription factor decoys are double- or single-stranded deoxyoligonucleotides 15-20 base pairs long designed to mimic the promoter region of a target gene recognized by a specific transcription factor. Theoretically, the transcription factor decoy binds to the DNA binding domain of the transcription factor, physically preventing it from binding to the DNA and transcribing its target gene. This approach is particularly attractive because as therapeutic targets, the transcription factors are easily identified, the synthesis of the decoy is straightforward, and knowing the exact molecular structure of the transcription factor is unnecessary.

Decoys have been designed and tested against a variety of transcription factors in preclinical models of disease (Table 2). An E2F decoy is the first transcription factor decoy to reach clinical trials. The E2F decoy (edifoligide) was extensively studied for its ability to inhibit smooth muscle cell proliferation in preclinical models of vein graft disease [58]. Yet, results of recent phase II and III clinical trials found that ex vivo E2F decoy treatment of lower extremity vein grafts did not significantly decrease the rate of vein graft failure in patients [59].

NF- κ B is a well characterized transcription factor that regulates genes involved in inflammation and cell adhesion, and inhibits apoptosis. Several NF- κ B transcription factor

decoys have been developed and studied in a wide variety of malignancies including gastric cancer, glioblastoma, prostate cancer, leukemia, and osteosarcoma [60-64]. Uetseka *et al.*, demonstrated an NF- κ B decoy could sensitize a chemoresistant stomach cancer cell line to 5-fluorouracil [64]. Another study found that a transcription factor decoy targeting NF- κ B inhibited cachexia, a common complication of cancer characterized by anorexia, anemia, decreased body weight and progressive tissue wasting, in a mouse model of colon adenocarcinoma [65]. NF- κ B decoys inhibited cell growth in a model of glioblastoma [60], and enhanced induction of apoptosis in models of prostate cancer and leukemia [62, 63]. Studies of the preclinical efficacy of NF- κ B decoys have been performed in other inflammatory diseases, including arthritis, asthma, and eczema [66, 67]. Furthermore, clinical trials of NF- κ B decoys are currently underway to investigate their clinical efficacy as a topical treatment for atopic dermatitis (Phase I/II) [68].

Sp1 has been inhibited by transcription factor decoys in preclinical models of disease as well. Sp1 regulates the expression of genes involved growth, apoptosis, angiogenesis, and tumorigenesis. An Sp1 transcription factor decoy suppressed proliferation and target gene expression in an *in vitro* model for diabetes [69]. Also, breast cancer cell migration was prevented by downmodulation of urokinase receptor expression by a Sp1 transcription factor decoy [70, 71]. When lung adenocarcinoma or glioblastoma multiforme cell lines were treated with an Sp1 decoy, VEGF was downmodulated and cell proliferation was inhibited [72]. In addition, an *in vivo* experiment further illustrated the therapeutic value of an Sp1 decoy when melanoma tumor growth was inhibited and VEGF and TNF- α protein expression was decreased in mice [73].

Table 2. Transcription factor decoys under investigation.

Transcription factor decoys are listed with the therapeutic application and references.

Transcription Factor Target	Therapeutic Application	References
β-catenin	Colon cancer	[74]
E2F1	Prevention of vein graft failure	[58, 59]
NF-κB	Arthritis Asthma Cancer: Colon cancer Gastric cancer Glioblastoma Prostate cancer Leukemia Osteosarcoma Eczema Ischemia Osteoporosis	[66] [67] [60-64] [75] [76] [77] [77]
Sp1	Cancer: Breast cancer Glioblastoma multiforme Lung cancer Melanoma Diabetes	[70, 71, 73] [69]
STAT1	Arthritis	[78]
STAT6	Allergic reactions Acute dermatitis	[79-81] [82]
STAT3	Prostate cancer SCCHN Skin cancer Psoriasis	[40] [53, 54] [56] [55]
NF-κB, E2F, and STAT3	Breast cancer Lung cancer	[83]

Finally, a single decoy containing binding sites for three transcription factors that are up-regulated in cancer and known to form multiprotein transcription factor complexes with each other—NF- κ B, E2F, and STAT3—has been developed [83]. Antitumor efficacy of the decoy was investigated in *in vitro* and *in vivo* models of breast cancer and lung cancer and found to significantly decrease tumor cell growth and target gene expression. This study demonstrated the ability to design more complex decoys targeting multiple transcription factor decoys.

1.4.2 STAT3 decoy design

The double stranded STAT3 decoy ODN developed by our laboratory is based on the Serum Inducible Element (SIE) of the human *c-fos* promoter with a high affinity modification (Figure 3) [53]. The 18-base pair decoy was designed to bind to the STAT3 DNA binding domain, abrogating its ability to bind to DNA response elements and induce transcription of target genes, eliciting antitumor effects through the down-regulation of STAT3 target genes. One of the limiting factors in using oligonucleotides is the rapid degradation of unmodified ODNs in serum and cells, so modifications that increase resistance to nucleases have been developed. One of the most common modifications is phosphorothioated bases, the replacement of a non-bridging oxygen with sulfur in phosphate linkages [84]. The internucleoside linkages between the first and last three base pairs of the STAT3 decoy and mutant control decoy are phosphorothioated to prevent degradation in serum and in cells. Studies have shown that this type of modification also increases cellular uptake and sequence-specific duplexes are more aptly formed. The entire sequence is not modified because studies have suggested that although fully

phosphorothioated ODNs have increased cellular retention, they also result in increased nonspecific binding compared to partially or unmodified ODNs [84].

STAT3 Decoy

5'-CAT TTC **CCG TAA ATC-3'**
3'-GTA AAG **GGC ATT TAG-5'**

Mutant Control Decoy

5'-CAT TTC **CCT TAA ATC-3'**
3'-GTA AAG **GGA ATT TAG-5'**

Figure 3. STAT3 decoy and mutant control decoy sequence.

The STAT3 decoy consists of an 18 nucleotide portion of the SIE promoter region of the human c-fos gene. The first and last three bases at both the 5' and 3' ends have been chemically modified with a phosphorothioate modification (underlined bases) to increase resistance to degradation by nucleases. A mutant control decoy differing by a single base pair mutation (in red) has no binding affinity for STAT3 and serves a negative control for all experiments.

The mutant control decoy differs from the mutant control decoy by a single base pair mutation (Figure 3). The mutant control decoy has previously demonstrated no DNA binding activity to STAT3 and does not inhibit STAT3 binding activity in EMSAs after SCCHN cells are treated [53]. In cell proliferation experiments, the mutant control decoy does not significantly decrease cell proliferation compared to an untreated control. Also, STAT3 target gene expression is not decreased by the mutant control decoy either. Therefore, the mutant control decoy serves as a control for all STAT3 decoy experiments.

1.4.3 STAT3 decoy in preclinical models

The STAT3 transcription factor decoy is designed to mimic the consensus sequence recognized by STAT3. The decoy binds to STAT3, inhibiting its potential to bind to DNA and transcribe target genes. Our lab previously demonstrated that the STAT3 decoy inhibited target gene expression, induced apoptosis, and decreased proliferation of a SCCHN cell line *in vitro* [53]. Experiments with normal oral keratinocytes showed that the STAT3 decoy was taken up in normal cells, although proliferation was not decreased. Furthermore, the STAT3 decoy significantly inhibited the growth of SCCHN xenografts in nude mice compared to the mutant control decoy [54]. In addition, when combined with cisplatin, the STAT3 decoy inhibited cell proliferation, increased apoptosis, and decreased expression of Bcl-X_L and Cyclin D1 both *in vitro* and *in vivo*, demonstrating improved therapeutic efficacy of combining the STAT3 decoy with an established treatment modality for SCCHN [54].

Also, the STAT3 decoy inhibited the growth of initiated keratinocytes expressing the constitutively active *Ha-Ras* gene in cell lines and mice, and inhibited the growth of skin tumors after direct injection [56]. STAT3 activation is necessary in keratinocytes for skin to heal after injury, and some reports have provided evidence for a role for STAT3 in the development psoriatic plaques, which may actually be the result of persistent wound-healing reactions [55]. Sano *et al.* showed that STAT3 activation in keratinocytes is responsible for the formation of human psoriatic lesions. This study also found that transgenic mice expressing constitutively active STAT3 developed skin lesions that are pathologically related to human psoriatic plaques. These psoriatic-like lesions were inhibited by treatment with the STAT3 decoy, clearly indicating that STAT3 plays a role in the development of psoriasis in a transgenic mouse model. A single-stranded STAT3 oligonucleotide induced mitochondrial-mediated apoptosis in prostate

cancer preclinical models [40]. *In vitro* experiments found that the single-stranded STAT3 decoy decreased mitochondrial transmembrane potential, inhibited survivin expression, and induced caspase cleavage in prostate cancer cell lines. Prostate cancer xenografts injected into nude mice were treated intratumorally with the single-stranded STAT3 decoy and resulted in slowed growth rate by inducing apoptosis. These studies indicate the therapeutic efficacy of the STAT3 decoy as a STAT3 inhibitor in human diseases in which STAT3 is a mediator of pathogenesis.

1.5 RATIONALE AND HYPOTHESES

Our laboratory previously demonstrated STAT3 decoy antitumor activity both *in vitro* and *in vivo* using SCCHN models, as well as augmentation of these effects when the STAT3 decoy is combined with chemotherapy *in vivo* [53, 54]. The goal of these studies was to elucidate the molecular mechanism of the STAT3 transcription factor decoy and to investigate the efficacy of a novel therapeutic strategy that incorporates the decoy with other clinically established treatment modalities.

To investigate the mechanism by which the STAT3 decoy elicits antitumor effects in SCCHN, experiments were performed to determine the role of STAT1, based on high sequence homology between STAT1 and STAT3, the presence of STAT1/3 heterodimers in SCCHN cell lines, and the presence of both STAT1 and STAT3 in SCCHN cell lines and tumors.

Furthermore, the STAT3 decoy was combined with an EGFR inhibitor and/or a Bcl-X_L inhibitor to investigate the hypothesis that targeting a single signaling pathway up-regulated in SCCHN by inhibiting the upstream receptor, intracellular signaling molecule and transcription

factor, and the downstream target gene would increase antitumor effects in SCCHN preclinical models.

2.0 STAT1 DOES NOT CONTRIBUTE TO OR MITIGATE THE STAT3 DECOY ANTIPROLIFERATIVE MECHANISMS

2.1 INTRODUCTION

2.1.1 STAT1

STAT1 was the first STAT protein identified after treatment with interferons resulted in transcription of its target genes [85]. STAT1 contains the same functional domains as STAT3—the N-terminal oligomerization domain, DNA binding domain, dimerization domain containing the SH2 domain and tyrosine residue, and the C-terminal transactivation domain. STAT1 and STAT3 share 72% sequence homology in the DNA binding domain, and STAT1/3 heterodimers have been identified in a variety of cell types, including SCCHN cell lines. Serine 727 is required for STAT1 to bind to other transcription factors such as MCM-5 and BRCA1 for maximal transcriptional activity [86].

2.1.2 STAT1 signaling pathways

STAT1 mediates signaling downstream of growth factor and cytokine receptors, including EGFR, PDGFR, and IFN receptors (IFNRs), in a ligand-dependent manner (Figure 4). The DNA binding specificity of STAT1 dimers is dependent on its binding partners, which

include STAT2, STAT3, and various other transcription factors [86]. STAT1 is activated by ligand binding of IFN- α or IFN- β to the IFNAR, which is activated by auto- and trans-phosphorylation of Jak1 and Tyk2. This results in the phosphorylation of Tyr466 of IFNAR1, Tyr 660 of STAT2, and Tyr 701 of STAT1. pSTAT1 and pSTAT2 dimerize and transcribe gamma activated sequence (GAS) elements, or the heterodimer can bind to p48, a member of the IRF family of transcription factors to form the ISGF3 complex.

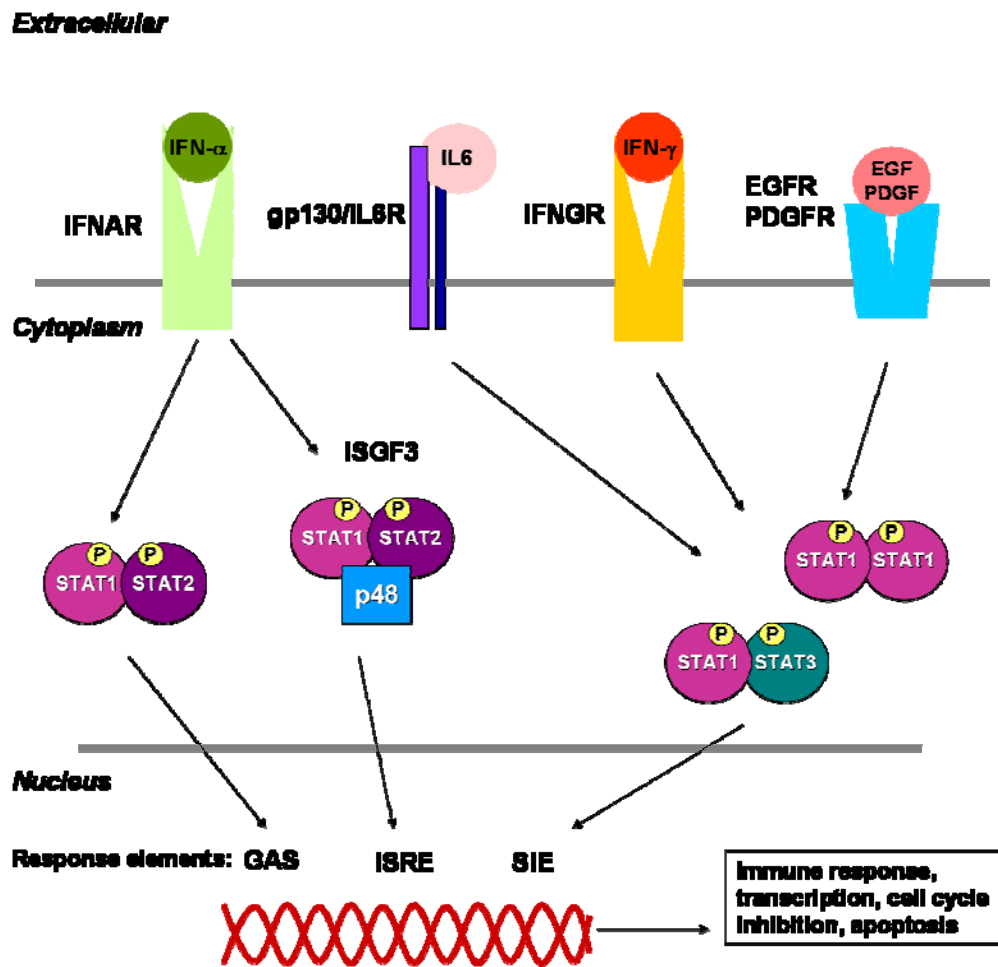


Figure 4. STAT1 Signaling Pathways.

STAT1 is activated by both cytokine and growth factor receptors. IFN- γ binds to and activates Interferon- α receptors (IFNARs) which dimerize and recruit STAT1 to the JAK1 and JAK2 sites, which

phosphorylate tyrosine 701 of STAT1. pSTAT1 then dimerizes through reciprocal interactions of phospho-Tyr 701 and the SH2 domain, with pSTAT2. This heterodimer can then transcribe target genes containing GAS elements or form a transcription complex with p48 to form ISGF3, which regulates genes containing ISREs. IL-6 binding to gp130/IL-6R, IFN- γ binding to Interferon- γ receptors (IFNGRs), EGF binding to EGFR, or PDGF binding to PDGFR phosphorylates Tyr 701 on STAT1, which then dimerizes with either pSTAT1 or pSTAT3 and then binds to serum inducible elements (SIE) to transcribe target genes as well.

The heterodimer or transcription factor complex translocates into the nucleus, binds to either GAS or interferon-stimulated response elements (ISREs) in the promoters of IFN- α or IFN- β inducible genes [87]. STAT1 is also phosphorylated via EGF binding to EGFR or PDGF binding to PDGFR. EGF binding to EGFR results in STAT1 and STAT3 activation, and subsequent homo- or heterodimerization, leading to transcription of target genes. Studies have identified two to five hundred STAT1 target genes, including IRF-1, p21^{waf1}, Fas and FasL, TRAIL, and caspases which modulate cell growth and induce apoptosis, providing evidence for STAT1 as a tumor suppressor [88].

2.1.3 STAT1 in cancer and SCCHN

Several studies have indicated that STAT1 is important in normal growth and have implicated STAT1 as a tumor suppressor. STAT1 knockout human fibroblasts are insensitive to TNF- α -mediated apoptosis [89]. STAT1 knockout mice have defects in IFN-mediated STAT1 signaling, resulting in decreased immune response and increased susceptibility to infection [90]. These mice developed tumors rapidly in response to chemical carcinogens but did not

spontaneously develop tumors [91]. In SCCHN cell lines overexpressing STAT1 and STAT3, loss of STAT1 by either antisense ODNs or dominant-negative constructs did not alter cell growth, indicating that STAT3 but not STAT1 is necessary for EGFR-mediated cell growth [26]. Despite its antiproliferative and pro-apoptotic effects, STAT1 is frequently overexpressed in a variety of malignancies including multiple myeloma, some leukemias, lung cancer, breast cancer and SCCHN [4, 24]. In all cases, STAT3 and/or STAT5 are also overexpressed, and STAT1 may be antagonizing the oncogenic activity of these proteins.

2.1.4 Rationale and hypotheses

Based on the presence of STAT1/3 heterodimers, the sequence homology between STAT1 and STAT3, as well as the overexpression of both proteins in SCCHN cell lines, we investigated the ability of the STAT1 pathway to mitigate the antiproliferative effects of the STAT3 decoy. We hypothesized that the STAT3 decoy inhibits STAT1 signaling, and that decreased STAT1 levels would have no effect on STAT3 decoy-mediated antitumor effects. In addition, stimulation of the STAT1 pathway would not mitigate the antitumor effects of the STAT3 decoy in SCCHN.

2.2 MATERIALS AND METHODS

2.2.1 Chemicals and reagents

Phospho-STAT1 (Tyr701), STAT1, and STAT3 antibodies were purchased from Cell Signaling Technology (Danvers, MA). The IRF-1 antibody and Enhanced Chemiluminescence (ECL) kit were purchased from Santa Cruz Biotechnology (Santa Cruz, CA). Beta actin antibody was obtained from Oncogene Science (San Diego, CA). Beta-tubulin antibody was purchased from Abcam (Cambridge, MA). Optifect transfection reagent, fetal calf serum, penicillin/streptomycin solution, and Opti-MEM[®]I Media were purchased from Invitrogen (Carlsbad, CA). Human recombinant IFN- γ was obtained from Roche Applied Science (Indianapolis, IN).

2.2.2 Cell culture

The SCCHN cell lines UM-22A, UM-22B, PCI-15B, 1483, and PCI-37A cells [92] were of human origin and maintained in DMEM with 10% heat-inactivated fetal calf serum and 1X penicillin/streptomycin mix (both from Invitrogen, Carlsbad, CA) at 37°C with 5 % CO₂. STAT1 knockout cells, the human fibroblast U3A cell line, were provided by Dr. Jacqueline Bromberg (Memorial Sloan Kettering Cancer Center, New York, NY) and cultured in DMEM containing 10% Cosmic Calf Serum (Hyclone, Logan, UT) and 1X Penicillin/Streptomycin mix at 37°C with 5 % CO₂ [93]. STAT3 knockout and wild-type mouse embryonic fibroblasts [94] were provided by Dr. David Levy (NYU School of Medicine, New York, NY) and were maintained in DMEM with 10 % heat-inactivated fetal calf serum (Invitrogen, Carlsbad, CA)

and 1X penicillin/streptomycin mix (Invitrogen, Carlsbad, CA) at 37°C with 5 % CO₂. STAT5A/B knockout and wild-type mouse embryonic fibroblasts [95] provided by Dr. James Ihle (St. Jude Children's Research Hospital, Memphis TN) were grown in DMEM with 10% heat-inactivated fetal calf serum and 1X Penicillin/Streptomycin mix at 37°C with 5 % CO₂.

2.2.3 Preparation and transfection of STAT3 decoy and mutant control decoy

STAT3 decoy (5'-CATTTCCTCGTAAATC-3' and 3'-GTAAAGGGCATTTAG-5') and the mutant control sequence (5'-CATTTCCTTAAATC-3' and 3'-GTAAAGGGAATTAG-5') were generated as previously described [53, 54]. The single-stranded sense and antisense oligonucleotides were synthesized and purified by means of β -cyanoethylphosphoramidite chemistry to minimize degradation of the oligonucleotides by endogenous nucleases by the DNA Synthesis Facility at the University of Pittsburgh (Pittsburgh, PA). Equal amounts of sense and antisense STAT3 decoy or mutant control decoy oligonucleotides were combined with TE buffer pH 8.0, and boiled for 5 mins. The denatured oligonucleotides were then annealed by cooling to room temperature over 2-3 hrs, then stored at -20°C.

For transfections, UM-22B or PCI-15B cells were plated to approximately 60-70% confluency and Opti-MEM[®]I Media containing the STAT3 decoy or mutant control with Optifect transfection reagent was added and incubated at 37°C with 5% CO₂ for 4h. Fresh DMEM containing 10% heat-inactivated fetal bovine serum and 1X Penicillin/Streptomycin mix was then added.

2.2.4 siRNA transfections

STAT1 siRNA SMART pool and STAT3 On-Target Plus SMART pool siRNA were purchased from Dharmacon (catalog numbers MU-003543-01 and L-003544-00, respectively). 1200 pmoles STAT1 siRNA was transfected into UM-22B or PCI-15B cells in T-75 flasks using Optifect according to manufacturer's instructions in Opti-MEM[®]I Media (Invitrogen, Carlsbad, CA) for 4 hrs. Media was then changed to DMEM + 10%FBS and 1X penicillin/streptomycin.

2.2.5 Western blotting

Cells were lysed in lysis buffer (1 % Nonidet-P40, 150 mM NaCl, 1 mM EDTA, 10 mM sodium phosphate buffer (pH 7.2), 0.25 mM DTT, 1 mM PMSF, 10 µg/ml leupeptin and 10 µg/ml aprotinin) for 30 mins at 4°C with rotation, scraped and transferred into microfuge tubes, and sonicated. The lysates were then centrifuged at 13,200 rpms for 5 mins at 4°C. 50-40 µg of whole cell protein lysate was combined with 4X loading dye, boiled 5 minutes, and loaded onto a 8% or 10% polyacrylamide gels and proteins were separated at 125V. Proteins were transferred onto nitrocellulose membrane using a semi-dry transfer apparatus for 50 min at 19V. The membrane was then blocked in 5% milk, 0.2 % Tween 20 in PBS (TBST) and then incubated in primary antibody diluted in 1% milk (beta actin, beta tubulin, pSTAT1, STAT1, STAT3, or IRF-1 antibodies). The membrane was then washed 4 times in TBS-T for 5 mins each, followed by incubation with appropriate secondary antibody diluted in 1% milk. After the membrane was washed 4 times in TBS-T for 5 mins each signals were visualized using the ECL kit (Santa Cruz Biotechnology).

2.2.6 Cell counting

Cell counting experiments were performed using trypan blue dye exclusion assay. Cells were trypsinized and after lifting off of the plate, trypsin was neutralized with DMEM. Cells were centrifuged and cell pellets were resuspended in fresh media. Cells were then combined with trypan blue and counted using a hemacytometer. The percent survival was then calculated relative to the untreated control.

2.2.7 MTT Assay

MTT (3-(4, 5-dimethylthiazol-2-yl)-2,5-diphenyltetrazolium bromide) assays were performed to determine the cell viabilities. Media was removed from the culture plates and replaced with 5 mg/ml MTT (Sigma, Catalog # M5655) and incubated at 37°C, 5% CO₂ for 15 min. MTT reagent was removed and dimethyl sulfoxide (DMSO) was added to lyse the cells. Plates were then read in a plate reader at 595 nm. Data was normalized to untreated control cells and the equation to calculate the percentage survival is $(OD_{\text{experimental}} / OD_{\text{untreated}}) \times 100\%$.

2.2.8 Statistics

Statistical analyses were performed using StatXact software (Cytel Software Corporation, Cambridge, MA) and p-values were obtained by the nonparametric Wilcoxon-Mann-Whitney test when comparing two groups or the Kruskal-Wallis test when comparing more than two groups ($p < 0.05$ was considered significant).

2.3 RESULTS

2.3.1 STAT1 pathway is intact in SCCHN cells

To determine that the STAT1 pathway is intact in SCCHN cell lines, we serum starved UM-22B cells for 48 hrs, followed by treatment with IFN- γ (200 U/ml) for 0 min, 10 min, 30 min, 4 hrs, 10 hrs, or 24 hrs in serum free DMEM to stimulate the STAT1 pathway (Figure 5). Whole cell lysates were prepared and 50 μ g of lysate/lane was immunoblotted for phospho-STAT1 (Tyr 701), total STAT1, and a STAT1 target gene, IRF-1. Beta actin was used as a loading control. Increased phosphorylation of STAT1 was observed as early as 10 mins, and began to decrease between 4 and 24 hrs. Expression of IRF-1 was also increased by 4 hrs after STAT1 stimulation. STAT1 protein levels were not altered by IFN- γ .

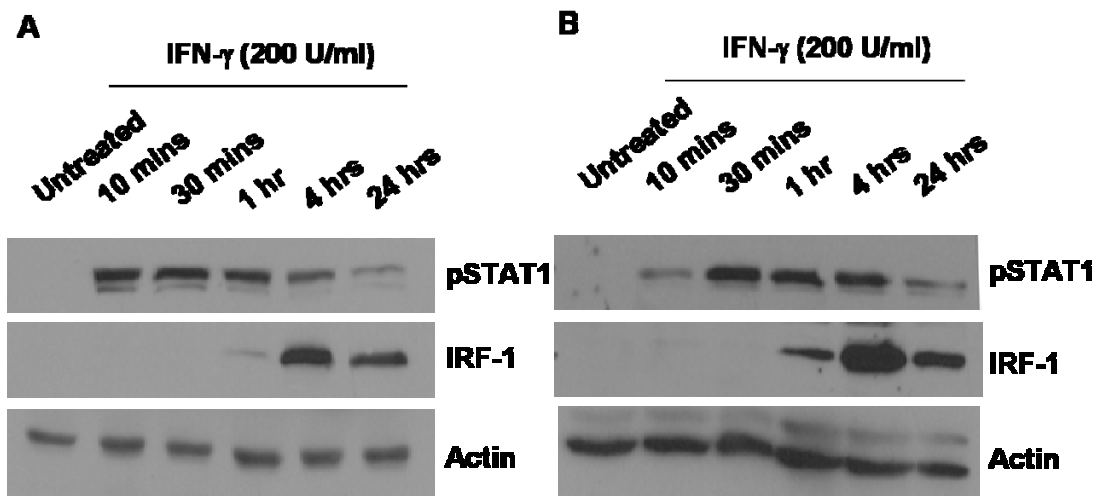


Figure 5. Time course of IFN- γ stimulation of SCCHN cells.

(A) UM-22B or (B) PCI-15B cells were serum starved for 48 hrs, then stimulated with IFN- γ (200U/ml) for 10 min, 30 min, 1 hr, 4 hrs, or 24 hrs. 50 μ g cell lysate were immunoblotted for phospho-STAT1 (Tyr701), IRF-1, or actin (loading control).

Additionally, UM-22B or PCI-15B cells were stimulated with increasing amounts of IFN- γ for 4hrs before lysates were collected and immunoblotted for IRF-1. Figure 6 shows a dose-dependent increase in STAT1 phosphorylation and IRF-1 protein. These results indicate that the STAT1 pathway functions in response to IFN- γ stimulation through the activation of STAT1 and subsequent expression of a known STAT1 target gene, IRF-1.

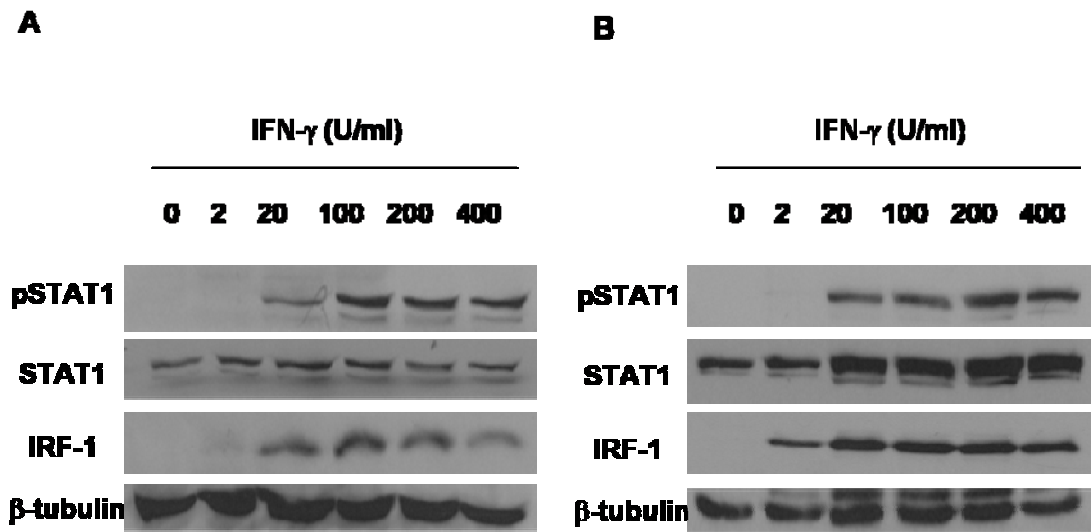


Figure 6. Dose-dependent induction of pSTAT1 by IFN- γ in SCCHN cells.

(A) UM-22B or (B) PCI-15B cells were serum starved for 48 hrs, then stimulated for 24 hrs with IFN- γ (0, 2, 20 100, 200 or 400 U/ml). 50 μ g cell lysate were immunoblotted for phospho-STAT1 (Tyr701), STAT1, IRF-1, or beta-tubulin (loading control).

2.3.2 SCCHN cell lines express STAT1 and STAT3 and are sensitive to STAT3 decoy-mediated cell death

Lysates from a panel of SCCHN cell lines including PCI-37A, 1483, PCI-15B, UM-22A, and UM-22B were prepared and 50 μ g of protein/lane was run on an 8% polyacrylamide gel,

transferred to nitrocellulose membrane, and probed for total STAT1 or STAT3 protein levels (Figure 7A). Beta tubulin served as a loading control. We found that the SCCHN cell lines, had similar levels of STAT1 or STAT3 protein. The experiment was performed three times and densitometric analysis was performed, normalizing STAT1 or STAT3 protein expression to the loading control (Figure 7B). There was no significant difference between either STAT1 or STAT3 protein expression across the five SCCHN cell lines examined ($p=0.06$ and $p=0.81$, respectively).

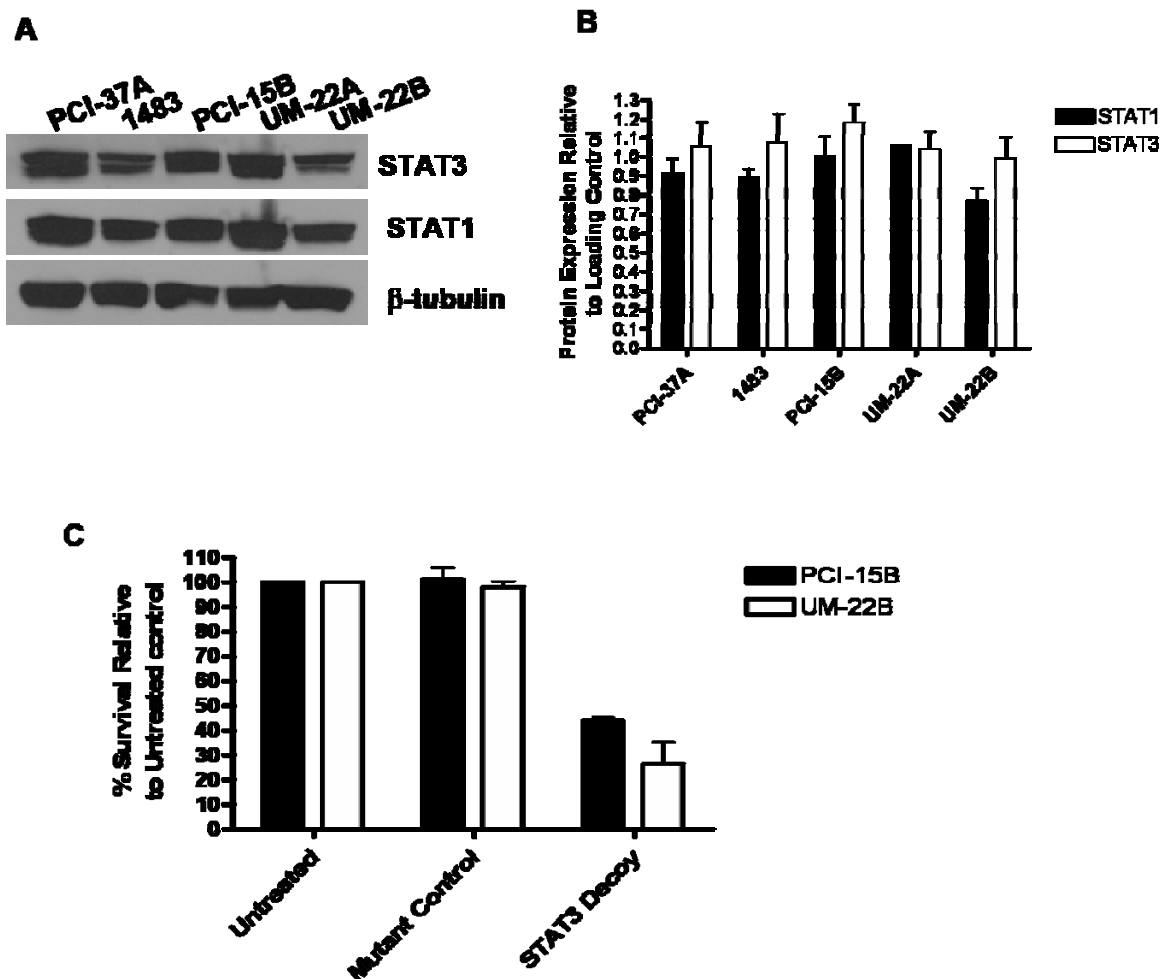


Figure 7. STAT1 levels do not correlate with SCCHN growth inhibition by the STAT3 decoy.

(A) Lysates from SCCHN cells (PCI-37A, 1483, PCI-15B, UM-22A, and UM-22B) were immunoblotted for STAT1, STAT3, or beta tubulin to assess expression levels of STAT1 and STAT3. (B) Densitometric analysis was performed and Kruskal Wallis test was performed and determined there was no significant

difference in either STAT1 or STAT3 protein levels in these cell lines ($p=0.06$ and $p=0.81$, respectively). (C) UM-22B or PCI-15B cells were transfected with 690 pM STAT3 decoy or the mutant control decoy and trypan blue dye exclusion was used to determine cell survival after 24 hrs. Experiment was performed three times with similar results.

UM-22B and PCI-15B cells were transfected with 690 pM STAT3 decoy or mutant control decoy, and viable cell counting was performed after 24 hrs to assess survival (Figure 7C). The STAT3 decoy treatment resulted in 26.4% ($\pm 8.95\%$) survival in UM-22B cells and 43.9% ($\pm 1.42\%$) survival in PCI-15B cells relative to the untreated control. These results indicate that SCCHN cells are sensitive to the growth inhibitory effects of the STAT3 decoy.

2.3.3 Stimulation of the STAT1 pathway does not mitigate STAT3 decoy-mediated antitumor effects in SCCHN cell lines.

To investigate if the activation of the STAT1 pathway mitigates the antitumor effects of the STAT3 decoy, UM-22B and 1483 cells were treated with the STAT3 decoy or mutant control (100 pM) in the presence or absence of IFN- γ (200 U/ml) for 4 hrs. Media was changed to fresh DMEM and lysates were collected after 24 hrs and immunoblotted for IRF-1 and β -tubulin (loading control) (Figure 8A and 8B). The experiment was repeated four times, and densitometry was performed on the immunoblots and showed a significant decrease in IRF-1 protein expression relative to loading control when the STAT3 decoy was added in the presence of IFN- γ ($p=0.0143$ for UM-22B or 1483 cells) (see Figure 8C and 8D). Additionally, MTT assays were performed and IFN- γ treatment did not decrease STAT3 decoy-mediated growth inhibition in either UM-22B or PCI-15B cells (Figure 8E and 8F).

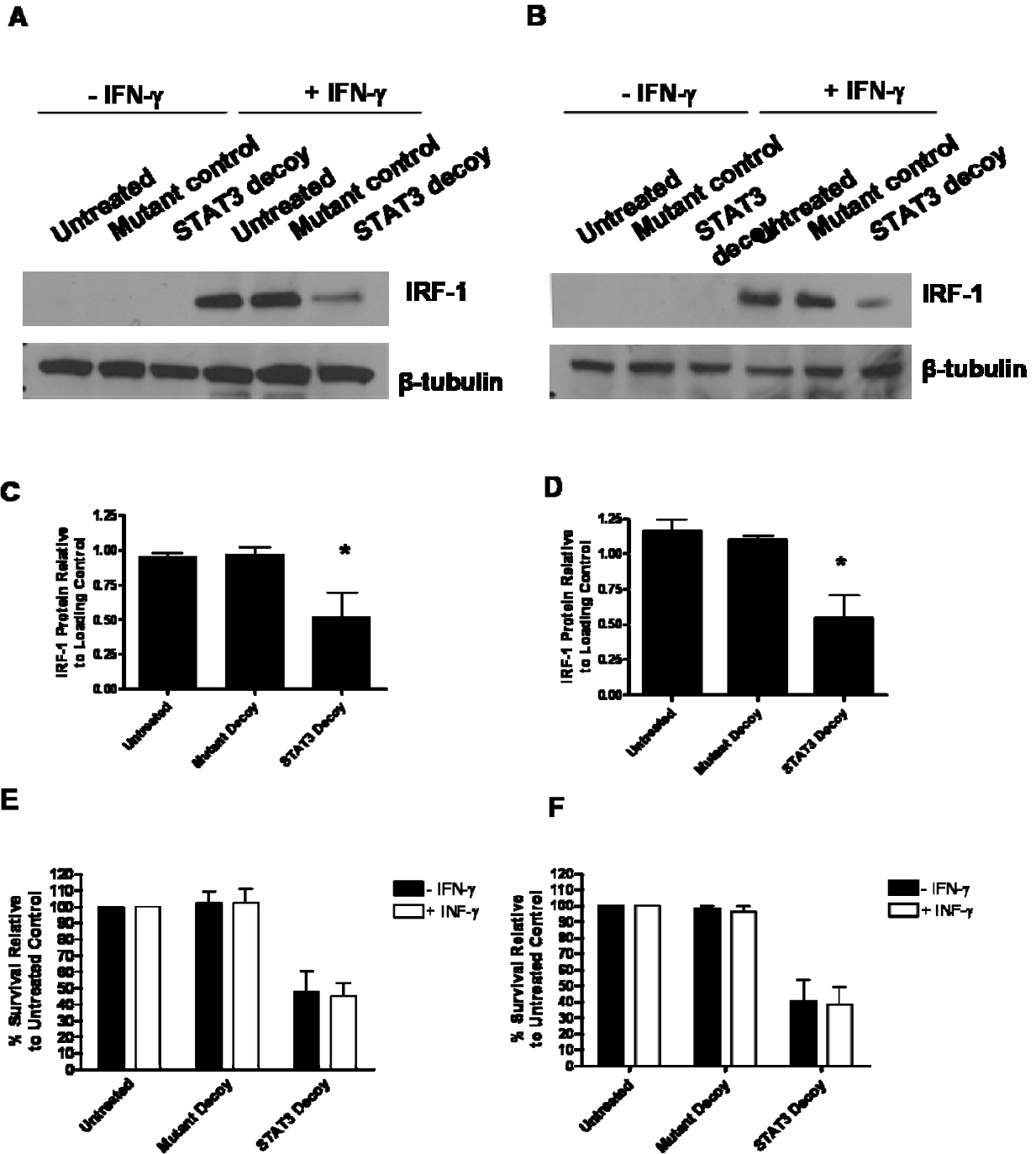


Figure 8. STAT3 decoy mediated inhibition of the STAT1 pathway or growth inhibition is not abrogated by stimulation with IFN- γ in SCCHN cell lines.

UM-22B or 1483 cells were transfected with 100 pM STAT3 decoy or mutant control decoy in the presence or absence of IFN- γ (200U/ml) for 4 hrs. Media was then changed to DMEM (10% FBS, P/S) and (A) UM-22B lysates or (B) 1483 were collected after 24 hrs for immunoblotting for IRF-1 and β -

tubulin. Densitometry was performed on the (C) UM-22B or (D) 1483 samples treated with IFN- γ , with IRF-1 protein levels normalized to the β -tubulin loading control (*p=0.0143) after the experiment had been performed four times. MTT assays were performed three times for both (E) UM-22B and (F) 1483 cells.

2.3.4 STAT1 siRNA down-regulates STAT1 protein expression and signaling in SCCHN cells.

We chose an siRNA approach to downmodulate STAT1 protein levels in SCCHN cells to investigate the role of STAT1 in the STAT3 decoy antitumor mechanism. siRNA transfection was optimized and the effects on protein expression, growth, and signaling were investigated. Pooled STAT1 siRNA (Dharmacon) was transfected into UM-22B or PCI-15B cells using Lipofectamine 2000 (Invitrogen), and cell lysates were collected at various time points (days 2 through 7). GFP siRNA was used as a negative control in these experiments. The lysates were immunoblotted for STAT1 protein and a marked decrease in STAT1 protein levels was observed from day 2 through 7 (beta tubulin served as the loading control) (Figure 9A and 9B). Growth curves were constructed for the siRNA-transfected UM-22B or PCI-15B cells and showed that STAT1 siRNA increased cell growth relative to the GFP siRNA transfected control cells (Figures 9C and 9D). The siRNA-transfected cells were also stimulated with IFN- γ for 4 hrs. Cell lysates were collected after 24 hrs and immunoblotted for STAT1, IRF-1, and beta-tubulin. STAT3 siRNA transfected cells were also treated and immunoblotted for STAT3, IRF-1, and beta-tubulin as an additional control. The immunoblots show that STAT1 siRNA (but not GFP or STAT3 siRNA) mitigates IFN- γ -induced IRF-1 protein expression in both UM-22B cells (Figures 9E).

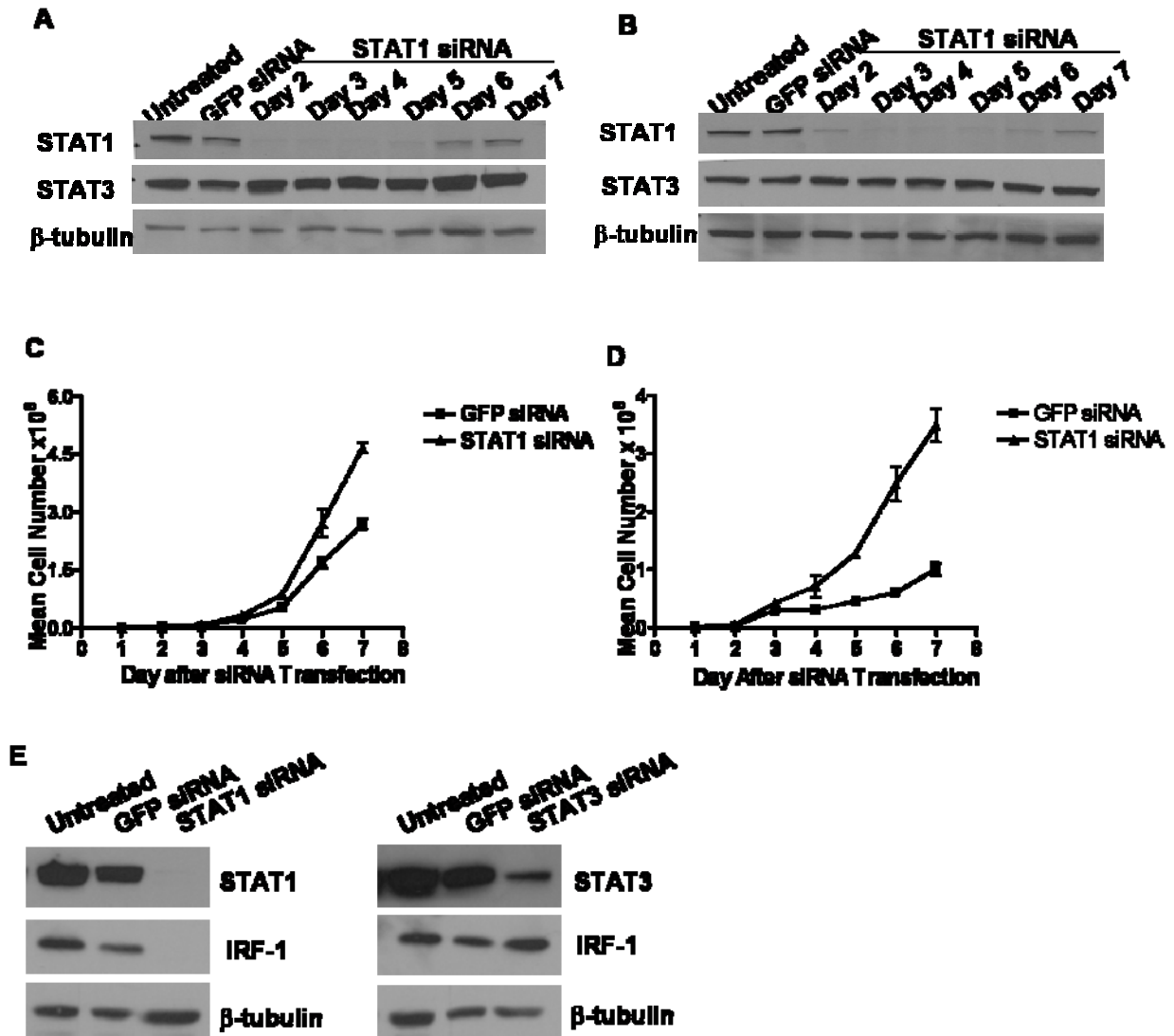


Figure 9. STAT1 siRNA downmodulates total STAT1 protein levels, increases proliferation, and decreases STAT1 signaling.

Pooled STAT1 siRNA was transfected into (A) UM-22B or (B) PCI-15B cells and protein lysates were from day 2 through days 7 after transfection were immunoblotted for STAT1, STAT3, or β -tubulin (loading control). The experiment was performed three times with similar results. Growth of (C) UM-22B or (D) PCI-15B cells transfected with either GFP siRNA or STAT1 siRNA. 20,000 or 10,000 cells, respectively, were plated for cell counting 24 hrs after siRNA transfections. Cell counts were taken for 7 days using trypan blue dye exclusion. The experiment was performed two times. (E) UM-22B cells transfected with GFP siRNA (control), STAT3 siRNA (control) or STAT1 siRNA were stimulated with IFN- γ (200U/ml) for 4 hrs. Lysates were collected after 24 hrs and probed for STAT1, STAT3, IRF-1, or β -tubulin (loading control).

2.3.5 Downmodulation of STAT1 does not mitigate the antiproliferative effects of the STAT3 decoy

We next investigated the potential contribution of STAT1 to the STAT3 decoy-mediated antitumor mechanism using an siRNA approach. STAT1 siRNA or GFP siRNA (control) was transfected into UM-22B or PCI-15B cells in T-75 flasks. Twenty-four hours after siRNA transfection, cells were trypsinized and replated in 24-well plates for transfection with either the STAT3 decoy or mutant control decoy and cell survival was assessed after 72 hrs using MTT assay. In UM-22B cells, treatment with the STAT3 decoy resulted in 54.2 % (\pm 0.8 %) survival in GFP siRNA transfectants, and 59 % (\pm 3.9 %) in STAT1 siRNA transfectants (Figure 10A). The mutant control decoy resulted in 100.4 % (\pm 1.8 %) and 111.6 % (\pm 2.0 %) survival and there was no significant difference in cell viability of STAT3 decoy transfected STAT1 siRNA cells or GFP siRNA cells (Figure 10A and 10B).

These results were also confirmed in a STAT1 knockout human fibroblast cell line (U3A) (Figure 10C). STAT1 knockout human fibroblasts were transfected with 1026 pM STAT3 decoy and resulted in 31.2 % (\pm 4.0 %) cell survival which did not significantly differ from that of wild-type mouse embryonic fibroblasts which served as a control in the experiment (35.7 % (\pm 7.0 %) survival) ($p=0.5$). These results from both UM-22B and PCI-15B cells indicate that down-regulation of STAT1 protein levels does not alter STAT3 decoy antiproliferative effects.

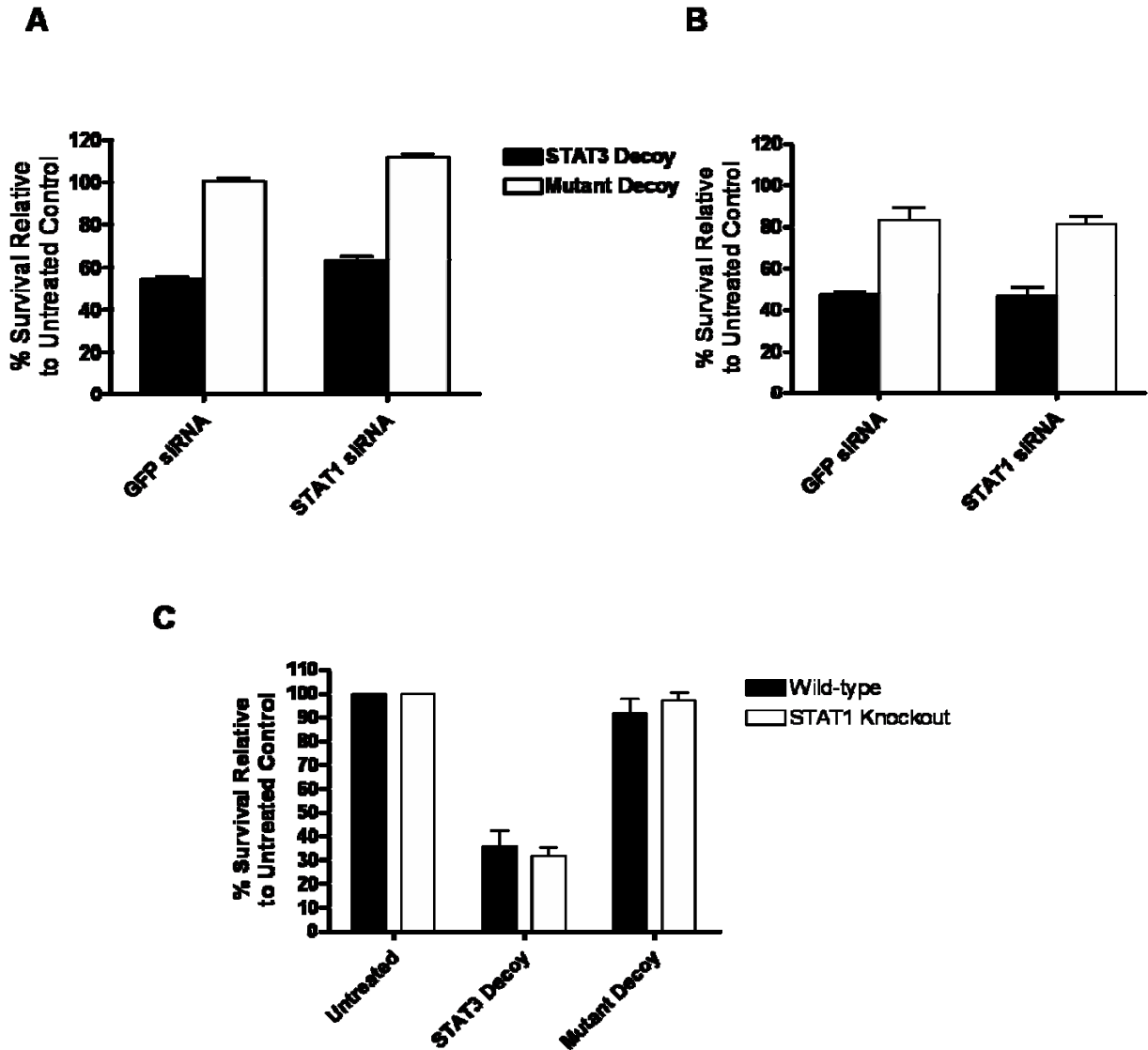


Figure 10. Downmodulation of STAT1 protein does not alter decreased cell viability mediated by the STAT3 decoy in SCCHN cells.

Cell viability of STAT1 siRNA transfected cells treated with the STAT3 decoy or GFP siRNA transfected control UM-22B cells was assessed 72 hrs after decoy transfection using MTT assay in **(A)** UM-22B or **(B)** PCI-15B cells. **(C)** STAT1 knockout cells (U3A cell line) or wild-type MEFs were transfected with 1026 pM STAT3 decoy or mutant control decoy. Cell counts using trypan blue dye exclusion assay were performed after 24 hrs. Data above represent the cumulative results from three independent experiments.

2.3.6 Characterization of STAT1 and STAT3 protein expression in STAT3 knockout and wild-type mouse embryonic fibroblast cell lines

Next, we wanted to determine if STAT3 is necessary for the growth inhibitory effects of the STAT3 decoy. STAT3 or STAT5 knockout or wild-type mouse embryonic fibroblasts (MEFs) were obtained and STAT protein expression and cell growth were first examined. Cell lysates from STAT3 knockout or wild-type MEFs were immunoblotted for STAT1, STAT3, or beta tubulin (loading control). STAT3 knockout MEFs expressed STAT1 at a comparable level to that of the wild-type MEFs (Figure 11A). The rate of growth of these cell lines was also investigated. The wild-type and STAT3 knockout cell lines were plated in 6-well plates and cell counts were performed using trypan blue dye exclusion at days 1 through 5. The STAT3 and STAT5 knockout MEFs were found to grow at a slower rate compared to the wild-type cells (Figure 11B and 11C). STAT1 and STAT3 protein expression was previously reported to be intact in STAT5 knockout and wild-type cells [95].

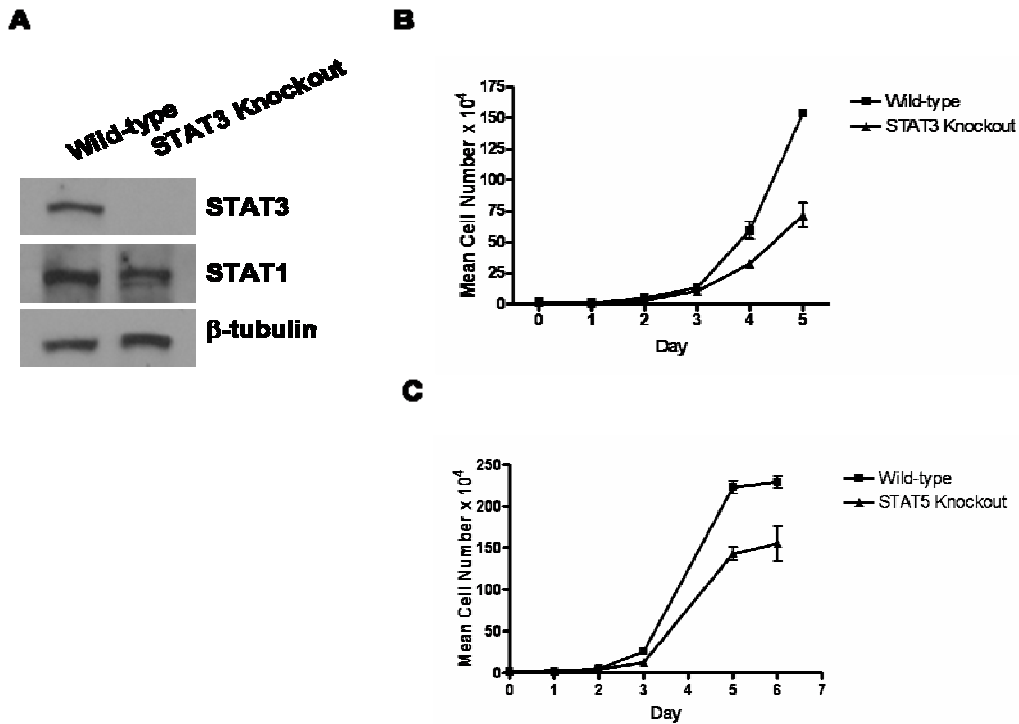


Figure 11. Characterization of STAT3 or STAT5 knockout and wild-type MEFs.

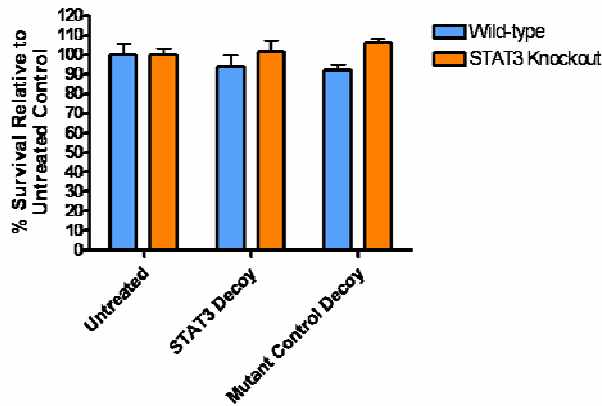
(A) Lysates from STAT3 knockout and wild-type MEFs were immunoblotted to determine that STAT1 protein expression was intact. (B) STAT3 knockout and wild-type MEFs were plated in 6-well plates and cell counts were performed at days 1 through 5 using trypan blue dye exclusion to investigate the growth of these cell lines. (C) Growth curves were also obtained for STAT5 knockout and wild-type MEFs with similar results.

2.3.7 STAT3 is necessary for the antiproliferative effects mediated by the STAT3 decoy

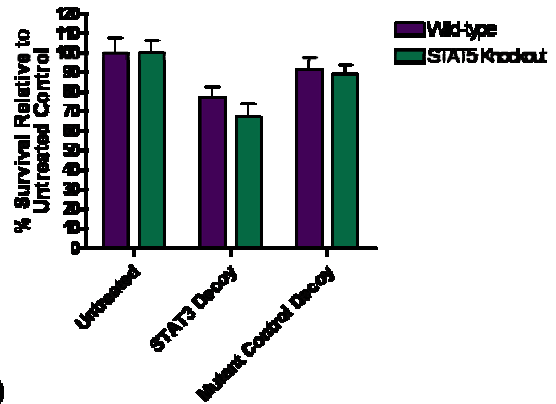
To determine if STAT3 is necessary for STAT3 decoy-mediated cell growth inhibition, STAT3 or STAT5 knockout and wild-type MEFs were transfected with 1026 pM or 102.6 pM STAT3 decoy or mutant control decoy and cell counts using trypan blue dye exclusion were performed after 24 hrs. Survival of the STAT3 knockout cells was unaffected after transfection with 1026 pM of STAT3 decoy, in contrast to the STAT3 wild-type cells, STAT5 knockout

cells, and STAT5 wild-type MEFs whose survival was dramatically decreased upon treatment with 1026 pM of the STAT3 decoy compared to the mutant control decoy (Figure 12C and 12D). Because MEFs express comparatively normal levels of STAT3 compared to SCCHN cell lines, in order to observe a decrease in cell viability, 10X the concentration of STAT3 decoy sufficient to decrease proliferation in SCCHN cells (1026 pM) was transfected into the MEFs. At 102.6 pM, there was no decrease in cell viability compared to the mutant control decoy in any of the four MEF cell lines used (Figure 12A and 12B).

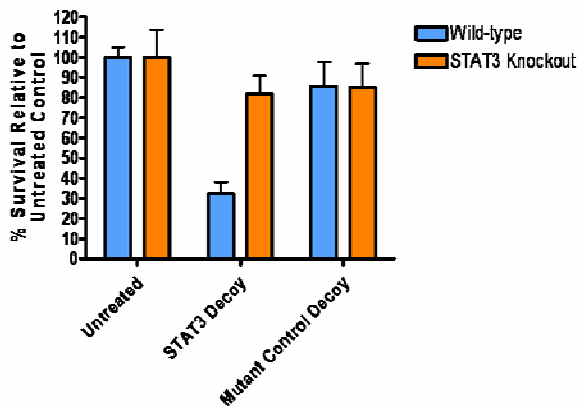
A



B



C



D

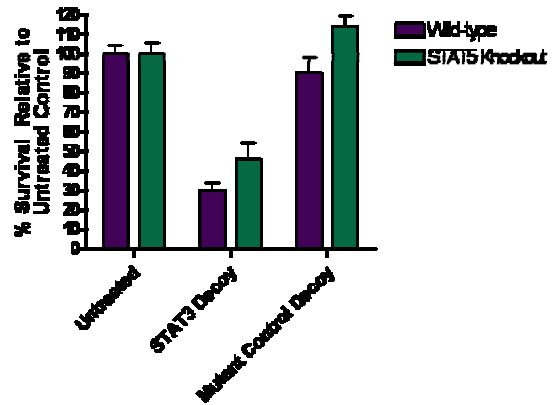


Figure 12. STAT3 but not STAT5 is necessary for STAT3 decoy-mediated decrease in cell survival.

(A) STAT3 knockout or wild-type MEFs or (B) STAT5 knockout or wild-type MEFs were transfected with 102.6 pM STAT3 decoy or mutant control decoy and cell counts were performed using trypan blue dye exclusion after 24 hrs. The experiments were also repeated using 1026 pM STAT3 decoy or mutant control decoy in the (C) STAT3 knockout or wild-type MEFs or the (D) STAT5 knockout or wild-type MEFs. The experiment was independently performed three times.

2.4 DISCUSSION

Our studies have previously focused on the antitumor activity of the STAT3 decoy in both *in vitro* and *in vivo* models of SCCHN [53, 54]. Others have reported that direct injection of the STAT3 decoy into skin tumors in a mouse model of epithelial cancer inhibited tumor growth [56]. The STAT3 decoy was also used to treat mice with psoriatic lesions induced by constitutive activation of STAT3 [55]. Sano *et al.*, found that the STAT3 decoy prevented the onset of psoriatic lesions and induced the regression of established lesions, providing evidence for STAT3 as a target in the treatment of psoriasis, and indicating that the STAT3 decoy could be an efficacious treatment for psoriasis patients.

To date, published reports using the STAT3 decoy have focused on its efficacy as a clinical therapy, assuming that STAT3 is the only target inhibited, leaving the exact mechanism of the STAT3 transcription factor decoy undefined [53-56]. To further elucidate the mechanism of the STAT3 decoy, the role of STAT1 and STAT3 in the STAT3 decoy-mediated antitumor mechanism in SCCHN was explored. The STAT3 transcription factor decoy was designed to bind to the DNA binding domain of STAT3, a known oncogene whose overexpression has been

correlated with poor clinical prognosis, decreased survival, and increased resistance to chemoradiation. We investigated the role of STAT1 in the mechanism of the STAT3 transcription factor decoy because of the high sequence homology in the DNA binding domain of STAT3 and STAT1, the presence of STAT1/3 heterodimers, and because both STAT1 and STAT3 are expressed in SCCHN cell lines. Also STAT1 has demonstrated the ability to function as a tumor suppressor in some malignancies [8, 19, 96-98], leading us to hypothesize that STAT1 may play a role in mediating the STAT3 decoy antitumor effects observed in SCCHN preclinical models. We found that although the STAT3 decoy inhibited the STAT1 pathway, STAT1 does not contribute to or mitigate STAT3 decoy-mediated antitumor effects. The role of STAT1 in cancer is unclear. Classified as a tumor suppressor, STAT1 is essential for interferon signaling and regulates cell death through transcription of caspases, death receptors and ligands, as well as cell cycle regulators such as p21^{waf1} [99]. Yet, a recent report described a role for STAT1 as a tumor promoter in leukemia [100]. STAT1 is involved in the expression of MHC class I molecules, which have been postulated to play a role in tumor cell evasion of the immune system. This study provided evidence for a model in which high MHC class I molecule expression protected tumor cells from elimination by the immune system and was a direct result of STAT1 activity.

In regards to SCCHN, we previously reported that STAT1 overexpression has been shown to induce increased sensitivity to chemotherapy in SCCHN [98]. In a syngeneic model murine squamous cell carcinoma, STAT1 deficiency in the host enhanced interleukin-12-mediated tumor regression [101]. It is possible that STAT1 functions as a tumor suppressor during the early stages of tumor initiation, and not during the progression of cancer after tumor cells are established. Therefore, inhibition of STAT1 activity by the STAT3 decoy in cancer cell

lines may not have an effect on proliferation. To investigate this, future studies could be performed to determine if STAT1 inhibition via the STAT3 decoy prevents tumor cell initiation using cancer prevention models.

Transcription factor decoys were initially used to investigate transcription factor mediated-gene expression [102, 103]. Since then, several transcription factor decoys targeting proteins shown to play a role in malignancy and other diseases [53, 54, 58, 60, 62, 66, 68-78]. Both STAT1 and STAT3 have been shown to interact with other proteins and transcription factors. For example, STAT1 binds to the TNF α receptor signaling complex and inhibit NF- κ B [104] and STAT1 binding to p53 has also been demonstrated [105]. Also, studies have documented that STAT3 interacts with other factors including PIAS3, GRIM-19 and EZ1 [106-108]. To date, the effects of a transcription factor decoy on other transcription factors or binding partners has not been explored. The ability of the decoy to inhibit activity of STAT1 in addition to its intended effects on inhibiting STAT3 raises the possibility that the STAT3 decoy may have actions beyond inhibiting STAT3 in cancer cells. This could potentially limit its use as a therapeutic reagent. Conversely, because transcription factors are known to function in large multiprotein complexes consisting of multiple regulatory proteins, co-factors and related DNA elements, use of a transcription factor decoy may be advantageous because it simultaneously inhibits multiple proteins in the transcription complex. These findings provide a rationale for similar mechanistic studies of other transcription factor decoys, prior to their entering the clinic.

Because the previous experiments determined that STAT1 neither contributes to nor mitigates STAT3 decoy-mediated antitumor effects, we hypothesized that STAT3 is the main target of the STAT3 decoy and is necessary for growth inhibitory effects. Both STAT3 knockout MEFs, STAT5 knockout MEFs, and wild-type MEFs were first characterized in regards to

STAT1 and STAT3 protein expression, and rate of growth in culture (Figure 11). The STAT3 and STAT5 knockout MEFs grew at a slower rate compared to the wild-type control MEFs, indicating that STAT3 and STAT5 contribute to growth and proliferation in these cell lines, but loss of either STAT3 or STAT5 protein does not kill the cells. Other published reports using these cell lines have not investigated alterations in cell growth, but have focused on changes in signaling and other phenotypical aspects of the cells [94, 95]. Based on results from cell survival assays, we found that STAT3 but not STAT5 was necessary for STAT3 decoy mediated decrease in survival (Figure 12). These results indicate that STAT3 is indeed the main target of the STAT3 decoy and further confirm the rationale for STAT3 as a therapeutic target in SCCHN.

3.0 COMBINING THE STAT3 DECOY WITH AN EGFR AND/OR A BCL-X_L INHIBITOR ENHANCES ANTITUMOR EFFECTS IN PRECLINICAL MODELS OF SCCHN

3.1 INTRODUCTION

3.1.1 EGFR

Epidermal growth factor (EGFR), also known as erbB1 or Her1, is a transmembrane protein tyrosine kinase receptor that mediates signal transduction and is critical for many metabolic and physiological cellular processes [109]. EGFR is a 170kd protein consisting of an extracellular ligand binding domain, a transmembrane domain, and an intracellular domain containing protein tyrosine kinase activity [110]. Ubiquitously expressed in normal epithelial tissues, EGFR activity is regulated by extracellular ligand binding including TGF- α , EGF, amphiregulin, and heparin binding EGF, which results in receptor homodimerization or heterodimerization and trans-phosphorylation of tyrosine residues in the carboxy-terminal domain of the receptors. EGFR signals through a number of different signaling pathways, including activation of Ras/mitogen-activated protein kinase (Ras/MAPK), phospholipase C- γ , phosphatidylinositol-3 kinase (PI3K), and STATs. Phospho-tyrosine binding proteins bind to activated EGFR, are phosphorylated on tyrosine residues and activated in order to perpetuate downstream signaling.

3.1.1.1 EGFR overexpression and mutation in SCCHN

EGFR and its ligand TGF- α are overexpressed in 80-90% of SCCHN tumors, implicating an autocrine regulatory pathway in carcinogenesis of the disease [111]. EGFR overexpression has been identified as an independent prognostic marker in SCCHN, and high EGFR levels correlate with poor advanced stage, increased tumor size, resistance to chemotherapy and radiation, increased recurrence, and decreased survival [28, 112].

Somatic mutations in the EGFR tyrosine kinase domain have been reported to confer increased sensitivity to EGFR targeting tyrosine kinase inhibitors (TKIs) in lung cancer [113, 114]. However, the somatic mutation rate in SCCHN is low compared to other epithelial malignancies and evidence suggests EGFR mutation status is unrelated to sensitivity to TKIs in SCCHN [115-117]. Recently, EGFRvIII, an EGFR mutant in glioma was reported in SCCHN [118]. This truncated mutant protein has a portion of the extracellular domain deleted, resulting in a constitutively active form of the receptor that studies have shown is only present in cancer cells. Because of this deletion, EGFRvIII function is independent of ligand binding. EGFRvIII has been found in brain, lung, prostate, and ovary cancer, and SCCHN [119]. In one study, EGFRvIII was found in 42% SCCHN tumors examined, and cell lines expressing the mutated protein demonstrated decreased sensitivity to an EGFR monoclonal antibody (cetuximab) [118].

3.1.2 EGFR as a therapeutic target for SCCHN

EGFR targeting using EGFR antisense gene therapy, monoclonal antibodies, or tyrosine kinase inhibitors in SCCHN preclinical models results in antitumor effects [120]. Furthermore, EGFR is overexpressed in SCCHN tumors and this overexpression correlates with patient survival, making EGFR a therapeutic target for SCCHN [28]. Several strategies to block EGFR

activity have been developed and include down-regulation of EGFR expression, inhibition of EGFR activation and/or phosphorylation, and inhibition of downstream signaling. Studies have focused on using a variety of inhibitors including toxin conjugates, antisense oligonucleotides, EGFR monoclonal antibodies (mAbs), or TKIs [109] (Table 3).

3.1.2.1 Monoclonal antibodies

Cetuximab (Erbix[®], C225; Imclone Systems), a monoclonal antibody specific for EGFR, was approved by the FDA for the treatment of unresectable SCCHN in combination with radiation and as a monotherapy for the treatment of platinum-based therapy-resistant SCCHN in 2006 [121]. However, cetuximab has resulted in limited efficacy as a monotherapy for SCCHN in the clinic [122]. Cetuximab is a mouse-humanized antibody specific for EGFR that competes with ligand and blocks ligand-induced activation of EGFR, induces receptor dimerization and subsequent receptor down-regulation [123-125]. Prior to FDA approval, studies documented antitumor effects in SCCHN preclinical models alone [126] or in combination with chemotherapeutic drugs such as cisplatin, paclitaxel or 5-fluorouracil [127, 128], or with radiation [129]. Several other EGFR antibodies have been developed and are currently undergoing investigation for treatment of SCCHN, including matuzumab (EMD7200) [130], panitumumab (ABX-EGF) [131, 132], and TheraXIM (hR3) [133].

Table 3. Summary of EGFR inhibitors studied for SCCHN.

EGFR inhibitors have reached various stages of development for SCCHN, from FDA approval to preclinical studies in progress and are listed below.

Inhibitor	Strategy	Phase of Development	References
Cetuximab (Erbix [®] , C225)	Chimeric mouse-humanized anti-EGFR antibody	FDA approved 2006 for SCCHN	[121-123, 125-129]
Gefitinib (Iressa [™] , ZD1839)	TKI	FDA approved in 2003 for locally advanced or metastatic NSCLC* Phase II for SCCHN	[134, 135]
Erlotinib (Tarceva [™] , OSI-779)	TKI	FDA approved in 2004 for locally advanced or metastatic NSCLC FDA approved in 2005 for pancreatic cancer in combination with gemcitabine Phase II for SCCHN	[136, 137]
Matuzumab (EMD-72000)	Humanized anti-EGFR antibody	Phase II for SCCHN	[130]
TheraXIM (hR3)	Humanized anti-EGFR antibody	Phase II for SCCHN	[133]
U6 promoter-driven EGFR AS	EGFR antisense gene therapy	Phase I for SCCHN	[138-142]
Panitumumab (ABX-EGF)	Human anti-EGFR monoclonal antibody	Preclinical for SCCHN	[131, 132]
Pseudomonas toxin-EGFR antibody conjugate	Toxin conjugate	Preclinical	[143, 144]
TGF- α -linked toxin	Toxin conjugate	Preclinical for SCCHN	[143, 144]

3.1.2.2 Targeting EGFR with TKIs

Tyrosine kinase inhibitors (TKIs), such as erlotinib (OSI-779, Tarceva™) and gefitinib (ZD1839, Iressa™) selectively inhibit tyrosine phosphorylation on EGFR, abrogating downstream signaling. Both erlotinib and gefitinib have been studied in clinical trials for various types of cancer but have demonstrated limited efficacy as monotherapies. Erlotinib and gefitinib inhibit adenosine triphosphate (ATP) binding to the intracellular tyrosine kinase domain of EGFR, preventing protein kinase activity and subsequent downstream signaling, leading to apoptosis [145].

Erlotinib is a quinazoline derivative and a reversible inhibitor of EGFR that has shown antitumor effects in a variety of human cancers including SCCHN [146]. Results of several phase I and II clinical trials investigating erlotinib alone or in combination with radiation and/or various chemotherapeutic drugs have been reported in SCCHN, with combination treatments showing increased antitumor effects (reviewed in [110]). Erlotinib is currently FDA approved for treatment of locally advanced or metastatic non-small cell lung cancer after failure of at least one prior chemotherapy regimen [136] and approved for use in combination with gemcitabine for the first-line treatment of patients with locally advanced, unresectable or metastatic pancreatic cancer [137].

Preclinical studies with gefitinib have shown antitumor activity as a monotherapy or in combination with chemotherapy in both tumor cell lines and xenografts [147, 148]. After phase I studies documented that the TKI is safe when administered daily and dose-dependent kinetics were performed, it was tested as a first or second-line therapy for SCCHN [149]. In this study, the response rate was 10.6%. In 2003, Gefitinib was approved as a third-line monotherapy for NSCLC, but later failed to prolong patient survival in two phase III trials when combined with

chemotherapy and was removed from development by the company in 2005 [134, 135]. However, several preclinical and clinical studies combining gefitinib with chemotherapy or radiation have demonstrated synergistic antitumor effects (reviewed in [110]), indicating that an EGFR TKI combined with cytotoxic strategies could serve as an efficient treatment for SCCHN.

3.1.2.3 EGFR antisense gene therapy

EGFR antisense gene therapy was investigated as a treatment for SCCHN in preclinical models. EGFR antisense-expression plasmids were previously tested *in vitro* and significantly decreased growth of SCCHN cell lines compared to normal mucosal epithelial cells [138]. *In vivo* EGFR antisense in a modified U6 expression construct demonstrated antitumor effects when combined with liposomes and directly injected into SCCHN tumor xenografts [139]. EGFR antisense ODNs were also combined with chemotherapeutic agents such as docetaxel, and resulted in increased cytotoxicity, reduced tumor growth, and decreased EGFR signaling [141]. A phase I clinical trial testing EGFR antisense gene therapy in SCCHN patients is currently underway [140].

3.1.2.4 Immunotoxin conjugates targeting EGFR

Immunotoxins composed of *Pseudomonas* or *Diphtheria* bacterial toxins conjugated to either EGFR-targeted monoclonal antibodies or EGFR-specific ligands have been developed. Such toxin conjugates use the antibody or ligand portion to bind to the EGFR receptor. After binding to the receptor, the toxin conjugate is internalized, where the toxin portion mediates cytotoxic effects. A study found that a toxin linked to TGF- α had antitumor effects in EGFR-positive cancer cell lines and in SCCHN tumor xenografts [144]. Another study of two *Pseudomonas* toxins linked to EGFR antibodies resulted in growth inhibition of SCCHN cell

lines *in vitro* and decreased tumor size *in vivo* [143]. Toxin conjugates targeting EGFR have not been evaluated in clinical trials in SCCHN to date.

3.1.3 Bcl-X_L

The Bcl-2 family of proteins regulates apoptosis and includes death antagonists such as Bcl-2, Mcl-1, Bcl-w, A-1, and Bcl-X_L, and death agonists such as Bax, Bak, Bik, Bad, and Bid. These proteins share at least one of four homologous Bcl homology (BH) domains, of which the BH3 domain has been indicated as critical for the protein-protein interactions between the Bcl-2 family proteins [150, 151]. Bcl-X_L, a STAT3 target gene, is found localized in the outer mitochondrial membrane where it binds to BH3 domains of pro-apoptotic proteins such as Bax, Bak, and Bad in order to function as a repressor of apoptosis [151]. The exact mechanism by which Bcl-2 family proteins regulate apoptosis remains unclear. Studies indicate that apoptotic signals trigger the formation of pores in the outer mitochondrial membrane by proapoptotic proteins (Bax, Bak, Bik, Bad, and Bid) through which cytochrome c is released from the mitochondria into the cytosol, triggering the activation of caspases and a signaling cascade that initiates the mitochondria-mediated apoptosis pathway. Certain members of this protein family have demonstrated the ability to form channels in synthetic lipid membranes [152-154]. Apoptosis is an important cellular process, and dysregulation of regulators of apoptosis, such as Bcl-X_L, results in a variety of diseases, including cancer.

3.1.3.1 Bcl-X_L as a therapeutic target for cancer

Several studies have provided evidence for Bcl-2 family proteins as therapeutic targets for cancer [155]. Recent studies have specifically focused on targeting Bcl-X_L. A negative

correlation between Bcl-X_L expression and sensitivity to chemotherapeutic drugs was shown in a panel of cancer cell lines [156]. Overexpression of Bcl-X_L has been reported in a variety of malignancies, including glioblastoma, breast, pancreatic, prostate, colorectal, and intestinal cancers, as well as SCCHN. While Bcl-2 and Bcl-X_L are homologous proteins, a previous study showed high protein expression of Bcl-X_L in 74% of laryngeal tumors, but only 15% of the 47 tumors examined expressed high levels of Bcl-2 protein [157].

3.1.3.2 Bcl-X_L targeting strategies

Previous studies have targeted anti-apoptotic Bcl-2 family members using antisense ODNs, siRNA, small molecular weight chemical inhibitors, and BH3 peptides. The general function of these inhibitors is to sensitize cancer cells to standard treatment modalities such as radiation or chemotherapy [155]. These strategies have also been applied to Bcl-X_L (Table 4). To date, no Bcl-X_L inhibitor has been FDA approved as a cancer treatment.

Table 4. Summary of Bcl-X_L targeting strategies.

Below is a comprehensive list of Bcl-X_L inhibitors and the mechanism by which they act is also described. To date, no Bcl-X_L inhibitor has been FDA approved for SCCHN or any other malignancy.

Inhibitor	Mechanism	References
Antisense ODNs	Inhibition of mRNA translation	[158-164]
Bispecific antisense ODN targeting Bcl-2 and Bcl-XL	Inhibition of mRNA translation	[165-168]
Bcl-X _L siRNA	Targeted mRNA degradation	[169-173]
Antisense chimeric peptide nucleic acid ODN	Modulates splicing of <i>Bcl-X</i> gene	[174]
2-methoxy antimycin A	Small molecule inhibitor that blocks mitochondrial electron transport at inner membrane ubiquinone-cytochrome c oxido-reductase	[175-178]
(-)-Gossypol	Small molecule inhibitor that blocks the BH3 domain	[179-188]
Bax and Bad BH3 peptides	Small molecule inhibitors that bind to Bcl-X _L	[151, 181, 182, 189-191]
ABT-737	Small molecule inhibitor of Bcl-2, Bcl-X _L and Bcl-w	[192-196]
TW-37	Small molecule inhibitor of Bcl-2, Bcl-X _L and Mcl-1	[197]
Chelerythrine and Sanguinarine	Natural benzophenanthridine alkaloids, small molecule inhibitors of Bcl-X _L by binding to BH groove and BH1 domain, respectively	[198]

3.1.3.3 Antisense and siRNA strategies to target Bcl-X_L

The strategy of inhibiting mRNA translation using both antisense ODNs and siRNA has been used to target Bcl-X_L. Antisense strategies targeting Bcl-X_L have shown antitumor efficacy when combined with chemotherapy or radiation in a variety of cancer models including glioblastoma, pancreatic cancer, prostate cancer, colorectal cancer, and mesothelioma [159-163, 199]. Interestingly, antisense ODNs specifically designed to target both Bcl-2 and Bcl-X_L, a “bispecific antisense ODN” has recently shown to induce apoptosis in a variety of cancer cell lines and enhanced sensitivity to chemotherapy in some preclinical models [165-168]. Another study coupled Bcl-X_L antisense ODNs with antennapedia, a peptide of 16 residues from the homeodomain of the *Drosophila* transcription factor that is easily internalized into cells in culture, increasing cellular uptake of the antisense ODNs, and increasing stability in the cytoplasm [164]. Treatment of pancreatic cancer cells with Bcl-X_L antisense ODNs coupled with antennapedia resulted in down-regulation of Bcl-X_L protein and increased sensitivity to radiation both *in vitro* and *in vivo*. Studies examining the efficacy of Bcl-X_L siRNA have reported decreased Bcl-X_L expression and increased apoptosis in preclinical models of hepatocellular carcinoma, gastric cancer, and colon cancer, esophageal cancer [169-172]. These studies using siRNA provide proof-of-principle for Bcl-X_L as a therapeutic target in cancer.

3.1.3.4 Small molecule inhibitors of Bcl-X_L

One promising approach to inhibit Bcl-X_L repression of apoptosis involves the administration of small molecules designed to bind to the BH3 domain of Bcl-X_L, preventing Bcl-X_L/pro-apoptotic protein interactions [150, 151, 183, 200-202]. Several small molecule inhibitors of Bcl-X_L have been identified and tested in preclinical models, including antimycin A, BH3 domain peptides, and the novel inhibitor ABT-737. Antimycin A and its analogs are

inhibitors of the mitochondrial electron transport chain that induce apoptosis in a variety of Bcl-X_L-overexpressing cancer cell lines [175-178]. Antimycin A, an antibiotic isolated from *Streptomyces* sp., induces apoptosis by binding to the hydrophobic groove of the BH3 domain of Bcl-X_L and Bcl-2, inhibiting Bcl-X_L and Bcl-2 activity, resulting in mitochondrial swelling, loss of mitochondrial membrane potential [176].

Another type of small molecule inhibitor of Bcl-X_L, synthetic BH3 peptides that mimic the BH3 domains of pro-apoptotic proteins such as Bax and Bak, has demonstrated the ability to disrupt heterodimerization of Bcl-X_L with its pro-apoptotic binding partners and induce the release of cytochrome c from mitochondria [190]. Studies investigated the ability of a Bad BH3 peptide to bind to Bcl-X_L in Bcl-X_L-overexpressing Jurkat leukemia cells and found that the Bad BH3 peptide efficiently inhibited Bcl-X_L and induced release of cytochrome c from mitochondria [151, 191]. These studies also concluded that the BH3 peptides were most effective in cells that overexpressed Bcl-X_L, and given that Bcl-X_L is overexpressed in SCCHN [157], the use of BH3 peptides may be an effective therapeutic strategy for SCCHN. Bax, Bad, and Bak BH3 peptides linked to antennapedia or polyarginine peptide transduction domains have been investigated in the UM-22A, UM-22B, and 1483 cell lines and a dose-dependent decrease in cell survival was observed (unpublished data).

The BH3 mimetic ABT-737 has also been investigated as a Bcl-X_L inhibitor for cancers that overexpress Bcl-2 family proteins. ABT-737 is unique because it inhibits Bcl-2, Bcl-X_L, and Bcl-w with a higher potency than any other reported small molecule inhibitor [192]. This compound has demonstrated antitumor effects in small cell lung cancer and chronic lymphocytic leukemia [196, 203]. One study attributed significant antitumor effects to ABT-737 when used to treat multiple myeloma cell lines and primary multiple myeloma cells from patients whose

disease was resistant to prior treatment with chemotherapy [192]. Yet, studies have found that the antitumor activity of ABT-737 is limited by Mcl-1—cell lines treated with Mcl-1 inhibitors in combination with ABT-737 demonstrated higher antitumor activity, and cells overexpressing Mcl-1 were more resistant to ABT-737 treatment, indicating that it may not be an effective monotherapy for all Bcl-2 family-overexpressing malignancies [194, 195, 204, 205]. Further investigation to identify the exact mechanism by which this inhibitor elicits an antitumor response are necessary to understand why it is effective in some malignancies, but not others, and what other inhibitors it can be combined with to increase its efficacy.

3.1.3.5 Gossypol

Gossypol, is a polyphenol isolated from the seed, roots, and stem of the cotton plant, and found in cottonseed oil, is another well studied small molecule inhibitor of Bcl-X_L. Racemic gossypol was originally studied because of its antifertility properties. In the 1970s, the Chinese government conducted a study in which men were given racemic gossypol daily (20 mg/day) as a contraceptive [206, 207]. Although it was effective and well tolerated, 10 % of patients had reduced blood potassium levels and 10 % had irreversible infertility after they discontinued use. As a result, development of racemic gossypol as a male antifertility drug has been slow.

Racemic gossypol was next studied as an anticancer drug after treatment of cancer cell lines both *in vitro* and *in vivo* showed that it had potent antitumor effects, but eventually produced less than impressive antitumor effects in phase I/II clinical trials of breast cancer, adrenal cancer, and a variety of other advanced stage cancers [208-214]. Such dismal results led one group to conclude that although gossypol was safe and well tolerated, it was unlikely that it would be useful as a therapeutic drug for cancer [214]. The failure of racemic gossypol to perform satisfactorily as an anticancer drug in clinical trials led researchers to examine the drug

more carefully in preclinical models and subsequent studies identified the (-) enantiomer ((-)-gossypol, or AT-101) as a potent cytotoxic drug.

((-)-gossypol, but not the positive enantiomer, binds to the BH3 domain of Bcl-X_L and Bcl-2 to cause apoptosis through induction of DNA fragmentation, PARP cleavage, loss of mitochondrial membrane potential, cytochrome c release, and activation of caspase-3, -8, and -9 [179, 180, 183, 215]. One report demonstrated that (-)-gossypol induced dose-dependent apoptosis and growth inhibition of a panel of SCCHN cell lines *in vitro* [181]. A recent study investigated the efficacy of (-)-gossypol in an orthotopic xenograft model of SCCHN and concluded that systemic treatment with (-)-gossypol resulted in decreased tumor growth and increased apoptosis [184]. These studies using SCCHN preclinical models provide evidence that (-)-gossypol may be an effective therapeutic modality for SCCHN when Bcl-X_L is overexpressed. Clinical trials using (-)-gossypol for the treatment of B cell malignancies, small cell lung cancer, chronic lymphocytic leukemia, prostate cancer, and brain and central nervous system tumors, are all currently underway [216].

3.1.4 Rationale and hypotheses

We hypothesized that combined targeting of the pathway including EGFR, STAT3, and Bcl-X_L would result in increased antitumor effects. EGFR, STAT3, and Bcl-X_L have been implicated as independent therapeutic targets in SCCHN, and monotherapeutic strategies to target these molecules in SCCHN have shown limited efficacy in the clinic. Combining new and innovative therapeutic approaches, such the STAT3 decoy, with established or emerging treatment modalities such as erlotinib and (-)-gossypol is a novel treatment strategy for SCCHN. By blocking a pathway at the level of the receptor, intracellular signaling molecule and

transcription factor, as well as the downstream target gene, the pathway can be effectively inhibited regardless of any crosstalk with other aberrant signaling pathways, and may also down-regulate parallel or convergent pathways involved to maximize antitumor effects.

3.2 MATERIALS AND METHODS

3.2.1 Chemicals and reagents

An antibody against procaspase 3 and an antibody to detect both the full-length and cleaved forms of PARP were obtained from Cell Signaling Technology, Inc. (Danvers, MA). Beta tubulin antibody was obtained from Abcam, Inc. (Cambridge, MA). MTT (3-(4, 5-dimethylthiazol-2-yl)-2,5-diphenyltetrazolium bromide) was obtained from Sigma (The enhanced chemiluminescence (ECL) kit was purchased from Santa Cruz Biotechnology, Inc. (Santa Cruz, CA). Erlotinib (OSI-774, Tarceva™) was provided by Ken Iwata (OSI Pharmaceuticals, Uniondale, NY) [146]. (-)-gossypol was a kind gift from Dr. Shaomeng Wang (University of Michigan, Ann Arbor, MI) [181].

3.2.2 Cell culture

Please refer to section 2.2.2 (pg. 45).

3.2.3 STAT3 decoy preparation and transfection

Please refer to sections 2.2.3 and 2.2.4 (pgs. 46-47).

3.2.4 Dose response and cell viability experiments

Dose response experiments were performed using 0.001-200 μM erlotinib or 0.03-30 μM (-)-gossypol in DMEM containing 10% heat-inactivated fetal bovine serum and 1X Penicillin/Streptomycin mix, incubated at 37°C with 5 % CO_2 . For dose response experiments, the concentration of STAT3 decoy ranged from 0.34 pM to 3.4 nM and was combined with the transfection reagents described above. After 72h MTT assays were performed as described previously (see section 2.2.7, pg. 48). Curve fit nonlinear regression analysis of sigmoidal dose response curves with variable slope was performed using GraphPad Prism version 4.03 for Windows, GraphPad Software (San Diego, CA, www.graphpad.com). MTT data was confirmed using trypan blue dye exclusion assays for counting viable cells, as described previously (see section 2.2.6, pg. 48).

3.2.5 Cell treatments

For combination experiments, UM-22B and PCI-15B cells were transfected with the IC_{50} values (10 pM or 40 pM, respectively) of the STAT3 decoy or mutant control decoy as described above. After 4h, transfection media was removed and DMEM (10 % heat-inactivated fetal bovine serum, 1X Penicillin/Streptomycin mix) containing 5 μM or 0.1 μM erlotinib alone, 3 μM (-)-gossypol alone, or a combination of both erlotinib and (-)-gossypol was added. Cell counts using trypan blue dye exclusion were performed after 72h to assess cell viability.

3.2.6 Western blotting of cell line lysates

Western blots were run using 50 µg of whole cell protein lysate per lane as previously described (see section 2.2.5, pg.47).

3.2.7 Animals and treatment regimen

4-6 week old female athymic nude mice were injected with 1×10^6 1483 cells in the left and right dorsal flanks, resulting in two tumors per animal. Fourteen days later, after tumors were palpable, animals were assigned to two treatment groups by stratified randomization based on flank ratio (5 mice in the STAT3 decoy or mutant control decoy only group, and 5 mice in the erlotinib and STAT3 decoy or mutant control decoy group). Daily intratumoral injections of STAT3 decoy or mutant control (50 µg in 50 µl) was delivered for 14 days. Erlotinib was dissolved in a 20% trappsol (hydroxypropyl-beta-cyclodextrin) solution (CTD, Inc, Cyclodextrin Resource, High Springs, FL). 90 mg/kg erlotinib was delivered by oral gavage daily for 14 days, and sacrificed at day 15 after treatment began. The dose was chosen based on the literature which found that the maximum tolerated dose of erlotinib in nude mice is 100 mg/kg in non-small cell lung cancer xenografts [217]. There are no published reports for the maximum tolerated dose of erlotinib in nude mice carrying 1483 xenografts.

3.2.8 Statistics

Refer to section 2.2.8 (pg.48) for statistics.

3.3 RESULTS

3.3.1 SCCHN cell lines have similar IC₅₀ values for (-)-gossypol but not for erlotinib or the STAT3 decoy

In order to determine the doses of the inhibitors to use in our cell lines for combination treatments, we first performed dose response experiments for erlotinib (0.001 μ M to 200 μ M), STAT3 decoy (0.34 pM to 3.4nM), or gossypol (0.03 μ M to 30 μ M). UM-22B, PCI-15B, and 1483 cells were treated with a range of doses of erlotinib, STAT3 decoy, or (-)-gossypol for 72hrs and MTT assays were performed to assess cell viability. Data was normalized to untreated control cells and the percentage of cytotoxicity was calculated. Curve fit nonlinear regression analysis of sigmoidal dose response curves with variable slope was performed using GraphPad Software to determine IC₅₀ values for erlotinib, STAT3 decoy, or (-)-gossypol in UM-22B, PCI-15B, and 1483 cell lines (Table 5).

The IC₅₀ for (-)-gossypol in all cell lines tested was approximately 3 μ M, which is consistent with other reports of (-)-gossypol in SCCHN cell lines [181]. The IC₅₀ for erlotinib was 10 μ M, 0.33 μ M, or 7 μ M for UM-22B, PCI-15B, and 1483 cell lines, respectively. Similarly, the IC₅₀ value for STAT3 decoy varied between the cell lines examined, 12.6 pM for UM-22B, 38.3 pM for PCI-15B, or 2.05 pM for 1483. These results imply that our panel of SCCHN cell lines has varying levels of sensitivity to erlotinib or the STAT3 decoy, but not to (-)-gossypol.

Table 5. IC₅₀ values for inhibitors in SCCHN cell lines.

Representative results of dose-response experiments for erlotinib, the STAT3 decoy, or (-)-gossypol are listed for three SCCHN cell lines.

Cell line	Erlotinib	STAT3 Decoy	(-)-gossypol
UM-22B	10 μ M	12.6 pM	2.7 μ M
PCI-15B	0.33 μ M	38.3 pM	3.0 μ M
1483	7 μ M	2.05 pM	2.1 μ M

3.3.2 Combining EGFR and STAT3 inhibitors enhances antiproliferative effects in SCCHN *in vitro*

To assess the antiproliferative effect of combining EGFR and STAT3 inhibition, we treated UM-22B cells with erlotinib and the STAT3 decoy. The STAT3 decoy alone resulted in 62.7 % (\pm 5.6 %) survival. Treatment with erlotinib and the mutant control decoy resulted in 48.7 % (\pm 5.5 %) survival. Treatment with both the STAT3 decoy and erlotinib resulted in 29.6 % (\pm 3.3 %) survival, which was significantly different from either the STAT3 decoy alone or erlotinib and the mutant control decoy ($p=0.004$ and $p=0.028$, respectively) (Figure 13A). Similar results were seen for PCI-15B cells (Figure 13B). Treatment with the STAT3 decoy resulted in 61.2 % (\pm 5.5 %) survival. Treatment with erlotinib and the mutant control decoy resulted in 59.4 % (\pm 5.0 %) survival, and treatment with both the STAT3 decoy and erlotinib resulted in 39.0 % (\pm 2.5 %) survival. In PCI-15B cells, the combination of the STAT3 decoy and erlotinib significantly decreased survival compared to the STAT3 decoy alone or erlotinib

and the mutant control decoy ($p=0.004$ and $p=0.016$, respectively). These results indicate that combining erlotinib with the STAT3 decoy enhances antiproliferative effects.

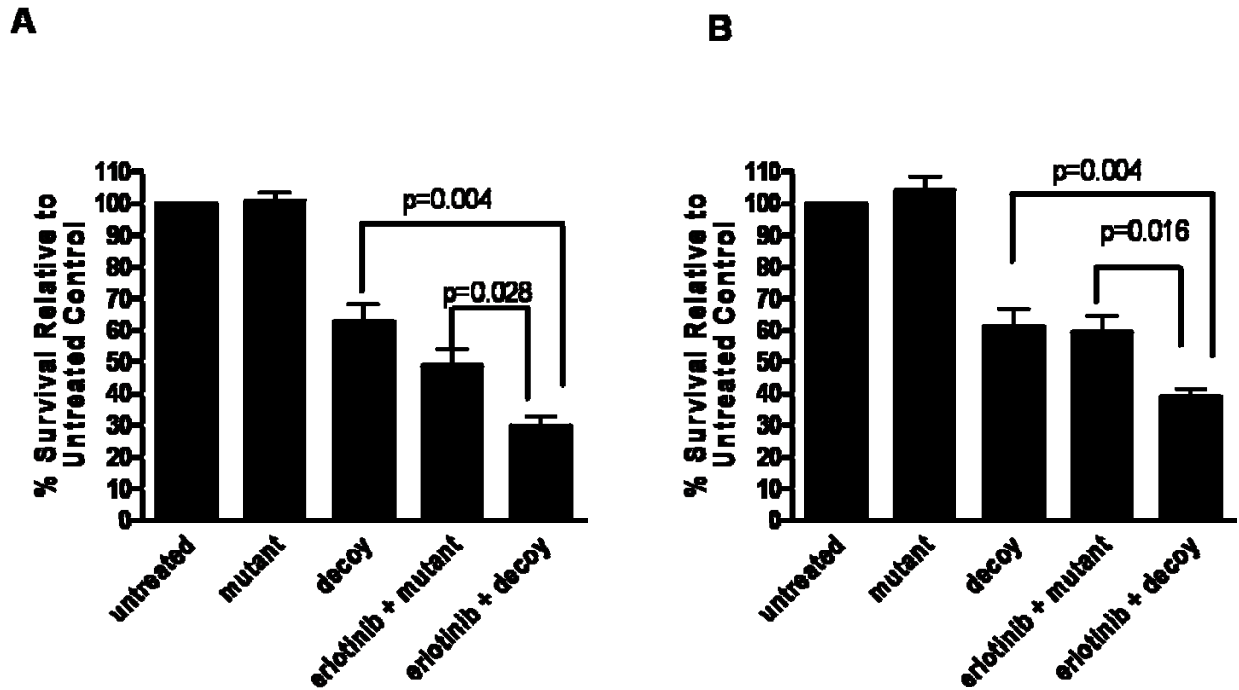


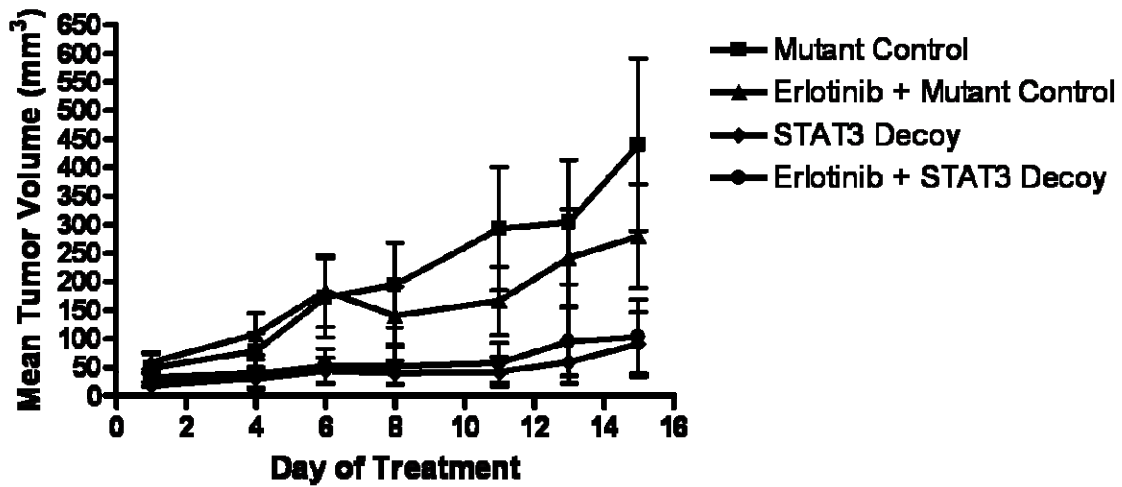
Figure 13. Combining the STAT3 decoy with erlotinib enhances growth inhibition *in vitro*.

(A) UM-22B cells were transfected with 10 pM STAT3 decoy or mutant control decoy for 4h. Transfection media was removed and DMEM containing 10 % FBS and 5 μ M erlotinib was added. Cells were then counted after 72h using trypan blue dye exclusion. When the STAT3 decoy was combined with erlotinib, survival was significantly reduced compared to STAT3 decoy ($p=0.004$) or erlotinib and the mutant control decoy ($p=0.028$) in UM-22B cells. (B) Similar results were seen for PCI-15B cells ($p=0.004$ and $p=0.016$) when treated with 0.1 μ M erlotinib and 40 pM STAT3 decoy. Cumulative results are shown from five separate experiments.

3.3.3 Targeting EGFR and STAT3 in an *in vivo* SCCHN preclinical model results in enhanced antitumor effects

To determine the therapeutic efficacy of combining an EGFR inhibitor with the STAT3 decoy *in vivo*, a xenograft model of SCCHN was used. Mice bearing 1483 tumors were treated with the STAT3 decoy or mutant control decoy by intratumoral injection with erlotinib or the vehicle control by oral gavage for two weeks (Figure 14). The STAT3 decoy inhibited growth of 1483 tumors compared to the mutant control decoy ($p < 0.05$ from day 8 to the end of the experiment) (Figure 14A and B). Erlotinib and the mutant control decoy also decreased tumor volume compared to the mutant control decoy alone ($p < 0.05$ at day 15) (Figure 14A and 14C). The combination of the STAT3 decoy and erlotinib did not significantly reduce tumor growth compared to the STAT3 decoy alone ($p = 0.393$ at day 15). This is because treatment with the STAT3 decoy alone was so effective at inhibiting tumor growth, the 50 $\mu\text{g}/\text{day}$ STAT3 decoy used in the experiment was too high to observe any enhanced growth inhibition when combined with erlotinib. However, two mice whose tumors were treated with the STAT3 decoy and erlotinib completely disappeared (Figure 14C).

A



B



C



Left tumor: mutant control decoy
Right tumor: STAT3 decoy

Figure 14. The STAT3 decoy inhibits SCCHN cell growth *in vivo*.

(A) 1483 cells (1×10^6) were inoculated subcutaneously in the right and left flanks of 10 athymic nude mice. After 14 days, the tumors were palpable and mice were randomized into two treatment groups. The tumor on the left flank was injected with the mutant control decoy and the tumor on the right flank was treated with the STAT3 decoy (50 μ g) daily for 14 days. Additionally, five mice received erlotinib (90 mg/kg) and five mice received vehicle control by oral gavage. The median tumor volumes are shown. (B) and (C) Photographs showing the dramatic decrease in tumor volume when the STAT3 decoy was injected (right flanks) compared to the mutant control decoy (left flanks). The mice in (C) received

erlotinib as well, and two of those mice whose tumors received the STAT3 decoy and erlotinib had no detectable tumor as early as day 17 after tumor inoculation (indicated by asterisks).

3.3.4 Combining STAT3 and Bcl-X_L inhibitors enhances antiproliferative effects in SCCHN cell lines

The STAT3 decoy was combined with (-)-gossypol in UM-22B and PCI-15B cells, and cell viability was assessed using trypan blue dye exclusion assay after 72hrs to determine the antiproliferative efficacy of combined inhibition of STAT3 and Bcl-X_L. Treatment of PCI-15B cells with the STAT3 decoy resulted in 54.2 % (\pm 4.2 %) survival. Treatment with the mutant control and (-)-gossypol resulted in 56.4 % (\pm 5.1 %) survival. Combined treatment of PCI-15B cells with the STAT3 decoy and (-)-gossypol resulted in 38.7 % (\pm 4.0 %) survival. Therefore, in PCI-15B cells, the combination of STAT3 decoy and (-)-gossypol significantly inhibited cell proliferation compared to either the STAT3 decoy alone, or the mutant control decoy with (-)-gossypol ($p=0.0278$ and $p=0.0278$, respectively) (Figure 15B). A similar trend was observed in UM-22B cells, where treatment with the STAT3 decoy resulted in 61.8 % (\pm 7.1 %) survival, treatment with the mutant control and (-)-gossypol resulted in 51.5 % (\pm 9.3 %) survival, and the combined treatment of the STAT3 decoy and (-)-gossypol resulted in 40.3 % (\pm 7.4 %) survival. Although the enhancement of growth inhibition elicited by the STAT3 decoy and (-)-gossypol was not statistically significant when compared to the STAT3 decoy alone ($p=0.075$) or to the mutant control and (-)-gossypol ($p=0.155$), the same trend was observed as that seen in the PCI-15B cell line (Figure 15A). These data indicate that the combination of the STAT3 decoy and (-)-gossypol enhance antiproliferative effects compared to either agent alone.

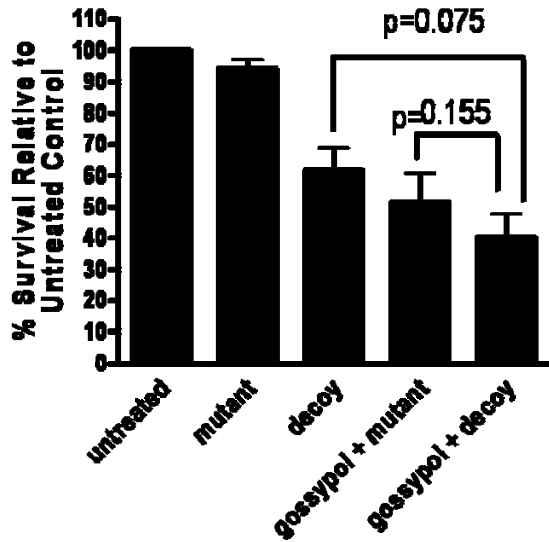
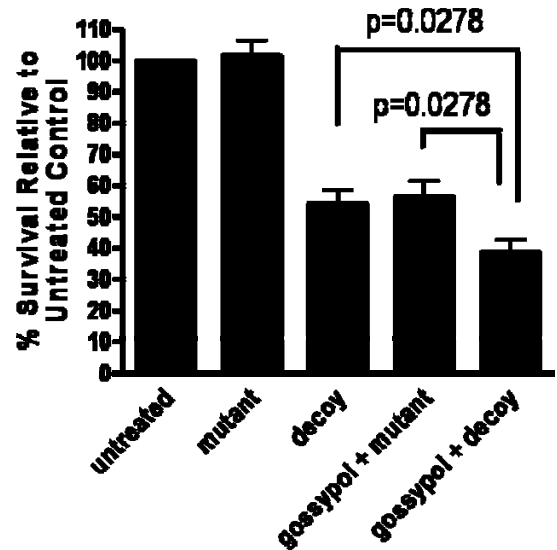
A**B**

Figure 15. A combination of the STAT3 decoy with (-)-gossypol inhibits growth of head and neck cancer cells.

(A) UM-22B cells were treated with 10 pM STAT3 decoy or mutant control decoy for 4h followed by treatment with 3 μ M (-)-gossypol for 72h. Cell counts were then performed using trypan blue dye exclusion. Combining the STAT3 decoy with (-)-gossypol augmented cell growth inhibition compared to STAT3 decoy alone or mutant control and (-)-gossypol in UM-22B ($p=0.075$ and $p=0.155$, respectively). (B) Similar results were seen when PCI-15B cells were treated with 40 pM STAT3 decoy and 3 μ M (-)-gossypol ($p=0.0278$ and $p=0.0278$). Cumulative results are shown from five separate experiments

3.3.5 A combination of EGFR, STAT3 and Bcl-X_L inhibitors enhances antiproliferative effects in SCCHN cell lines

We next investigated the antitumor efficacy of combined inhibition of EGFR, STAT3, and Bcl-X_L using a combination of erlotinib, the STAT3 decoy, and (-)-gossypol. We treated

UM-22B cells with 5 μ M erlotinib, 10 pM STAT3 decoy, and 3 μ M (-)-gossypol and compared it to cells treated with the STAT3 decoy alone or the combination of erlotinib, the mutant control decoy, and (-)-gossypol. After 72hrs, we performed cell counting using trypan blue dye exclusion assay, and found that the combination of erlotinib, the STAT3 decoy, and (-)-gossypol resulted in 21.3 % (\pm 4.1 %) survival. Treatment with the STAT3 decoy alone resulted in 54.3 % (\pm 3.4 %) survival, while treatment with erlotinib, the mutant control, and (-)-gossypol resulted in 30.7 % (\pm 2.2 %) survival (Figure 16A). The triple combination of erlotinib, the STAT3 decoy, and (-)-gossypol significantly inhibited survival compared to either the STAT3 decoy alone ($p=0.004$) or compared to erlotinib, the mutant control, and (-)-gossypol ($p=0.0476$). Similar results were seen with PCI-15B cells, where erlotinib, the STAT3 decoy, and (-)-gossypol significantly inhibited survival compared to the STAT3 decoy alone ($p=0.004$) or erlotinib, the mutant control decoy, and (-)-gossypol ($p=0.008$) (Figure 16B).

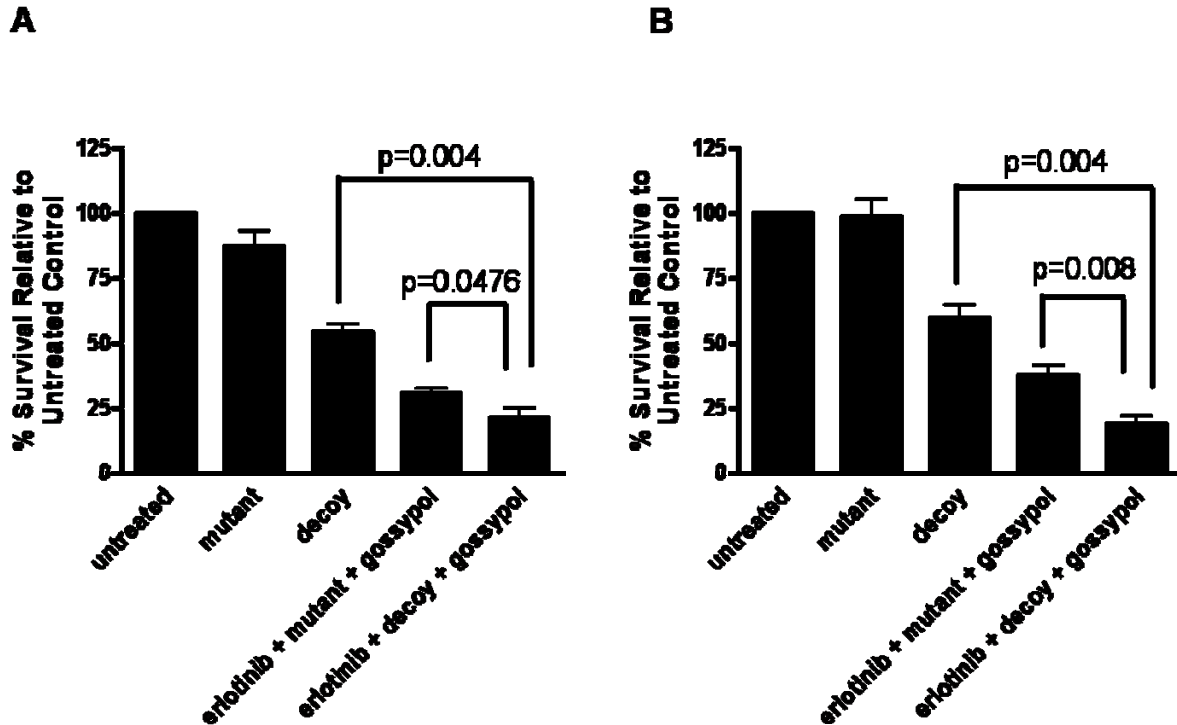


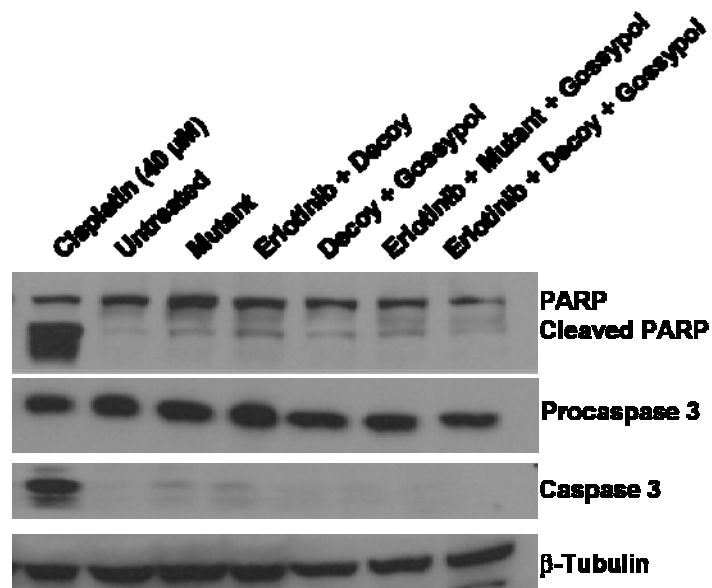
Figure 16. Combining erlotinib, STAT3 decoy and (-)-gossypol further enhances growth inhibition but not apoptosis in SCCHN cells compared with treatment using either the STAT3 decoy alone or a combination of erlotinib, mutant control decoy, and (-)-gossypol.

(A) UM-22B cells were plated in 96-well plates and treated with 5 μ M erlotinib, 10 pM STAT3 decoy and/or 3 μ M (-)-gossypol. Cell counts were performed by trypan blue dye exclusion at 72h. Combining erlotinib, STAT3 decoy and (-)-gossypol enhanced cell growth inhibition compared to STAT3 decoy alone ($p=0.004$) or erlotinib, mutant control, and (-)-gossypol ($p=0.0476$). (B) Similar results were seen with PCI-15B treated with 0.1 μ M erlotinib, 40 pM STAT3 decoy and 3 μ M (-)-gossypol ($p= 0.004$ and 0.008, respectively). Cumulative results are shown from five separate experiments.

3.3.6 A combination of EGFR, STAT3 and Bcl-X_L inhibitors does not increase induction of apoptosis in an SCCHN cell line

To investigate the effect of combined targeting of EGFR, STAT3, and Bcl-X_L on apoptosis, 1483 cells treated with erlotinib, the STAT3 decoy, and/or (-)-gossypol were harvested after 24 hrs and whole cell lysates subjected to Western blot analysis for PARP and cleaved PARP, procaspase 3 and caspase 3, and β -tubulin (loading control) (Figure 17A). Treatment of 1483 cells with combinations of the STAT3 decoy with erlotinib and/or (-)-gossypol appears to decrease total PARP levels. Yet, we do not observe any increase in the cleaved form of PARP. Also, procaspase 3 levels and activated caspase 3 levels are not altered upon treatment. Densitometry was performed to quantify the ratio of PARP to cleaved PARP (Figure 17B). Treatment with the double combinations (STAT3 decoy in combination with either erlotinib or (-)-gossypol) both appear to decrease the PARP/cleaved PARP levels compared to the mutant control (0.69 ± 0.09 and 0.64 ± 0.23 , respectively). Treatment with the triple combinations (erlotinib, the mutant control, and (-)-gossypol or erlotinib, the STAT3 decoy, and (-)-gossypol) appear to further decrease the PARP/cleaved PARP ratio (0.47 ± 0.13 and 0.50 ± 0.11 , respectively) compared to the double combinations. Yet, when the ratios of PARP to cleaved PARP for all of the treatment groups were compared using a nonparametric Kruskal Wallis Test, there was no significant difference between them ($p=0.205$). These results indicate that treatment with the STAT3 decoy in combination with erlotinib and/or (-)-gossypol does not increase apoptosis of 1483 cells after 24 hrs.

A



B

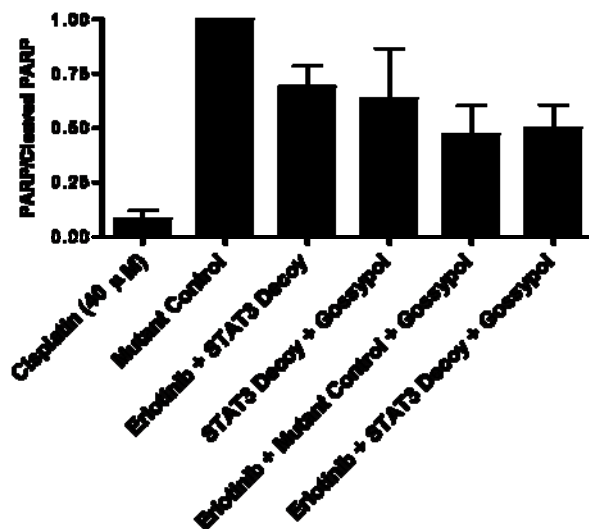


Figure 17. Combined inhibition of STAT3 with erlotinib and (-)-gossypol does not significantly increase apoptosis *in vitro*.

(A) 1483 cells were treated with the STAT3 decoy (2 pM), erlotinib (3.5 μ M), and/or (-)-gossypol (3 μ M) for 24 hrs. Cisplatin (40 μ M) was used as a positive control for apoptosis induction. Cell lysates were collected and immunoblotted for PARP, cleaved PARP, procaspase 3 and caspase 3, and β -tubulin (loading control). The experiment was performed three times with similar results to those shown above. (B) Densitometry was performed on three separate immunoblots to analyze the ratio of PARP to cleaved PARP as a measure of induction of apoptosis.

3.4 DISCUSSION

Because there are no published reports of IC₅₀ concentrations for erlotinib, the STAT3 decoy, or (-)-gossypol in the UM-22B, PCI-15B or 1483 SCCHN cell lines, dose-response experiments were performed to determine the IC₅₀ values of erlotinib, the STAT3 decoy, or (-)-gossypol (Table 5). IC₅₀ values for erlotinib have not been reported for the cell lines used in our experiments, but have been reported for other EGFR overexpressing cancer cell lines including breast, colon, and head and neck, and vary from 100 nM to 7 μM [218]. The human esophageal squamous cell carcinoma cell lines Kyse-30, Kyse-70, and Kyse-140 had IC₅₀s of 13.9 μM, 19.2 μM, and 0.7 μM, respectively [219]. We found that the IC₅₀ value for either erlotinib or the STAT3 decoy varied amongst the three cell lines examined (0.33 μM to 10 μM and 2.05 pM to 38.3 pM, respectively). One group reported a mean IC₅₀ value of 5.30 (± 1.55) μM of (-)-gossypol in 10 SCCHN cell lines, which is comparable to the 3.0 μM IC₅₀ we calculated using our cell lines [181]. To perform combination experiments, in order to assess an enhanced effect on cell growth or apoptosis, the IC₅₀ values of the STAT3 decoy and (-)-gossypol were used, while half of the IC₅₀, or the IC₂₅ concentration was used for erlotinib. This is because the sigmoidal dose response curves for the STAT3 decoy and (-)-gossypol in the SCCHN cell lines was quite steep, indicating that the IC₂₅, IC₅₀, and IC₇₅ concentrations are within a very narrow range (data not shown).

Because of the complexity of signaling pathways and the multi-level cross-stimulation of parallel pathways in a cell, novel inhibitors have not performed satisfactorily as monotherapies in clinical trials [220]. Preclinical studies have focused on combining EGFR inhibitors or Bcl-X_L inhibitors with standard treatments—either radiation or chemotherapy [148, 159, 160, 162-164,

168, 169, 182, 187, 221, 222]. Because no STAT3 inhibitor has reached the clinic to date, there is no clinical data on the therapeutic efficacy of a STAT3 inhibitor in combination with either standard treatments or experimental treatments such as EGFR or Bcl-X_L inhibitors. Therefore, the strategy of combined targeting of molecules in a pathway whose component proteins are up-regulated in cancer has only begun to be explored.

For example, investigations of the clinical efficacy of combined targeting for the treatment of NSCLC reported increased response rates, prolonged time to progression of disease, and increased median survival time for patients that received inhibitors targeting VEGF and EGFR [220]. To date, there are few published reports of combined inhibition of STAT3 and EGFR and no published reports of combined inhibition of STAT3 and Bcl-X_L. One study showed enhanced growth inhibition of an human cervical cancer cell line overexpressing EGFR when an EGFR inhibitor and a STAT3 inhibitor were combined *in vitro* [223]. The SCCHN cell lines were treated with the transcription factor decoy targeting STAT3, combined with either the EGFR tyrosine kinase inhibitor erlotinib, or the Bcl-X_L inhibitor, (-)-gossypol. The effects on cell survival were investigated *in vitro* and the data indicate that combining the STAT3 decoy with either erlotinib or (-)-gossypol enhances inhibition of cell growth. Results also indicate that the STAT3 decoy combined with erlotinib *in vivo* did not significantly decrease the growth of 1483 xenografts in nude mice, probably due to the striking efficacy of the STAT3 decoy alone at this particular concentration (50 µg/day). This experiment should be repeated using a lower dose of STAT3 decoy (35 µg/day) in order to determine if the combination of the STAT3 decoy with erlotinib is therapeutically efficacious for SCCHN.

Few studies investigating the therapeutic efficacy of combined targeting of three molecules have been reported. The combined inhibition of EGFR, its downstream signaling

molecule, PKA, and the downstream target gene, COX-2 resulted in enhanced antitumor effects compared to single inhibitors or combinations of two inhibitors both *in vitro* and *in vivo* [224]. Studies have shown that EGFR has a structural interaction with PKA, and that EGFR may activate expression of COX-2 [225-227]. One study performed in both colon and breast cancer *in vitro* and *in vivo* models combined EGFR, PKA, and Bcl-2/Bcl-X_L inhibitors and again found that targeting multiple proteins in a pathway which are also points of convergence for other up-regulated pathways that control proliferation, apoptosis, angiogenesis, and metastasis was therapeutically efficacious [224]. Our study combined EGFR, STAT3, and Bcl-X_L inhibitors and found enhanced growth inhibition but we did not observe an induction of apoptosis *in vitro* after 24 hrs in 1483 cells. Regardless, given the growth inhibitory effects observed, the triple combination of the STAT3 decoy, erlotinib, and (-)-gossypol may be an efficacious treatment modality for SCCHN.

4.0 CONCLUSIONS AND FUTURE DIRECTIONS

4.1 CONCLUSIONS

This dissertation focused on two objectives: to elucidate the contribution if any of STAT1 in the STAT3 decoy-mediated antitumor mechanism and to determine the therapeutic efficacy of combining the STAT3 decoy with EGFR and/or Bcl-X_L inhibitors in preclinical models of SCCHN. We found that the STAT1 pathway is intact in SCCHN cell lines, and that the STAT3 decoy mitigates STAT1 signaling *in vitro*. Downmodulation of STAT1 protein by transient transfection of STAT1 siRNA did not alter STAT3 decoy-mediated growth inhibition in SCCHN cell lines. Similar results were seen when a STAT1 knockout cell line was transfected with the STAT3 decoy. Therefore, STAT1 does not contribute to the growth inhibitory effects elicited by the STAT3 decoy. Stimulation of the STAT1 pathway did not mitigate STAT3 decoy-mediated growth inhibition either. Further studies using STAT3 knockout cells demonstrated that STAT3 is necessary for STAT3 decoy-mediated growth inhibition. These results lead us to conclude that the STAT3 decoy may be safely used as a therapy for cancers that express STAT3 and STAT1. Also, this study provides evidence that the mechanism of any transcription factor decoy should be thoroughly explored. Transcription factors form complexes with other transcription factors and co-activators whose signaling may also be affected by the use of a transcription factor decoy.

EGFR, STAT3, and Bcl-X_L are all overexpressed in SCCHN and correlated with decreased survival, poor prognosis, and increased resistance to chemotherapy and radiation. These three proteins are related in that Bcl-X_L is a downstream target gene expressed by the transcription factor, STAT3, which is activated in response to EGFR activation. In addition, each protein is a point of convergence for many signaling pathways upregulated in SCCHN, including MAPK, PI3K/Akt, mTOR, Src, STAT5, and IL6/gp130. We found that the combination of the STAT3 decoy, with either an EGFR inhibitor (erlotinib) or a Bcl-X_L inhibitor ((-)-gossypol) elicited enhanced growth inhibition in SCCHN cell lines compared to single treatments. We also looked at the ability of the combinations of inhibitors to induce apoptosis, but we did not see a significant increase in apoptosis when the STAT3 decoy was combined with either erlotinib or (-)-gossypol. Erlotinib is an FDA approved inhibitor, but there are currently no FDA approved Bcl-X_L inhibitors, so we combined erlotinib with the STAT3 decoy in an *in vivo* model of SCCHN. The STAT3 decoy elicited a strong growth inhibitory effect on SCCHN xenografts, which did not allow us to observe any effect of the combined treatment.

4.2 FUTURE DIRECTIONS

4.2.1 Investigation of other signaling molecules involved in the mechanism of the STAT3 decoy

Given the results implicating that the STAT3 decoy inhibits STAT1 signaling, we hypothesize that the STAT3 decoy may inhibit other molecules that are related to STAT3 or whose signaling pathways crosstalk with the STAT3 pathway such as STAT5 and mTOR.

STAT5 and mTOR are both up-regulated in cancer, particularly SCCHN, and are associated with STAT3 in various ways that are described in detail below. Therefore, studies to further elucidate the mechanism by which the STAT3 decoy elicits antitumor effects in preclinical models should be performed to investigate if these proteins also play a role in the STAT3 decoy mechanism. After further elucidating the mechanism of the STAT3 decoy, investigations into the therapeutic efficacy of combined targeting approaches can also be performed.

4.2.1.1 Role of STAT5 in the STAT3 decoy mechanism

STAT5 is an oncogenic protein whose overexpression has been reported in a variety of malignancies, including breast, prostate, non-small cell carcinoma, melanoma, and SCCHN [2, 4, 228-234]. STAT5 overexpression usually accompanies overexpression of STAT3, although the role of STAT5 overexpression in cancer is not clearly understood at this time [2, 3, 235]. STAT5 does not share the same degree of homology with STAT3 as STAT1 does (about 62% in the DNA binding domain)—but the oncogenic effects of STAT5 have been clearly demonstrated in the literature. The STAT5 pathway is intricately interwoven with that of STAT3—EGFR and Src are upstream mediators of STAT5 transcription of target genes, and the list of STAT5 target genes has considerable overlap with that of STAT3, including Bcl-X_L. Additionally, we have identified the formation of STAT3/5 heterodimers in SCCHN cell lines (unpublished data). The role of the STAT heterodimers is unclear. Studies to determine if STAT3 decoy binding to STAT3 disrupts STAT3/5 heterodimer formation and/or signaling should be performed to further elucidate the mechanism of the STAT3 decoy and determine a possible role for STAT5 in the STAT3 decoy-mediated antitumor effects. In addition, the prolactin receptor specifically activates STAT5 after stimulation with prolactin, resulting in the expression of STAT5 target genes, such as Pim-1 (a known oncogene) [236]. This signaling pathway can be used to study

the role of STAT5 in the STAT3 decoy mechanism just as we used the STAT1 pathway (stimulated by IFN-gamma, with IRF-1 as the target gene) in the studies described in Chapter 2 of the dissertation. Preliminary data suggest that prolactin receptor is expressed in UM-22B, PCI-15B, 1483, and UM-22A cells, and STAT5b is expressed in UM-22B, 1483, and UM-22A cells under normal culture conditions (Figure 18). Dose-response and time course experiments should be performed to determine optimal concentration of PRL and the best time point to observe PRL-mediated induction of STAT5 phosphorylation and downstream signaling. Additionally, the STAT3 and STAT5 knockout MEFs would be useful in these experiments to examine the function of the STAT3/5 heterodimers, and to investigate their role in the STAT3 decoy mechanism.

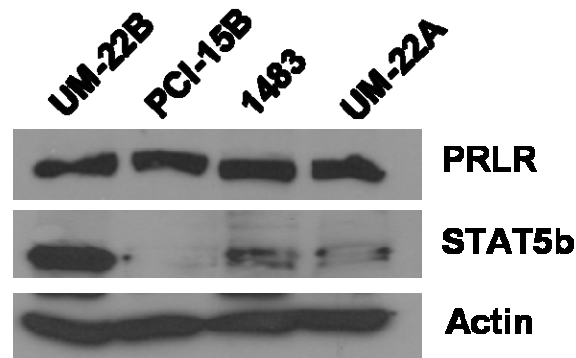


Figure 18. Prolactin receptor and STAT5b protein expression in SCCHN cell lines.

Panel of SCCHN cell lines (UM-22B, PCI-15B, 1483, and UM-22A) were immunoblotted for the prolactin receptor (PRLR) and actin (loading control).

We took an siRNA approach to examine the effects of STAT5b, but not STAT5a, on STAT3-decoy mediated growth inhibition. Our lab previously demonstrated that STAT5b but not STAT5a is responsible for tumorigenesis of squamous cells *in vitro* [233], therefore, we

focused on two STAT5b siRNA duplexes (5'-AAGCCUGGGACUCAAUAGAUCUU-3' and 5'-AAGUACUACACACCGGUCCCCUU-3') [237] from Dharmacon and tested them alone and in combination in UM-22B cells (Figure 19A). The combination of both siRNA duplexes down-regulated STAT5b protein levels at days 2 and 3. The growth of the STAT5b siRNA-transfected cells did not differ from that of untransfected control UM-22B (Figure 19B).

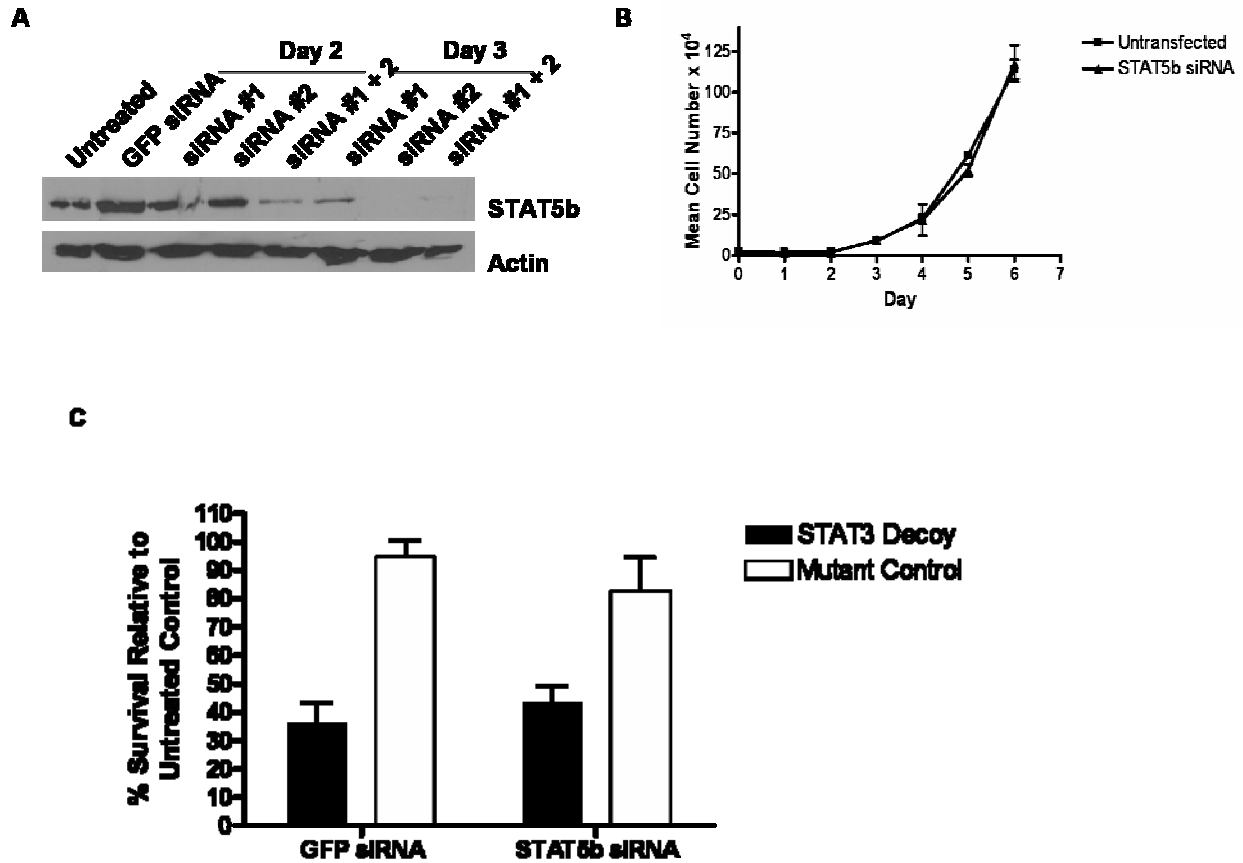


Figure 19. STAT5b is not necessary for STAT3 decoy-mediated growth inhibition of SCCHN cells.

(A) Transfection of a combination of two STAT5b siRNA duplexes into UM-22B cells was performed and protein lysates from day 2 and 3 after transfection were immunoblotted for STAT5b or β -actin (loading control). (B) Growth curves of untransfected and STAT5b siRNA-transfected UM-22B cells. (C) Cell viability of STAT5b siRNA transfected cells treated with the STAT3 decoy or GFP siRNA transfected control UM-22B cells. The experiment was performed independently three times.

After optimizing STAT5b siRNA transfection conditions, transfectants were treated with either the STAT3 decoy or mutant control decoy (Figure 19C). There was no significant difference between STAT5b siRNA-transfected cells or GFP-siRNA-transfected control cells treated with the STAT3 decoy ($43.3 \% \pm 6.0 \%$ survival compared to $35.9 \% \pm 7.4 \%$ survival, respectively, $p=0.3155$). The STAT5b siRNA data was confirmed by the previously described experiment using the STAT5 knockout MEFs (Figure 12B and 12D). These results indicate that like STAT1, STAT5b may not be necessary for STAT3 decoy-mediated growth inhibition in SCCHN cells. Further experiments to determine if stimulation of the STAT5 pathway mitigates STAT3 decoy-mediated growth inhibition should be performed.

4.2.1.2 Role of mTOR in the STAT3 decoy mechanism

Studies have provided strong evidence for mTOR as a therapeutic target in SCCHN [238, 239]. Crosstalk between mTOR and the following signaling pathways has been demonstrated: EGFR, STAT3, NF- κ B, and the prolactin receptor (PRLR) [240-244]. EGFR signals not only through the STAT3 pathway, but also through the PI3K-Akt pathway with subsequent downstream activation of mTOR. mTOR-mediated downstream effectors include p70S6 kinase (P70S6K) and eukaryotic initiation factor 4E binding protein 1 (4E-BP1), which both regulate eukaryotic protein translation. In particular, unphosphorylated 4E-BP1 binds to and represses eukaryotic initiation factor 4E (eIF4E), a protein that regulates cell growth. Gene amplification and overexpression of eIF4E protein has been reported in SCCHN, and is associated with both tumor progression and a marker for tumor recurrence [245, 246].

When an mTOR inhibitor was combined with an EGFR inhibitor in glioblastoma preclinical models, synergistic antitumor effects were observed [240]. mTOR has also been

shown to mediate serine phosphorylation (at serine 727) in the transactivation domain of STAT3, resulting in maximal activation of STAT3 [241, 243]. Given the crosstalk of mTOR with STAT3, we hypothesize that the STAT3 decoy may inhibit the mTOR pathway, contributing to the antitumor effects elicited by the STAT3 decoy.

Also, we hypothesize that combining the STAT3 decoy with an mTOR inhibitor, such as rapamycin (RAPA, sirolimus) or RAD001 (everolimus, Novartis Oncology) may result in synergistic antitumor effects for SCCHN. Rapamycin is an antibiotic that has displayed antiproliferative and antitumor activity and analogs of rapamycin are in clinical trials [247]. RAD001, an mTOR specific inhibitor that exhibits antiangiogenic activity by inhibition of VEGF production and cell proliferation [240], is orally administered and currently under phase I and II clinical trials for multiple tumor types. To date, no one has investigated the therapeutic effects of combined targeting of STAT3 and mTOR. Rao *et al.* found that combining an mTOR inhibitor (rapamycin) with an EGFR inhibitor resulted in synergistic antitumor effects in glioblastoma multiforme cell lines [240]. Preclinical *in vitro* studies combining the STAT3 decoy with an mTOR inhibitor would determine if combined inhibition of STAT3 and mTOR synergistically decreases cell survival, increases apoptosis, or decreases invasion. This therapeutic strategy can also be investigated *in vivo* using SCCHN xenograft-bearing nude mice treated with the STAT3 decoy or mutant control decoy with or without systemic administration of RAD001. Such a therapeutic strategy could be efficacious for the treatment of malignancies in which both STAT3 and mTOR are up-regulated.

4.2.2 Determining the molecular pathways affected by combined targeting of EGFR and STAT3 *in vivo*

To determine if combined targeting of EGFR and STAT3 with erlotinib and the STAT3 decoy alters SCCHN signaling *in vivo*, tumors from the mice treated with combinations of the STAT3 decoy or mutant control and/or erlotinib (Figure 14) were harvested and lysates were prepared. 50 µg protein lysate will be immunoblotted for STAT3 target gene protein expression including Bcl-X_L, VEGF, and Cyclin D1, and phosphorylation of EGFR and proteins downstream, including mTOR and p70S6 kinase. We expect that treatment with the STAT3 decoy decreased expression of the STAT3 target genes Bcl-X_L, VEGF, and cyclin D1, indicating that the STAT3 decoy inhibited the intended target. Treatment with erlotinib should inhibit phosphorylation of EGFR, as well as activation of proteins downstream of EGFR, specifically mTOR and p70S6 kinase. Such results would indicate that the STAT3 decoy inhibits STAT3 activity and that erlotinib inhibited activation of EGFR and subsequent downstream signaling. These experiments assessing intracellular signaling and pathway activation in xenografts should indicate if there is any benefit to combining erlotinib with the STAT3 decoy at the concentrations used on a molecular level. In addition, this experiment should be repeated with a lower dose of STAT3 decoy (35 µg/day). This lowering of the STAT3 decoy concentration from the previous experiment should reduce the growth inhibitory effects in the xenografts, and allow us to assess if the combination of the STAT3 decoy with erlotinib reduces tumor growth *in vivo*.

4.2.3 Future studies to investigate the therapeutic potential of EGFR, STAT3, and Bcl-X_L combined targeting for SCCHN

Studies to investigate the mechanism by which combined targeting of EGFR, STAT3, and Bcl-X_L elicits growth inhibition *in vitro* will be conducted. Western blotting for EGFR activation, STAT3 activation, and downstream signaling of EGFR (mTOR, p70S6 kinase) and STAT3 (Bcl-X_L, cyclin D1, VEGF, MMP-2, MMP-9) will be performed.

We found that apoptosis was not induced by combined targeting of erlotinib, the STAT3 decoy, and/or (-)-gossypol *in vitro*. These results are contrary to previous reports using the STAT3 decoy [54] or (-)-gossypol [179, 181, 184] in which apoptosis was induced. 24 hrs may not be the optimal time point to investigate PARP cleavage. The experiment will be repeated at earlier time points (10 minutes, 1 hr, and 12 hrs). To determine the effects of the triple combination of inhibitors, apoptosis will also be measured by procaspase 3 activation using an ELISA and by annexin V staining and subsequent cell counting of annexin V positive cells to determine induction of apoptosis. Flow cytometry will also be performed for propidium iodide staining to investigate changes in the cell cycle upon treatment of SCCHN cells with erlotinib, the STAT3 decoy, and/or (-)-gossypol. The growth inhibitory effects observed in our study may be due to inhibition of cell cycle progression as well.

The combined targeting of EGFR, STAT3, and Bcl-X_L with erlotinib, the STAT3 decoy and (-)-gossypol inhibited the growth of SCCHN cells *in vitro*. This therapeutic strategy will be investigated in an *in vivo* model of SCCHN. Nude mice bearing human SCCHN xenografts on their dorsal flanks will be treated with the STAT3 decoy delivered by intratumoral injection with erlotinib by oral gavage and/or (-)-gossypol by intraperitoneal injection.

4.2.4 Limitations of the STAT3 decoy as a treatment for SCCHN and other malignancies

This dissertation has focused on the STAT3 decoy as a treatment for SCCHN. We and others have documented the therapeutic efficacy of the STAT3 decoy for SCCHN and other malignancies [54-56]. Yet, limitations to the STAT3 decoy as a treatment in the clinic must be considered. The delivery of the STAT3 decoy by intratumoral injection is a substantial limitation to its use in the clinic. SCCHN is one disease in which the tumor is accessible in many cases, but very few malignancies have this characteristic, limiting the diseases for which the STAT3 decoy can be administered. Another limitation is the daily treatment regimen used in our *in vivo* experiments. *In vivo* studies should be performed to determine the maximum tolerated dose of the STAT3 decoy via intratumoral injection. Also, *in vivo* experiments to determine if dose of STAT3 decoy can be increased and the frequency of administration can be decreased should be performed because it is unrealistic to design a drug for the clinic that must be administered by intratumoral injection daily. Daily intratumoral injection has been the standard treatment regimen in our *in vivo* experiments. In cells, most unmodified DNA or RNA oligos have a half-life of 15 minutes or shorter [248]. Preliminary data has determined the STAT3 decoy remains intact as a double-stranded oligo for no more than 15 minutes *in vivo* (data not shown). To determine if the STAT3 decoy functions as a single-stranded decoy, *in vitro* and *in vivo* experiments comparing double- and single-stranded STAT3 decoy should be performed. One group reported that single-stranded STAT3 decoy induced apoptosis in prostate cancer cell lines *in vitro* and *in vivo*, indicating that annealing the STAT3 decoy may be unnecessary [40].

To increase biostability of the STAT3 decoy, chemical modifications can be made in addition to the phosphorothioate modification currently performed during synthesis. By

modifying the STAT3 decoy using peptide nucleic acid (PNA) technology, the STAT3 decoy efficacy may be improved. PNAs are synthetic mimics of DNA that have a modified deoxyribose phosphate backbone that is uncharged and flexible, resulting in increased binding affinity for complementary sequences and biostability [249]. Also, because PNAs have an uncharged polyamide backbone, they are not subject to the same degree of non-specific binding seen by DNA duplexes, and the half-life is at least 48 hrs [248]. Another advantage to PNAs is that they can be administered at high concentrations without toxicity. One study found that a Sp1 decoy with PNA modification inhibited Sp1 transcription, resulting in decreased expression of urokinase-type plasminogen activator receptor [250]. By combining the STAT3 decoy with PNA technology the biostability and antitumor efficacy of the STAT3 decoy could be improved. Yet, a distinct disadvantage to PNA technology is the low rate of cellular uptake observed in preclinical studies. Fisher *et al.* reported that binding of an NF- κ B transcription factor decoy to complementary PNA linked to a cell-penetrating peptide (transportan) increased cellular uptake and decreased concentrations necessary to inhibit NF- κ B binding activity *in vitro* [251]. Such a strategy could be applied to the STAT3 decoy as well to increase cellular uptake and subsequent antitumor effects.

4.3 CONCLUDING REMARKS

This dissertation has focused on the STAT3 transcription factor decoy previously designed in our laboratory. We have investigated the mechanism by which the STAT3 decoy elicits antitumor effects in SCCHN preclinical models. We found that the STAT3 decoy inhibits STAT1 signaling but that neither loss nor activation of STAT1 mitigates STAT3 decoy growth

inhibition. Also, we demonstrated that STAT3 is necessary for the STAT3 decoy-mediated growth inhibition. Our results provide rationale for mechanistic studies of transcription factor decoys. We then went on to investigate the therapeutic efficacy of combining the STAT3 decoy with an EGFR inhibitor and/or a Bcl-X_L inhibitor. We found that the triple combination of erlotinib, the STAT3 decoy, and (-)-gossypol resulted in enhanced growth inhibition of SCCHN cell lines *in vitro*. The studies performed for this dissertation have further characterized the STAT3 decoy as a therapeutic modality for SCCHN and provided evidence for combined targeting of EGFR, STAT3, and (-)-gossypol as a treatment strategy for this malignancy.

APPENDIX A

PUBLISHED WORK

Antiproliferative Mechanisms of a Transcription Factor Decoy Targeting STAT3: the Role of STAT1

Vivian Wai Yan Lui¹, **Amanda L. Boehm**², Priya Koppikar³, Rebecca J. Leeman³, Daniel Johnson^{4,5}, Michelene Ogagan³, Erin Childs³, Maria Freilino³ and Jennifer Rubin Grandis^{3,4*}

Department of ¹Clinical Oncology, The Chinese University of Hong Kong, Shatin, Hong Kong, Departments of ²Pathology, ³Otolaryngology, ⁴Pharmacology and ⁵Medicine, University of Pittsburgh and University of Pittsburgh Cancer Institute, Pittsburgh, PA 15213, USA

* Corresponding Author: Jennifer Rubin Grandis
Corresponding Address: Suite 500 Eye and Ear Institute
203 Lothrop Street
University of Pittsburgh
Pittsburgh, PA 15213
Telephone number: 412-647-5280

Fax number: 412-647-0108

Email: jgrandis@pitt.edu

Running title: STAT3 decoy effect on STAT1 signaling in SCCHN

Keywords: STAT3, STAT1 signaling, transcription factor decoy

Abbreviations: Squamous cell carcinoma of the head and neck (SCCHN); Signal Transducers and Activators of Transcription (STATs)

Text pages: 22

Number of figures: 5

Number of references: 29

Words in Abstract: 235

Words in Introduction: 437

Words in Discussion: 822

ABSTRACT

We previously developed a transcription factor decoy targeting STAT3 and reported antitumor activity in both *in vitro* and *in vivo* models of squamous cell carcinoma of the head and neck (SCCHN). Based on the known existence of STAT1-STAT3 heterodimers, the high sequence homology between STAT1 and STAT3, as well as expression of both STAT1 and

STAT3 in SCCHN, we examined whether the STAT3 decoy interferes with STAT1 signaling. SCCHN cell lines with different STAT1 expression levels (but similar STAT3 levels) were used. Both cell lines were sensitive to the growth inhibitory effects of the STAT3 decoy compared to a mutant control decoy. Intact STAT1 signaling was demonstrated by interferon-gamma (IFN- γ)-mediated induction of STAT1 phosphorylation (Tyr701) and interferon-regulatory factor-1 (IRF-1) expression. Treatment with the STAT3 decoy (but not a mutant control decoy) resulted in inhibition of IRF-1 protein expression in both cell lines, indicating specific inhibition of STAT1 signaling by the STAT3 decoy. As STAT1 is a potential tumor suppressor, we also investigated whether the therapeutic efficacy of the STAT3 decoy was mitigated by STAT1 signaling. In both PCI-15B and UM-22B cells, STAT1 siRNA treatment resulted in decreased STAT1 expression, without altering the antitumor activity of the STAT3 decoy. Similarly, the antitumor effects of the STAT3 decoy were not altered by STAT1 activation upon IFN- γ treatment. These results suggest that the therapeutic mechanisms of STAT3 blockade using a transcription factor decoy are independent of STAT1 activation.

INTRODUCTION

Signal Transducer and Activator of Transcription 3 (STAT3) has emerged as a potential molecular target for cancer therapy. STAT3 is constitutively activated and over-expressed in a variety of human malignancies, including breast, lung, prostate, brain, leukemia, multiple myeloma as well as squamous cell carcinoma of the head and neck (SCCHN) (Grandis et al., 1998; Turkson and Jove, 2000). The expression levels of activated or tyrosine phosphorylated

STAT3 have been reported to correlate with decreased survival in several cancers, including oral tongue carcinoma (Masuda et al., 2002). Molecular targeting of STAT3 using a variety of strategies in preclinical models of human cancer has been shown to inhibit tumor growth (Turkson and Jove, 2000). We previously developed a transcription factor decoy based on the STAT3 DNA binding element and demonstrated that this decoy interferes with STAT3 signaling and decreases SCCHN tumor growth *in vitro* and *in vivo* (Leong et al., 2003; Xi et al., 2005).

Transcription factor decoys are double-stranded DNA oligonucleotides that resemble the transcription factor-binding site in the promoters of target genes. Transcription factor decoys presumably bind transcription factors and sequester the targeted transcription factor, rendering it unavailable for transcription of downstream target genes. The sequence of the STAT3 decoy was derived from the serum-inducible element (SIE) of the human c-fos promoter. The therapeutic effects of the STAT3 decoy have also been demonstrated by another group in a chemically-induced skin carcinogenesis model (Chan et al., 2004) as well as in psoriasis, where STAT3 hyperactivation plays a major role (Sano et al., 2005). The regulation of STATs and the role of STAT proteins in carcinogenesis remain incompletely understood. Theoretically, targeting STAT3 using a transcription factor decoy approach may also affect the function of STAT3-associated proteins. Elucidation of the antitumor mechanisms of a STAT3 transcription factor decoy is necessary to optimize the design of clinical studies using this strategy to inhibit STAT3 signaling.

The protein sequence of STAT1 is 72% homologous with STAT3, and STAT1 has been shown to form heterodimers with STAT3. In contrast to the growth stimulatory and anti-apoptotic functions of STAT3, STAT1 is generally recognized to have a tumor suppressor function (Bromberg et al., 1998; Bromberg et al., 1996; Chin et al., 1997; Thomas et al., 2004;

Xi et al., 2006). Given the frequent expression of both STAT1 and STAT3 in cancers including SCCHN, we examined the effects of the STAT3 decoy on STAT1 signaling and the potential role of STAT1 in mediating the antitumor effects of the decoy in SCCHN. Our results demonstrate that while the STAT3 decoy disrupts STAT1 signaling, the therapeutic efficacy of the decoy is independent of STAT1 activation or expression levels.

MATERIALS AND METHODS

Plasmids and reagents:

The Gamma-activated sequence (GAS)-containing luciferase reporter plasmid, pGAS-Luc, was purchased from Stratagene (La Jolla, CA). Human interferon- γ (IFN- γ) was obtained from Roche Applied Science (Indianapolis, IN). Antibodies against STAT1, phospho-STAT1 (Tyr701), STAT3, or phospho-STAT3 (Tyr 705) were purchased from Cell Signaling Technologies (Beverly, MA). Antibodies against IRF-1 (C-20) and beta-actin were from Santa Cruz Biotechnology, Inc. (Santa Cruz, CA) and Oncogene Science, Inc (NY), respectively. Beta tubulin antibody (catalog number ab6046) was obtained from Abcam Inc. (Cambridge, MA). STAT1 (M-22) and STAT3 (C-20) antibodies used for electrophoretic mobility shift assay were purchased from Santa Cruz Biotechnology, Inc. (Santa Cruz, CA). Enhanced Chemiluminescence (ECL) kit was purchased from Santa Cruz Biotechnology, Inc. (Santa Cruz, CA). Transfection reagents, Lipofectamine 2000 and Optifect were purchased from Invitrogen (Carlsbad, CA).

Cell culture and generation of stable clones:

All head and neck squamous cell carcinoma cell lines (PCI-37A, 1483, PCI-15B, UM-22A, UM-22B) were of human origin (Lin et al., 2006). 1483 was a kind gift from Dr. Gary Clayman (MD Anderson Cancer Center, Houston, TX) and UM-22A and UM-22B lines were provided by Dr. Thomas Carey (University of Michigan, Ann Arbor, MI). The PCI-37A and PCI-15B lines were created at the University of Pittsburgh (Heo et al., 1989). Cells were maintained in DMEM with 10 % heat-inactivated fetal calf serum (Invitrogen, Carlsbad, CA) and 1x Penicillin/Streptomycin mix (Invitrogen, Carlsbad, CA) at 37°C with 5 % CO₂. STAT3 knockout and wild-type mouse embryonic fibroblasts were provided by Dr. David Levy (NYU School of Medicine, New York, NY) and were maintained in DMEM with 10 % heat-inactivated fetal calf serum (Invitrogen, Carlsbad, CA) and 1X Penicillin/Streptomycin mix (Invitrogen, Carlsbad, CA) at 37°C with 5 % CO₂ (Lee et al., 2002). STAT5A/B knockout and wild-type mouse embryonic fibroblasts provided by Dr. James Ihle (St. Jude Children's Research Hospital, Memphis TN) were grown in DMEM with 10% heat-inactivated fetal calf serum and 1X Penicillin/Streptomycin mix at 37°C with 5 % CO₂ (Teglund et al., 1998). U3A cells that do not express STAT1 were provided by Dr. Jacqueline Bromberg (Memorial Sloan Kettering Cancer Center, New York, NY). U3A cells were cultured in DMEM containing 10% Cosmic Calf Serum (Hyclone, Logan, UT) and 1X Penicillin/Streptomycin mix at 37°C with 5% CO₂ (Muller et al., 1993). For the generation of stable clones, UM-22B cells were transfected with pGAS-Luc (Stratagene, La Jolla, CA, Catalog# 219093) or pIRF-1-Luc (Panomics Inc., Redwood City CA, Catalog # LR0039) and co-transfected with pcDNA3.1 (+) carrying a G418 selection marker. Two days after transfection, cells that stably expressed luciferase were selected by G418 treatment (2 mg/ml) and stable

clones were expanded. Expression of luciferase in these clones stably expressing either pGAS-Luc or pIRF-1-Luc was confirmed by luciferase assays.

STAT3 decoy and siRNA transfection:

The STAT3 decoy and the mutant control decoy sequences (double-stranded dexoyribonucleotides with phosphorothioate modifications in the first three bases and last three bases of the sequences) were generated as previously described (Leong et al., 2003). The mutant control decoy, carrying a single base mutation, was used as a control as in previous studies (Leong et al., 2003; Xi et al., 2005). The DNAs were synthesized and purified using an oligonucleotide purification cartridge (OPC) method by the DNA Synthesis Facility at the University of Pittsburgh (Pittsburgh, PA). STAT1 siRNA SMART pool (catalog number MU-003543-01) and STAT3 On-Target Plus SMART pool siRNA was purchased from Dharmacon (catalog number L-003544-00). Decoy transfection was performed as described in the manufacturer's manual. In brief, SCCHN cells were plated ($2.5-3 \times 10^5$ /well in a 6 well tissue culture plate or 0.8×10^5 /well in a 24 well tissue culture plate). Eighteen hours after plating, cells were transfected with 102.6-1026 pM STAT3 decoy or mutant control decoy as a control. For cytotoxicity studies, the transfection medium was replaced with complete DMEM after 5 hrs of transfection. For STAT1 signaling studies, IFN- γ was added into the transfection medium 1 hr after transfection. For siRNA transfection, 1200 pmoles of siRNA was used to transfect a T-75 flask of cells.

Electrophoretic mobility shift assay:

20 µg UM-22B cell lysate was incubated for 1 hr with STAT1 and/or STAT3 antibodies (Santa Cruz). Radiolabeled high affinity serum inducible element (hSIE) duplex oligonucleotide or a mutant hSIE duplex oligonucleotide was incubated with the cell extract and antibodies (Wagner et al., 1990). Samples were then run on 4% nondenaturing polyacrylamide gels which were dried at 65°C for 1 hr. Supershifted proteins were then visualized by autoradiography.

Western blotting:

Cells were lysed in western lysis buffer [1 % Nonidet-P40, 150 mM NaCl, 1 mM EDTA, 10 mM sodium phosphate buffer (pH 7.2), 0.25 mM DTT, 1 mM PMSF, 10 µg/ml leupeptin and 10 µg/ml aprotinin] for 5 mins at 4°C. Lysates were then centrifuged at 4°C, 12000 rpm for 15 mins, and supernatants were collected for protein quantitation. Protein quantitation was performed using the Protein Assay Solution (BioRad Laboratories, Hercules, CA). Proteins (50 µg/lane) were then resolved on 10 % SDS-PAGE gels and transferred onto Trans-Blot nitrocellulose membranes (BioRad Laboratories, Hercules, CA) using a semi-dry transfer machine (BioRad Laboratories, Hercules, CA). Following transfer, membranes were incubated at 4°C overnight in blocking solution containing 5% non-fat dry milk, 0.2 % Tween 20 in 1 x PBS (TBST). Membranes were then incubated with primary antibody at room temperature for 2 hrs, then washed 3 times with TBST (10 mins/wash). The membranes were then incubated with secondary antibody for 1 h at room temperature, followed by 3 washes in TBST. Blots were developed using ECL, according to the manufacturer's instruction (Santa Cruz Biotechnology, Inc., Santa Cruz, CA).

MTT assay and cell counting:

To determine survival of SCCHN cells in response to various treatments, MTT assays were performed in 24 well plates. MTT solution was prepared from MTT powder (Sigma, Catalog # M5655) in 1x PBS (final concentration of 5mg/ml). Twenty-four hrs after the STAT3 decoy treatment, MTT solution was added to each well and incubated at 37°C for 1 h. MTT solution was then removed and DMSO (300 µl) was added to each well. The optical density of each well was determined using a microplate reader set at 570 nm. The percentage cell proliferation was calculated using the following equation: Percentage proliferation = (Treatment/Untreated) x 100 %.

Cell counting experiments were performed using trypan blue dye exclusion assay. Cells were trypsinized and after lifting off of the plate, trypsin was neutralized with DMEM. Cells were centrifuged and pellet was resuspended in fresh media. Cells were then combined with trypan and counted using a hemacytometer. Cell proliferation was then calculated relative to the untreated control using the following equation: Percentage proliferation = (Treatment/Untreated) x 100 %.

Luciferase assay:

Stable clones of pGAS-Luc or pIRF-1-Luc were generated in the UM-22B cell line using G418 selection media as described above. Transient transfections of STAT3 decoy and mutant control decoy were performed as described above using 690 pM STAT3 decoy or mutant control decoy. 5 hr after transfection, the transfection medium was removed and replaced with DMEM (10% FBS, 1X Penicillin/Streptomycin) with or without 200 U/ml of IFN- γ . After 24 hours cells were

lysed in luciferase lysis buffer (0.05% Triton X-100, 2 mM EDTA and 0.1 M Tris-HCl at pH 7.8) for 5 mins on ice. Lysates were then centrifuged at 14,000 rpm for 5 min at 4°C. Supernatants were collected and assayed for luciferase activity using the luciferase assay kit from Promega (Madison, WI). Luminescence was measured with a luminometer (Wallac Inc., Gaithersburg, MD). Luciferase activity was normalized as relative light units per microgram of total protein in the supernatant (RLU/ μ g protein). Fold changes with reference to the untreated control were calculated.

Statistical analysis:

Using StatXact software with Cytel Studio (Cytel Software Corporation, Cambridge, MA, USA). P-values were obtained by the Wilcoxon-Mann-Whitney test ($p < 0.05$ was considered significant).

RESULTS

STAT3 decoy inhibition of SCCHN growth does not correlate with STAT1 levels

Given the expression of both STAT1 and STAT3 in SCCHN, we investigated the potential role of STAT1 signaling on the antitumor activity of the STAT3 decoy in SCCHN cell lines. We first examined the expression levels of STAT1 and STAT3 in a panel of SCCHN cell lines, including PCI-37A, 1483, PCI-15B, UM-22A, and UM-22B in order to compare the effects of the decoy in cells expressing different levels of STAT1 (Fig. 1A). STAT1 was expressed at high levels in two SCCHN cell lines (PCI-15B, and UM-22A), and expressed at relatively lower levels in PCI37A, 1483 and UM-22B. All five SCCHN cell lines expressed high levels of STAT3. Two

SCCHN cell lines, PCI-15B and UM-22B, which expressed similar levels of STAT3 but different levels of STAT1 protein, were then chosen for further study. PCI-15B expressed a higher level of STAT1 than UM-22B. As shown in Figure 1B, treatment of PCI-15B cells with 690 pM STAT3 decoy resulted in only 34% ($\pm 1.8\%$) proliferation at 24 hrs, while the mutant control decoy treatment resulted in 94.1% ($\pm 6.7\%$) cell proliferation. In UM-22B, the SCCHN cell line expressing lower STAT1 levels, treatment with the STAT3 decoy resulted in 17.0% ($\pm 1\%$) cell proliferation, while the control decoy treatment resulted in 75.5% ($\pm 1.1\%$) proliferation. Similar results were observed by trypan blue dye exclusion assay (Figure 1C), in which the STAT3 decoy treatment resulted in 26.4% ($\pm 8.9\%$) proliferation in UM-22B cells while the control decoy treatment resulted in 98.0% ($\pm 2.3\%$) proliferation. PCI-15B cells treated with the STAT3 decoy resulted in 43.9% ($\pm 1.4\%$) cell proliferation, and 101% ($\pm 5.0\%$) of the control decoy treated cells proliferated after 24 hrs. These results demonstrate that SCCHN cell lines (PCI-15B and UM-22B) with high or low expression levels of STAT1, were equally sensitive to the cytotoxic effects of the STAT3 decoy. These results are supported by our previous observations that 1483, a SCCHN cell line with relatively lower levels of STAT1 and high levels of STAT3, was also sensitive to the cytotoxicity of the STAT3 decoy (Leong et al., 2003; Xi et al., 2005).

STAT1 signaling is intact in SCCHN cells

Since the cytotoxic effect of the STAT3 decoy was not diminished in SCCHN cell lines over-expressing STAT1, we next examined whether the STAT1 activation pathway was intact in SCCHN cells. IFN- γ is known to activate the STAT1 pathway through tyrosine phosphorylation of STAT1 (Tyr 701) and induction of the STAT1 target gene, IRF-1. Both PCI-15B and UM-

22B cells were serum-starved for 48 hrs and then treated with IFN- γ for up to 24 hrs (Fig. 2). In both cell lines, short-term IFN- γ treatment induced a dramatic and persistent phosphorylation of STAT1 (Tyr 701) without significant changes in total STAT1 levels until the 24 hr time point. In addition, intact IFN- γ -induced STAT1 signaling was further demonstrated by the rapid induction of IRF-1 expression, a known STAT1 target gene. Maximal IRF-1 induction was observed at 4 and 24 hrs after IFN- γ treatment in both cell lines. In fact, IRF-1 expression persisted for up to 72 hrs following IFN- γ treatment, although at much lower levels (data not shown). Therefore, STAT1 signaling is intact in SCCHN cell lines that are susceptible to the cytotoxic effects of the STAT3 decoy.

STAT3 decoy disrupts STAT1 signaling

We and others have previously shown that the STAT3 decoy inhibits STAT3 signaling in several disease models including SCCHN, skin cancer and psoriasis (Xi et al., 2005) (Chan et al., 2004; Leong et al., 2003; Sano et al., 2005). STAT1 shares the highest homology with STAT3 among the STAT family members and it is known to associate with STAT3 through direct heterodimer formation. Theoretically, targeting STAT3 using a transcription factor decoy approach may also affect the function of STAT3-associated proteins. Among the known STAT3-associated proteins, STAT1 is also of particular interest in this context because contrary to the growth stimulatory and anti-apoptotic functions of STAT3, STAT1 is generally recognized to have tumor suppressor functions (Xi et al., 2006). Therefore, we investigated the effects of the STAT3 decoy on STAT1 signaling by examining the effects of the decoy on STAT1 transcriptional activity and STAT1 target gene expression. SCCHN cells were stably transfected with a STAT1 reporter construct expressing luciferase from a pGAS-Luc, containing 4 gamma activated sequence (GAS)

enhancer elements, which are specific for STAT1 (Fig. 3A). In the absence of IFN- γ , the pGAS-Luc stable cell line expressed a low level of luciferase (41.3 ± 1.4 RLU/ μ g protein), indicating a low level of endogenous STAT1 activation. Treatment with the STAT3 decoy slightly inhibited luciferase activity (13.2 ± 0.3 RLU/ μ g protein) when compared with the mutant control decoy (38.1 ± 1.5 RLU/ μ g protein). The pGAS-Luc stable cell line was highly responsive to IFN- γ , indicating intact STAT1 signaling. In the presence of IFN- γ , luciferase activity increased markedly by 57 fold (from 41.3 ± 1.4 to 2350 ± 39.6 RLU/ μ g protein). Treatment with the STAT3 decoy, but not the mutant control decoy, completely abrogated luciferase activity in the pGAS-Luc stable cell line (STAT3 decoy treatment: 25.8 ± 1.8 RLU/ μ g protein; control decoy treatment: 2260 ± 13.3 RLU/ μ g protein). We next investigated whether expression of the STAT1 target gene, IRF-1, was affected by the STAT3 decoy. When SCCHN cells were treated with the STAT3 decoy for only 5 hrs (in the presence or absence of IFN- γ), induction of IRF-1 protein was markedly inhibited (Fig. 3B). Consistent with this result, we observed significant inhibition of IRF-1 transcriptional activity using a reporter gene system. A SCCHN cell line stably expressing an IRF-1-Luc reporter gene (carrying 6 copies of IRF-1-responsive element) was employed (UM-22B). Treatment with the STAT3 decoy, but not the mutant control decoy, completely abrogated the IFN- γ -induced expression of luciferase in the IRF-1-Luc stable cell line (Fig. 3C). We previously reported that the STAT3 decoy abrogates STAT3 DNA binding on gel shift assays (Leong et al., 2003). To determine the effect of the decoy on STAT dimers, we performed supershift experiments using STAT1 and/or STAT3-specific antisera. As shown in Figure 3D, STAT1 homodimers, STAT3 homodimers, as well as STAT1/3 heterodimers were all supershifted from the DNA binding complex on gel shift. Taken together, these results demonstrated that STAT3 decoy inhibited STAT1-mediated DNA binding and transcription.

These cumulative results suggest that the STAT3 decoy (but not the mutant control decoy) may sequester STAT1 in addition to STAT3 (or sequester STAT1/STAT3 heterodimer) and hence, disrupt STAT1 function and transcriptional activity.

STAT1 does not mediate the cytotoxic effects of the STAT3 decoy

STAT1 has been reported to function as a tumor suppressor in human cancer including SCCHN (Xi et al., 2006). We therefore investigated whether STAT1 contributes to the cytotoxic effects of the STAT3 decoy in SCCHN cells. STAT1 SMART pool siRNA was used to specifically down-regulate the expression of STAT1 in SCCHN cells. As shown in Figure 4A, STAT1 siRNA transfection of UM-22B for 4 hrs resulted in a knockdown of STAT1 expression for up to 6 days. Similar results were observed in PCI-15B cells (data not shown). To determine whether STAT1 knockdown using siRNA abrogated STAT1 signaling, we examined the effects of IFN- γ on IRF-1 expression in the presence and absence of STAT1 siRNA. As shown in Figure 4B, treatment of the SCCHN cells with STAT1 siRNA led to the failure of IFN- γ to induce IRF-1 expression in these cells. In contrast, treatment of the same cells with siRNA directed against STAT3 did not mitigate IFN- γ induction of IRF-1 (Figure 4C). We then evaluated the impact of STAT3 decoy on cells transfected with STAT1 siRNA (or GFP siRNA as control). After transfection with STAT1 siRNA, cells were replated for STAT3 decoy treatment. After an additional 72 hrs, cell viabilities were determined. As shown in Figure 4D, STAT1 siRNA transfection did not alter the growth inhibitory effects of the STAT3 decoy in both PCI-15B and UM-22B cells. In PCI-15B cells, STAT3 decoy treatment resulted in 47.4 % (\pm 1.5 %) and 46.9 % (\pm 4.3 %) cell proliferation in the GFP siRNA transfected and STAT1 siRNA transfected PCI-15B cells, respectively. The mutant control decoy resulted in 83 % (\pm 6.2 %) and 81.3 % (\pm 4.1

%) cell proliferation in the GFP siRNA and STAT1 siRNA transfected PCI-15B cells, respectively. Similar results were observed in UM-22B cells where STAT3 decoy treatment elicited 54.5 % (\pm 1.3 %) cell proliferation in GFP siRNA transfectants, and 63.1 % (\pm 2.0 %) in STAT1 siRNA transfectants. The mutant control decoy failed to inhibit cell proliferation. To confirm these results in a genetically defined system, the effects of the decoy was examined in STAT1 knockout MEFs. As shown in Figure 4E the STAT3 decoy inhibited the growth of STAT1 deficient cells as well as cells derived from wild-type MEFs. These results suggest that expression of STAT1 neither contributes to nor is required for the cytotoxic effects of the STAT3 decoy in SCCHN cells.

STAT1 activation does not alter the cytotoxicity of the STAT3 decoy

We next examined whether activation of STAT1 by IFN- γ would affect the cytotoxicity of the STAT3 decoy. As shown in Figure 4F, treatment of STAT3 decoy-transfected cells with increasing doses of IFN- γ did not result in any significant changes in the cytotoxicity of the STAT3 decoy ($p=0.9$ in PCI-15B and $p=0.6$ in UM-22B). In PCI-15B cells, the percentage cell proliferation with the STAT3 decoy alone, or the STAT3 decoy plus IFN- γ was 17% \pm 1.0 %, and 18.3% \pm 0.17 %, respectively. Similar results were observed in UM-22B cells, where the STAT3 decoy alone, or the STAT3 decoy plus IFN- γ resulted in 10.7% \pm 1.2 % and 13.1 \pm 1.0 % proliferation relative to control, respectively. Thus, activation of STAT1 pathway by IFN- γ does not alter the growth inhibitory effects of the STAT3 decoy in SCCHN cells. This suggests that the efficacy of the STAT3 decoy is independent of STAT1 activation, and that the STAT3 decoy can inhibit tumor cell growth even in the presence of STAT1 signaling.

STAT3 is required for growth inhibition by the STAT3 decoy

To determine if STAT3 is necessary for decoy-mediated cell killing, we examined the growth inhibitory effects of the decoy on STAT3 knockout and wild-type murine embryonic fibroblasts (MEFs) (a kind gift from Dr. David Levy). We first confirmed that the STAT3 knockout cells did not express STAT3 compared with the wild-type cells, and also found that both cell lines express comparable levels of STAT1 (data not shown). The MEFs were plated at a density of 5×10^4 cells in 12 well plates and transfected with 1026 pM STAT3 decoy or mutant control decoy. Cell counts, performed after 24hrs of transfection demonstrated that the percentage survival of the STAT3 knockout MEFs treated with the STAT3 decoy was $81.8 \pm 9\%$ as compared to $29.5 \pm 6\%$ survival of the wild-type MEF cells (Fig. 5A). We previously reported a lack of cytotoxic effects of the STAT3 decoy on normal epithelial cells when used at a concentration of 250.3 nM without lipid-mediated transfection (Leong et al., 2003). To verify that the growth inhibition of the wild-type MEFs by the STAT3 decoy was due to the higher concentrations of the decoy used in this assay, we repeated the experiment using a lower concentration of the decoy that we previously used to treat the SCCHN cell lines (102.6 pM) and observed that the survival of wild-type or STAT3 knockout MEFs was not impacted when this lower dose of the STAT3 decoy was employed (94% and 102%, respectively) (data not shown). To determine the specific requirement of STAT3 to mediate the growth inhibitory effects of the STAT3 decoy, cells derived from STAT5 deficient mice (and cells from their wild-type counterparts) were also treated with the high concentration of the STAT3 decoy. These cells have been previously reported to express STATs 1 and 3 (Teglund et al., 1998). In contrast to the results obtained in the STAT3-deficient cells, there was no difference in the effects of the STAT3 decoy on the growth of the STAT5 knockout cells or cells derived from their wild-type littermates (Fig. 5B).

These results indicate that STAT3 is specifically required for the antiproliferative effects of the STAT3 decoy.

DISCUSSION

In this study, we investigated the potential role of STAT1 on the antiproliferative effects of a STAT3 transcription factor decoy and the reciprocal effects of the STAT3 decoy on STAT1 signaling in SCCHN cells. STAT1 is a potential tumor suppressor that is known to associate with STAT3. Our results demonstrate that the STAT3 decoy inhibits SCCHN growth independent of STAT1 levels and STAT1 activation status. SCCHN cells with either high or low levels of STAT1 were equally sensitive to the growth inhibitory effects of the decoy. Down-regulation of STAT1 levels by siRNA or activation of STAT1 signaling by IFN- γ did not affect the growth inhibitory effects of the STAT3 decoy. In addition, we found that the STAT3 decoy disrupts STAT1 signaling, inhibits STAT1 target gene levels and STAT1 transcriptional activity. These results suggest that STAT1 does not contribute to the antitumor activity of the STAT3 decoy in SCCHN cells. Therefore, a STAT3 decoy has therapeutic potential for treating cancers with active STAT3 and STAT1 signaling.

Transcription factor decoys are double-stranded DNA oligonucleotides that closely resemble the transcription factor-binding site (or DNA binding sequence) in the promoters of target genes. Decoys presumably bind and sequester the targeted transcription factor, rendering it unavailable for transcription of downstream target genes, thus resulting in specific transcriptional inhibition. A transcription factor decoy approach was originally used for the study of gene expression mediated by transcription factors (Cho et al., 2002; Gambarotta et al., 1996). Because

of the sequence specific characteristics of a transcription factor decoy, it is an attractive approach to target transcription factors. Transcription factor decoys targeting a variety of transcription factors have been developed for E2F, NF- κ B, p53, AP-1, ets, Sp1 and estrogen receptor in a variety of disease models [reviewed in (Gambari, 2004)]. Many transcription factors have important roles in carcinogenesis and a number of transcription factor decoys have been shown to inhibit human cancer growth in preclinical models (Ahn et al., 2003; Alper et al., 2001; Ishibashi et al., 2000; Kuratsukuri et al., 1999; Leong et al., 2003; Xi et al., 2006). Both STAT1 and STAT3 interact with other proteins and transcription factors. STAT1 binds to the TNF α receptor signaling complex and inhibit NF- κ B (Wang et al., 2000). STAT1 has also been demonstrated to bind to p53 through protein-protein interactions (Townsend et al., 2004). STAT3, like STAT1, interacts with other factors including PIAS3, GRIM-19 and EZ1 (Chung et al., 1997; Nakayama et al., 2002; Zhang et al., 2003). Although the signal transduction events mediated by STAT1 and STAT3 were initially characterized in the context of DNA binding, it now appears that a co-activator mechanism that does not involve DNA binding, can explain some of the consequences of STAT activation. However, the effects of transcription factor decoys designed to inhibit a specific transcription factor, on other transcriptions factors or interacting proteins is largely unexplored.

Theoretically, inhibition of a tumor suppressor function should lead to enhanced tumor growth. However, this does not seem to be the case when STAT1 signaling is inhibited by the STAT3 decoy. This could be explained by the fact that the function of STAT1 in cancer is still incompletely understood. In addition to a potential tumor suppressor role, STAT1 may also have other unknown functions such as regulation of apoptosis (Thomas et al., 2004). STAT1 overexpression has been shown to induce chemosensitization in SCCHN (Xi et al., 2006) and

STAT1-deficient cells are resistant to tumor necrosis factor-alpha-induced apoptosis (Kumar et al., 1997). In addition, it is possible that the tumor suppressor activity of STAT1 is restricted to cancer development and not cancer progression. Therefore, abrupt inhibition of STAT1 activity by the decoy may not have an effect on cancer cell proliferation. In a syngeneic model murine squamous cell carcinoma, STAT1 deficiency in the host enhanced interleukin-12-mediated tumor regression (Torrero et al., 2006). These cumulative results suggest that the effects of STAT1 signaling on tumor formation and progression are likely dependent on the specific growth factors, cytokines and other transcription factors that are present in the tumor microenvironment. The ability of the decoy to inhibit STAT1 as well as STAT3 action, raises the possibility that the STAT3 decoy may have actions beyond inhibiting STAT3 in cancer cells, which might limit its potential usefulness as a therapeutic reagent.

Our findings have several clinical implications. Although STAT1 and STAT3 (with relatively opposed functions) are both expressed in a wide variety of cancers, including SCCHN, targeting of STAT3 using a transcription factor decoy approach can still be safely used as an anticancer treatment since inhibition of STAT1 signaling does not mitigate the therapeutic efficacy of the STAT3 decoy. Molecular targeting using a transcription factor decoy approach should be accompanied by a careful examination of the effects on other transcription factors or proteins associated with the transcription factor that is being specifically targeted. In this case, targeting of STAT3 by the STAT3 decoy disrupts STAT1 signaling in SCCHN. Transcription factors are known to function in large multiprotein complexes comprising multiple regulatory proteins, co-factors and related DNA elements. Therefore, targeting using a transcription factor decoy approach may offer an advantage (compared with an siRNA or antisense approach) of simultaneously inhibiting multiple proteins in the transcription complex.

FIGURE LEGENDS

Figure 1. STAT1 levels do not correlate with SCCHN growth inhibition by the STAT3 decoy. (A) Expression levels of STAT1 and STAT3 in a panel of SCCHN cell lines (PCI-37A, 1483, PCI-15B, UM-22A, UM-22B). Fifty micrograms of protein were loaded for immunoblotting with antibodies against STAT1 and STAT3. Beta-actin was performed as a loading control. (B) STAT3 decoy effects on proliferation in two SCCHN cell lines expressing different levels of STAT1. Both PCI-15B and UM-22B cells (0.6×10^5 cells) were transfected with 690 pM STAT3 decoy or the mutant control decoy and compared with an untransfected control (untreated). Inhibition of cell proliferation was determined by MTT assay at 24 hrs post-transfection. (C) STAT3 decoy effects on cell proliferation was also examined by trypan blue dye exclusion assays. PCI-15B and UM-22B cells were transfected with 690 pM STAT3 decoy or control decoy and compared to an untransfected control (untreated). Experiments were performed in triplicate wells and performed 3 times with similar results.

Figure 2. STAT1 signaling is intact in SCCHN cells. PCI-15B and UM-22B cells were first serum-starved for 48 hrs and then stimulated with IFN- γ (200 U/ml) for 10 mins, 30 mins, 1, 4 and 24 hrs, respectively. The levels of phospho-STAT1 (Tyr 701), total STAT1, and IRF-1 were determined by immunoblotting (50 μ g of protein were loaded). Beta-actin was performed as a loading control. The experiment was performed 3 times with similar results.

Figure 3. STAT3 decoy disrupts STAT1 signaling. (A) The STAT3 decoy inhibited the expression of STAT1 promoter activity in a cell line (UM-22B) stably expressing pGAS-Luc. The stable cell line was transfected with 690 pM STAT3 decoy or the mutant control decoy. Luciferase assay was performed 24 hrs after transfection. Fold change was calculated with reference to the untransfected control (without IFN- γ). Experiments were performed in triplicate wells and performed a total of 3 times with similar results obtained in each independent experiment. (B) Expression of an IFN- γ -responsive STAT1 target gene, IRF-1, was specifically down-regulated by the STAT3 decoy upon IFN- γ treatment. SCCHN cells were transfected with the STAT3 decoy or mutant control decoy for a total of 5 hrs (in a 6 well plate). In the IFN- γ -treated group, IFN- γ (200 U/ml) was added 1 h after transfection for an additional 4 hrs. Cells were then collected for immunoblotting for IRF-1. Beta-actin was performed as a loading control. Experiments were performed a total of 3 times with similar results obtained in each independent experiment. (C) Specific down-regulation of the transcriptional activity of IRF-1 by the STAT3 decoy. A SCCHN cell line (UM-22B) stably expressing IRF-1-Luc was used to examine the effect of the STAT3 decoy on IRF-1 transcriptional activity. Cells were transfected with 690 pM of the STAT3 decoy or the mutant control decoy. Luciferase assay was performed 24 hrs after transfection. Fold change was calculated with reference to the untreated (no decoy or IFN- γ) IRF-1-Luc control cells. Experiments were performed in triplicate wells and independently performed 3 times with similar results. (D) STAT 1 homodimers, STAT3 homodimers and STAT1/3 heterodimers can be supershifted from the DNA binding complex following treatment with the STAT3 decoy, but not the mutant control decoy. 20 μ g whole cell lysate from UM-22B cells was

preincubated with STAT1 and/or STAT3 antibodies and then radiolabeled using hSIE or a mutant hSIE probe.

Figure 4. STAT1 does not contribute to the cytotoxic effects of the STAT3 decoy in SCCHN cells. (A) UM-22B cells (a T-75 flask) were transfected with 1200 pmoles of GFP siRNA (control) or STAT1 siRNA for 4 hrs. Cells were collected at days 2, 3 and 4 for the analysis of STAT1 protein levels by immunoblotting. (B) Untreated, GFP siRNA, or STAT1 siRNA transfected UM-22B cells were stimulated with IFN- γ (200U/ml) for 4 hrs. Lysates were collected after 24 hrs and were immunoblotted for STAT1, IRF-1, and β -tubulin. (C) Untreated, GFP siRNA, and STAT3 siRNA transfected UM-22B cells were stimulated with IFN- γ (200U/ml) for 4 hrs. Lysates were collected after 24 hrs and were immunoblotted for STAT3, IRF-1, and β -tubulin. (D) Down-regulation of endogenous STAT1 by STAT1 siRNA did not affect the cytotoxic effects of the STAT3 decoy in SCCHN cell lines. PCI-15B and UM-22B cells were first transfected with the STAT1 siRNA (or GFP siRNA as control) and plated for STAT3 decoy treatment. MTT assay was performed 72 hrs after decoy treatment. The percentage proliferation after STAT3 decoy treatment (filled bars) and the mutant control decoy (open bars) was calculated using untransfected cells as control. Experiments were performed in triplicate wells and independently repeated 3 times. (E) STAT3 decoy-mediated decrease in cell survival in STAT1 knockout cells is not significantly different from that of wild-type cells ($p=0.5$). STAT1 knockout cells (U3A) and wild-type MEFs were transfected with 1026 pM STAT3 decoy or mutant control decoy. After 24 hrs, cell counts using trypan blue dye exclusion assay were performed. Experiment was performed independently in

triplicate 3 times. (F) Activation of STAT1 signaling by IFN- γ did not affect the cytotoxic effects of the STAT3 decoy in HNSCC. Both PCI-15B and UM-22B cells were transfected with 540 pM of the STAT3 decoy or mutant control decoy. At 5 h after transfection, the transfection medium was removed and replaced with either complete DMEM, DMEM + 200 U/ml of IFN- γ . MTT assay was performed at 24 hrs after transfection. Experiments were performed in triplicate wells and independently performed in triplicate wells and independently performed 3 times with similar results.

Figure 5. STAT3 is required for STAT3 decoy-mediated growth inhibition. (A) STAT3 knockout or wild-type MEFs (4×10^4 cells) were plated in 12-well plates and transfected with 1025 pM of the decoy or the mutant control decoy. Cell counts were performed 24hrs after transfection. EGFP control plasmid was used to measure transfection efficiency (80-90%). This figure represents cumulative results of three independent experiments. (B) STAT5 knockout or wild-type MEFs were plated in 12 well plates and transfected with 1025 pM of the decoy or mutant control decoy. Cell counts were performed 24 hrs after transfection, and the data represent the cumulative results of 3 independent experiments.

Acknowledgements: This work was supported by NIH grants RO1-CA101840, R01-CA77308 and P50-CA097190 (to JRG).

REFERENCES

- Ahn JD, Kim CH, Magae J, Kim YH, Kim HJ, Park KK, Hong S, Park KG, Lee IK and Chang YC (2003) E2F decoy oligodeoxynucleotides effectively inhibit growth of human tumor cells. *Biochem Biophys Res Commun* 310(4):1048-1053.
- Alper O, Bergmann-Leitner ES, Abrams S and Cho-Chung YS (2001) Apoptosis, growth arrest and suppression of invasiveness by CRE-decoy oligonucleotide in ovarian cancer cells: protein kinase A down-regulation and cytoplasmic export of CRE-binding proteins. *Mol Cell Biochem* 218(1-2):55-63.
- Bromberg JF, Fan Z, Brown C, Mendelsohn J and Darnell JE, Jr. (1998) Epidermal growth factor-induced growth inhibition requires Stat1 activation. *Cell Growth Differ* 9(7):505-512.
- Bromberg JF, Horvath CM, Wen Z, Schreiber RD and Darnell JE, Jr. (1996) Transcriptionally active Stat1 is required for the antiproliferative effects of both interferon alpha and interferon gamma. *Proc Natl Acad Sci U S A* 93(15):7673-7678.
- Chan KS, Sano S, Kiguchi K, Anders J, Komazawa N, Takeda J and DiGiovanni J (2004) Disruption of Stat3 reveals a critical role in both the initiation and the promotion stages of epithelial carcinogenesis. *J Clin Invest* 114(5):720-728.
- Chin YE, Kitagawa M, Kuida K, Flavell RA and Fu XY (1997) Activation of the STAT signaling pathway can cause expression of caspase 1 and apoptosis. *Mol Cell Biol* 17(9):5328-5337.
- Cho YS, Kim MK, Cheadle C, Neary C, Park YG, Becker KG and Cho-Chung YS (2002) A genomic-scale view of the cAMP response element-enhancer decoy: a tumor target-based genetic tool. *Proc Natl Acad Sci U S A* 99(24):15626-15631.
- Chung CD, Liao J, Liu B, Rao X, Jay P, Berta P and Shuai K (1997) Specific inhibition of Stat3 signal transduction by PIAS3. *Science* 278(5344):1803-1805.
- Gambari R (2004) New trends in the development of transcription factor decoy (TFD) pharmacotherapy. *Curr Drug Targets* 5(5):419-430.

- Gambarotta G, Boccaccio C, Giordano S, Ando M, Stella MC and Comoglio PM (1996) Ets up-regulates MET transcription. *Oncogene* 13(9):1911-1917.
- Grandis JR, Drenning SD, Chakraborty A, Zhou MY, Zeng Q, Pitt AS and Tweardy DJ (1998) Requirement of Stat3 but not Stat1 activation for epidermal growth factor receptor- mediated cell growth in vitro. *J Clin Invest* 102(7):1385-1392.
- Heo DS, Snyderman C, Gollin SM, Pan S, Walker E, Deka R, Barnes EL, Johnson JT, Herberman RB and Whiteside TL (1989) Biology, cytogenetics, and sensitivity to immunological effector cells of new head and neck squamous cell carcinoma lines. *Cancer Res* 49(18):5167-5175.
- Ishibashi H, Nakagawa K, Onimaru M, Castellanos EJ, Kaneda Y, Nakashima Y, Shirasuna K and Sueishi K (2000) Sp1 decoy transfected to carcinoma cells suppresses the expression of vascular endothelial growth factor, transforming growth factor beta1, and tissue factor and also cell growth and invasion activities. *Cancer Res* 60(22):6531-6536.
- Kumar A, Commane M, Flickinger TW, Horvath CM and Stark GR (1997) Defective TNF-alpha-induced apoptosis in STAT1-null cells due to low constitutive levels of caspases. *Science* 278(5343):1630-1632.
- Kuratsukuri K, Sugimura K, Harimoto K, Kawashima H and Kishimoto T (1999) "Decoy" of androgen-responsive element induces apoptosis in LNCaP cells. *Prostate* 41(2):121-126.
- Lee CK, Raz R, Gimeno R, Gertner R, Wistinghausen B, Takeshita K, DePinho RA and Levy DE (2002) STAT3 is a negative regulator of granulopoiesis but is not required for G-CSF-dependent differentiation. *Immunity* 17(1):63-72.
- Leong PL, Andrews GA, Johnson DE, Dyer KF, Xi S, Mai JC, Robbins PD, Gadiparthi S, Burke NA, Watkins SF and Grandis JR (2003) Targeted inhibition of Stat3 with a decoy oligonucleotide abrogates head and neck cancer cell growth. *Proc Natl Acad Sci U S A* 100(7):4138-4143.
- Lin CJ, JR G, Carey TE, Whiteside TL, Gollin SM, Ferris RL and Lai SY (2006.) Head and neck Squamous cell carcinoma cell lines: Established models and rationale for selection. *Head and Neck*, Published online in advance of print.

- Masuda M, Suzui M, Yasumatu R, Nakashima T, Kuratomi Y, Azuma K, Tomita K, Komiyama S and Weinstein IB (2002) Constitutive activation of signal transducers and activators of transcription 3 correlates with cyclin D1 overexpression and may provide a novel prognostic marker in head and neck squamous cell carcinoma. *Cancer Res* 62(12):3351-3355.
- Muller M, Laxton C, Briscoe J, Schindler C, Improta T, Darnell JE, Jr., Stark GR and Kerr IM (1993) Complementation of a mutant cell line: central role of the 91 kDa polypeptide of ISGF3 in the interferon-alpha and -gamma signal transduction pathways. *Embo J* 12(11):4221-4228.
- Nakayama K, Kim KW and Miyajima A (2002) A novel nuclear zinc finger protein EZI enhances nuclear retention and transactivation of STAT3. *Embo J* 21(22):6174-6184.
- Sano S, Chan KS, Carbajal S, Clifford J, Peavey M, Kiguchi K, Itami S, Nickoloff BJ and DiGiovanni J (2005) Stat3 links activated keratinocytes and immunocytes required for development of psoriasis in a novel transgenic mouse model. *Nat Med* 11(1):43-49.
- Teglund S, McKay C, Schuetz E, van Deursen JM, Stravopodis D, Wang D, Brown M, Bodner S, Grosveld G and Ihle JN (1998) Stat5a and Stat5b proteins have essential and nonessential, or redundant, roles in cytokine responses. *Cell* 93(5):841-850.
- Thomas M, Finnegan CE, Rogers KM, Purcell JW, Trimble A, Johnston PG and Boland MP (2004) STAT1: a modulator of chemotherapy-induced apoptosis. *Cancer Res* 64(22):8357-8364.
- Torrero MN, Xia X, Henk W, Yu S and Li S (2006) Stat1 deficiency in the host enhances interleukin-12-mediated tumor regression. *Cancer Res* 66(8):4461-4467.
- Townsend PA, Scarabelli TM, Davidson SM, Knight RA, Latchman DS and Stephanou A (2004) STAT-1 interacts with p53 to enhance DNA damage-induced apoptosis. *J Biol Chem* 279(7):5811-5820.

- Turkson J and Jove R (2000) STAT proteins: novel molecular targets for cancer drug discovery. *Oncogene* 19(56):6613-6626.**
- Wagner BJ, Hayes TE, Hoban CJ and Cochran BH (1990) The SIF binding element confers sis/PDGF inducibility onto the c-fos promoter. *Embo J* 9(13):4477-4484.**
- Wang Y, Wu TR, Cai S, Welte T and Chin YE (2000) Stat1 as a component of tumor necrosis factor alpha receptor 1-TRADD signaling complex to inhibit NF-kappaB activation. *Mol Cell Biol* 20(13):4505-4512.**
- Xi S, Dyer KF, Kimak M, Zhang Q, Gooding WE, Chaillet JR, Chai RL, Ferrell RE, Zamboni B, Hunt J and Grandis JR (2006) Decreased STAT1 expression by promoter methylation in squamous cell carcinogenesis. *J Natl Cancer Inst* 98(3):181-189.**
- Xi S, Gooding WE and Grandis JR (2005) In vivo antitumor efficacy of STAT3 blockade using a transcription factor decoy approach: implications for cancer therapy. *Oncogene* 24(6):970-979.**
- Zhang J, Yang J, Roy SK, Tininini S, Hu J, Bromberg JF, Poli V, Stark GR and Kalvakolanu DV (2003) The cell death regulator GRIM-19 is an inhibitor of signal transducer and activator of transcription 3. *Proc Natl Acad Sci U S A* 100(16):9342-9347.**

FIGURES

Figure 1A

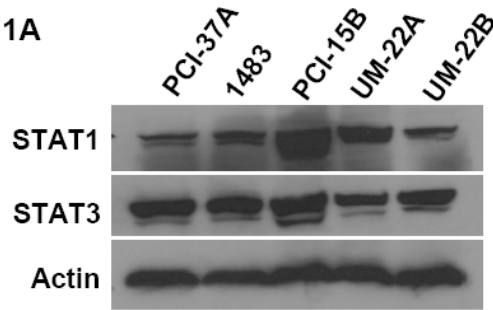


Figure 1B

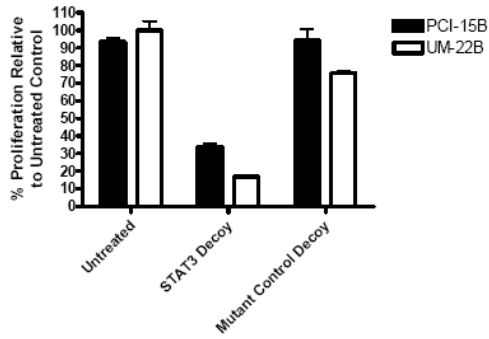


Figure 1C

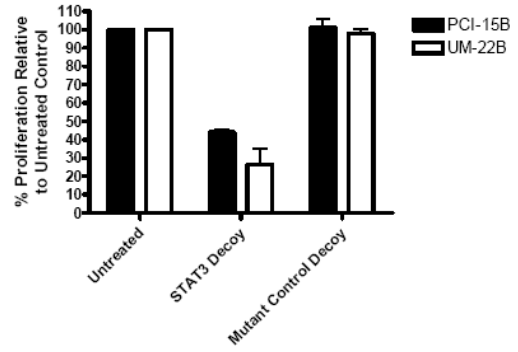
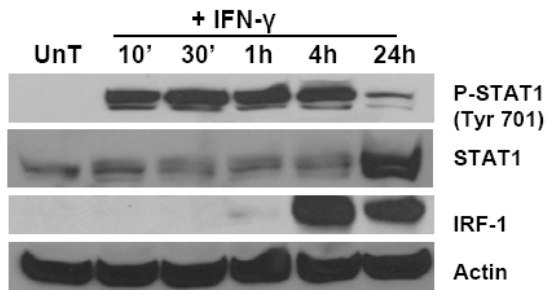


Figure 2

PCI-15B



UM-22B

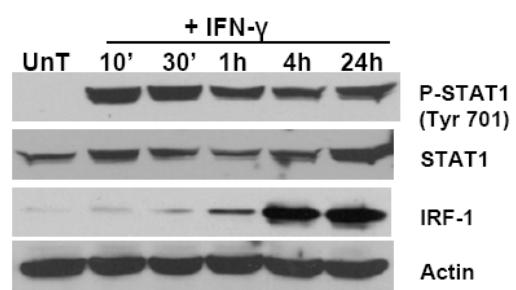


Figure 3A

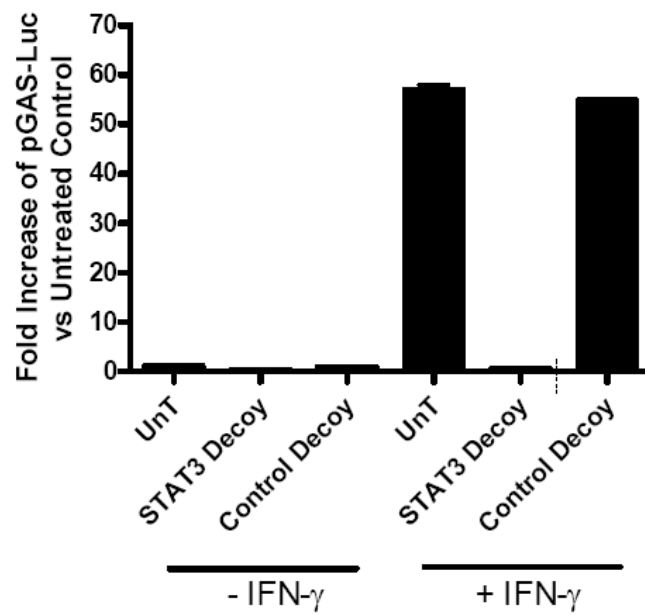


Figure 3B

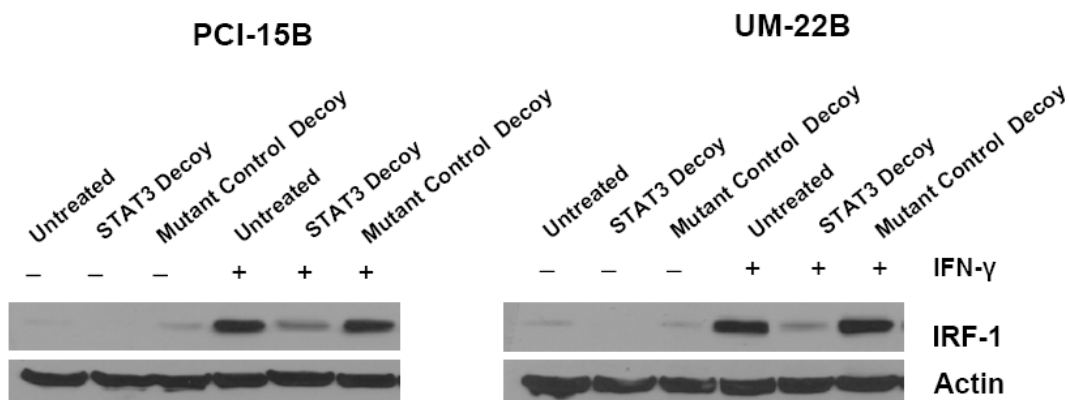


Figure 3C

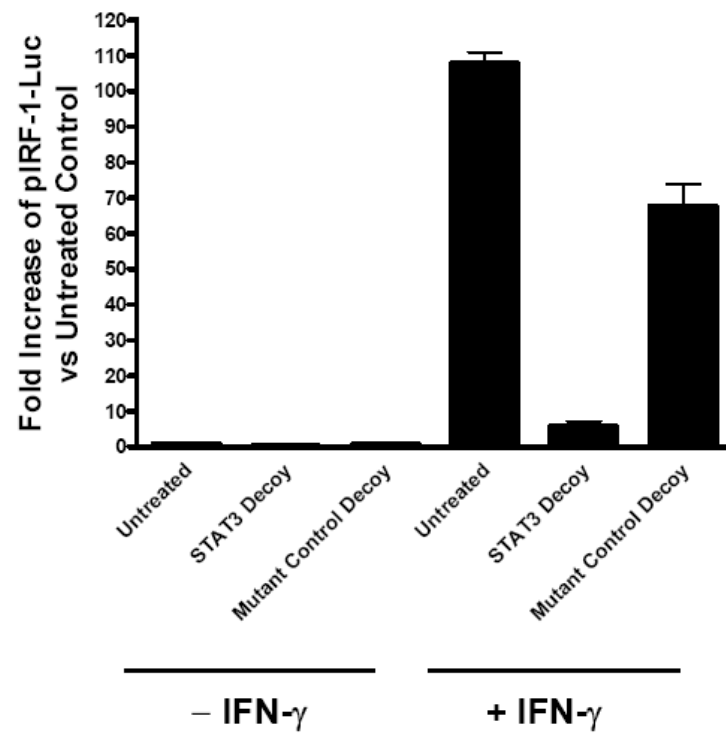
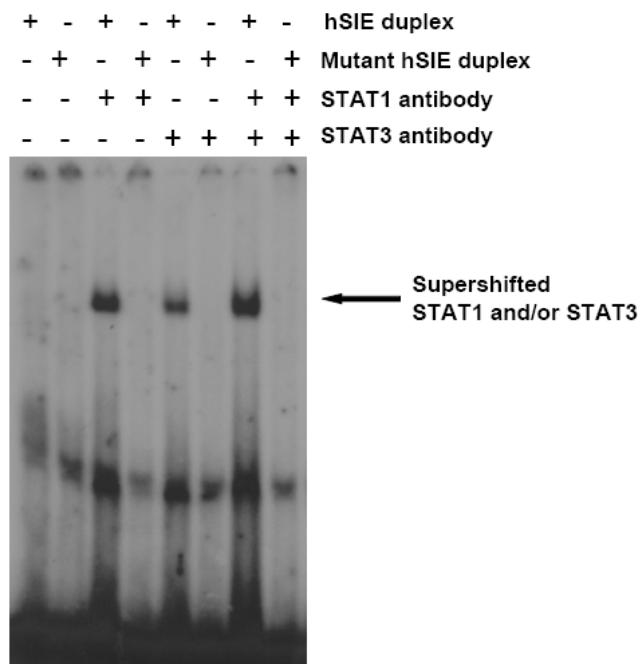


Figure 3D



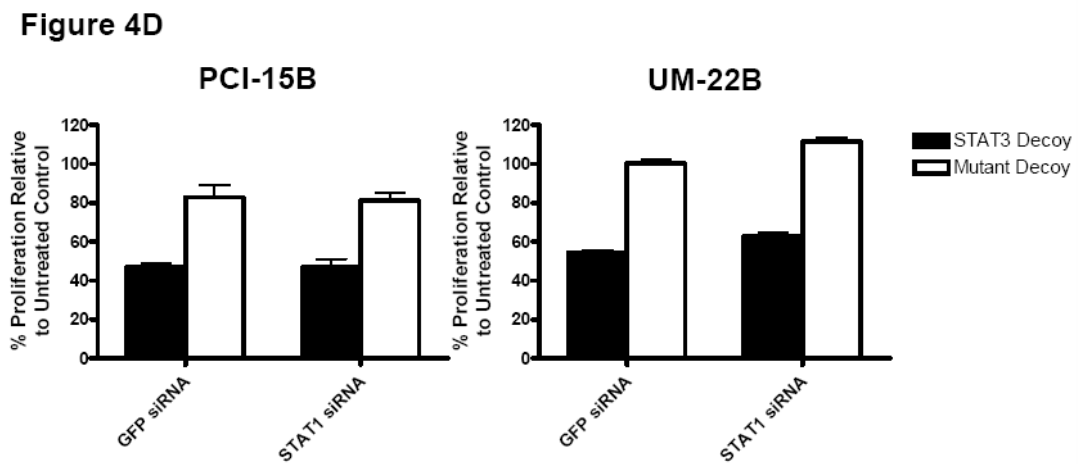
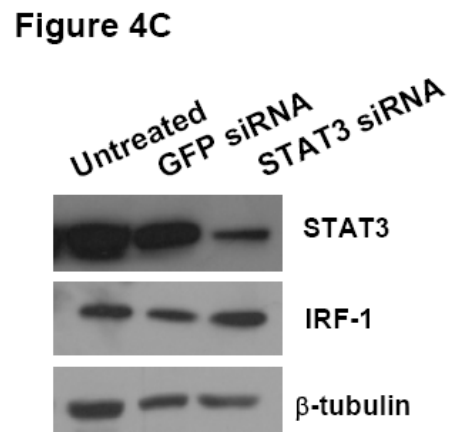
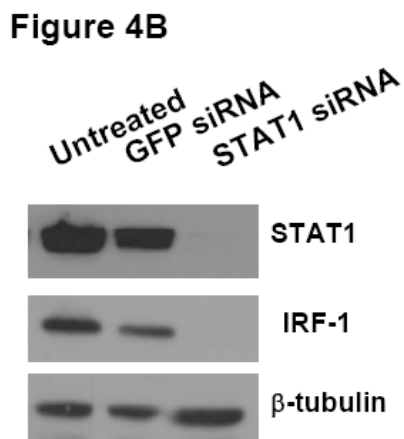
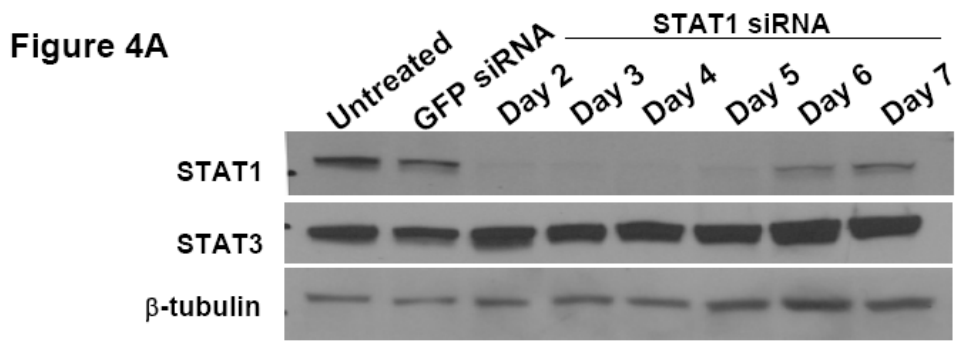


Figure 4E

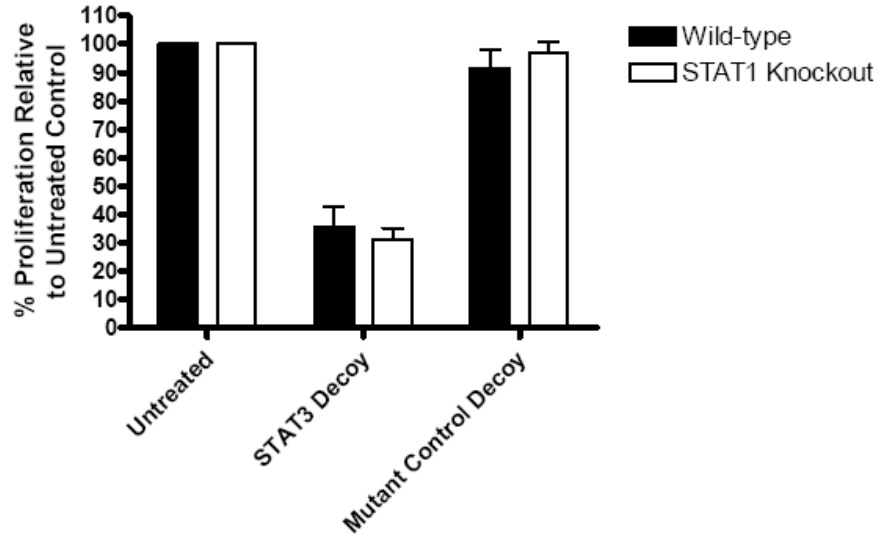


Figure 4F

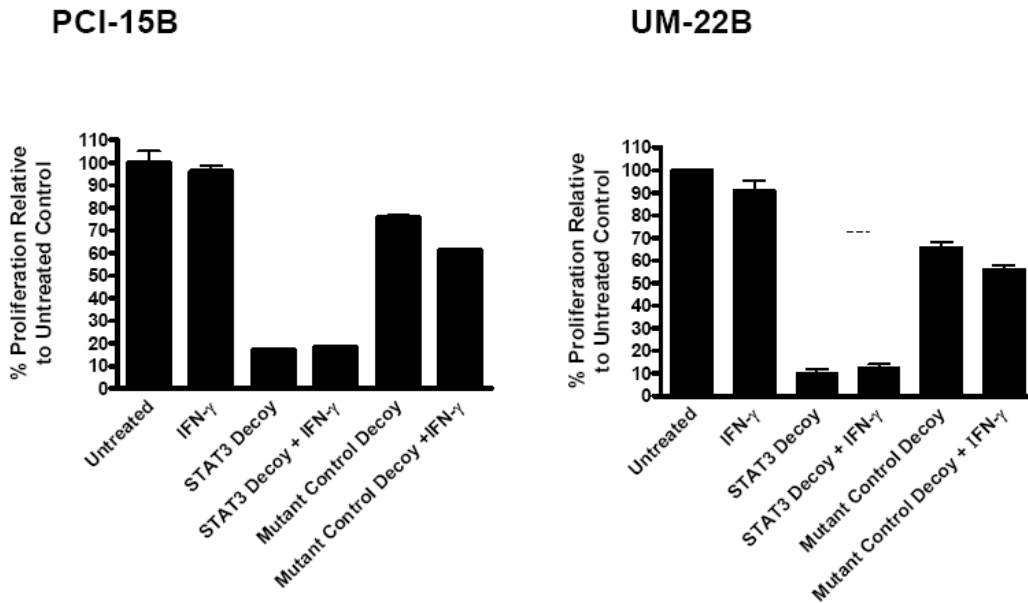


Figure 5A

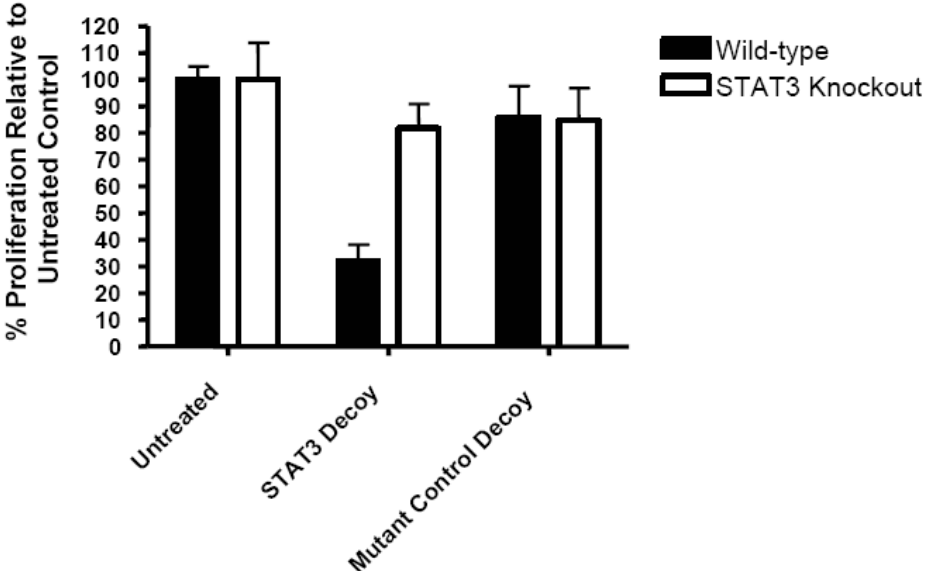
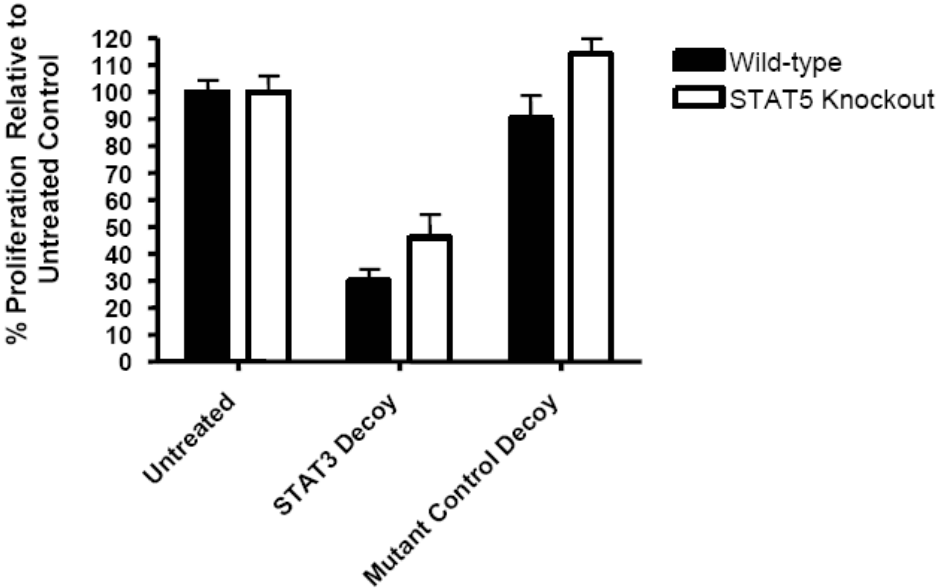


Figure 5B



BIBLIOGRAPHY

1. National Cancer Institute: Head and neck cancer: questions and answers. <http://www.cancer.gov/cancertopics/factsheet/Sites-Types/head-and-neck/print?page=&keyword=>
2. Buettner, R., L.B. Mora, and R. Jove. Activated STAT signaling in human tumors provides novel molecular targets for therapeutic intervention. *Clinical Cancer Research*, 2002. **8**: p. 945-954.
3. Bowman, T., et al. STATs in oncogenesis. *Oncogene*, 2000. **19**: p. 2474-2488.
4. Calo, V., et al. STAT proteins: from normal control of cellular events to tumorigenesis. *Journal of Cellular Physiology*, 2003. **197**: p. 157-168.
5. Hovarth, C.M., Z. Wen, and J.E.D. Jr. A STAT protein domain that determines DNA sequence recognition suggests a novel DNA-binding domain. *Genes and Development*, 1995. **9**: p. 984-994.
6. Xu, X., Y.-L. Sun, and T. Hoey. Cooperative DNA binding and sequence selective recognition conferred by the STAT amino-terminal domain. *Science*, 1996. **273**: p. 794-797.
7. Shuai, K., et al. Interferon activation of the transcription factor STAT91 involves dimerization through SH2-phosphotyrosyl peptide interactions. *Cell*, 1994. **76**: p. 821-828.
8. Bromberg, J., et al. Transcriptionally active STAT1 is required for the antiproliferative effects of both interferon alpha and interferon gamma. *Proceedings of the National Academy of Sciences*, 1996. **93**: p. 7673-7678.
9. Turkson, J., et al. Requirement for Ras/Rac1-mediated p38 and c-Jun N-terminal kinase signaling in STAT3 transcriptional activity induced by the Src oncoprotein. *Molecular and Cellular Biology*, 1999. **19**: p. 7519-7528.
10. Levy, D.E. and C.-k. Lee. What does STAT3 do? *The Journal of Clinical Investigation*, 2002. **109**: p. 1143-1148.
11. Takeda, K., et al. Targeted disruption of the mouse STAT3 gene leads to early embryonic lethality. *Proceedings of the National Academy of Sciences*, 1997. **94**(3801-3804).
12. Darnell, J. STATs and gene regulation. *Science*, 1997. **277**: p. 1630-1635.
13. Ruff-Jamison, S., et al. Epidermal growth factor and lipopolysaccharide activate STAT3 transcription factor in mouse liver. *Journal of Biological Chemistry*, 1994. **269**(35): p. 21933-21935.
14. Shao, H., et al. Identification and characterization of signal transducer and activator of transcription 3 recruitment sites within the epidermal growth factor receptor. *Cancer Research*, 2003. **63**: p. 3923-3930.

15. Sriuranpong, V., et al. Epidermal growth factor receptor-independent constitutive activation of STAT3 in head and neck squamous cell carcinoma is mediated by the autocrine/paracrine stimulation of the interleukin 6/gp130 cytokine system. . *Cancer Research*, 2003. **63**: p. 2948-2965.
16. Turkson, J., et al. Stat3 activation by Src induces specific gene regulation and is required for cell transformation. . *Molecular and Cellular Biology*, 1998. **18**: p. 2545-2552.
17. Zhong, Z., Z. Wen, and J.E. Darnell. STAT3: a STAT family member activated by tyrosine phosphorylation in response to epidermal growth factor and interleukin-6. *Science*, 1994. **264**: p. 95-98.
18. Leeman, R., W. Lui, and J. Grandis. STAT3 as a therapeutic target in head and neck cancer. *Expert Opinion in Biological Therapeutics*, 2006. **6**: p. 231-241.
19. Bromberg, J.F., et al. STAT3 activation is required for cellular transformation by *v-src*. *Molecular and Cellular Biology*, 1998. **18**: p. 2553-2558.
20. Bromberg, J., et al. Stat3 as an oncogene. *Cell*, 1999. **98**: p. 295-303.
21. Catlett-Falcone, R., et al. Constitutive activation of Stat3 signaling confers resistance to apoptosis in human U266 myeloma cells. *Immunity*, 1999. **10**: p. 105-115.
22. Galm, O., et al. SOCS-1, a negative regulator of cytokine signaling is frequently silenced by methylation in multiple myeloma. *Blood*, 2003. **101**: p. 2784-2788.
23. He, B., et al. SOCS-3 is frequently silenced by hypermethylation and suppresses cell growth in human lung cancer. *Proceedings of the National Academy of Sciences*, 2003. **100**(24): p. 14133-14138.
24. Yu, H. and R. Jove. The stats of cancer--new molecular targets come of age. *Nature Reviews*, 2004. **4**: p. 97-104.
25. Garcia, R. and R. Jove. Activation of STAT transcription factors in oncogenic tyrosine kinase signaling. *Journal of Biomedical Science*, 1998. **5**: p. 79-85.
26. Grandis, J.R., et al. Requirement of Stat3 but not Stat1 activation for epidermal growth factor receptor-mediated cell growth *in vitro*. *Journal of Clinical Investigation*, 1998. **102**: p. 1385-1392.
27. Masuda, M., et al. Constitutive activation of signal transducers and activators of transcription 3 correlates with cyclin D1 overexpression and may provide a novel prognostic marker in head and neck squamous cell carcinoma. *Cancer Research*, 2002. **62**: p. 3351-3355.
28. Grandis, J.R., et al. Levels of TGF- α and EGFR protein in head and neck squamous cell carcinoma and patient survival. *Journal of the National Cancer Institute*, 1998. **90**: p. 824-832.
29. Turkson, J. and R. Jove. STAT proteins: novel molecular targets for cancer drug discovery. *Journal of Biological Chemistry*, 2000. **279**: p. 5811-5820.
30. Chiarle, R., et al. STAT3 is required for ALK-mediated lymphomagenesis and provides a possible therapeutic target. *Nature Medicine*, 2005. **11**: p. 623-629.
31. Chiarle, R., et al. NPM-ALK transgenic mice spontaneously develop T-cell lymphomas and plasma cell tumors. *Blood*, 2003. **101**: p. 1919-1927.
32. Zamo, A., et al. Anaplastic lymphoma kinase (ALK) activates STAT3 and protects hematopoietic cells from cell death. *Oncogene*, 2002. **21**: p. 1038-1047.
33. Konnikova, L., et al. Knockdown of STAT3 expression by RNAi induces apoptosis in astrocytoma cells. *BMC Cancer*, 2003. **3**(23).

34. Cattaneo, E., et al. Variations in the levels of the JAK/STAT and ShcA proteins in human brain tumors. *Anticancer Research*, 1998. **18**: p. 2381-2387.
35. Rahaman, S.O., et al. Inhibition of constitutively active STAT3 suppresses proliferation and induces apoptosis in glioblastoma multiforme. *Oncogene*, 2002. **21**: p. 8404-8413.
36. Lian, J.P., et al. Modulation of the constitutive activated STAT3 transcription factor in pancreatic cancer prevention: effects of indole-3-carbinol (I3C) and genistein. *Anticancer Research*, 2004. **24**: p. 133-137.
37. Scholz, A., et al. Activated signal transducer and activator of transcription 3 (STAT3) supports the malignant phenotype of human pancreatic cancer. *Gastroenterology*, 2003. **125**(891-905).
38. Wei, D., et al. STAT3 activation regulates the expression of vascular endothelial growth factor and human pancreatic cancer angiogenesis and metastasis. *Oncogene*, 2003. **22**: p. 319-329.
39. Barton, B.E., et al. IL-6 signaling by STAT3 participates in the change from hyperplasia to neoplasia in NRP-152 and NRP-154 rat prostatic epithelial cells. *BMC Cancer*, 2001. **1**(19).
40. Barton, B.E., et al. Novel single-stranded oligonucleotides that inhibit signal transducer and activator of transcription 3 induce apoptosis *in vitro* and *in vivo* in prostate cancer cell lines. *Molecular Cancer Therapeutics*, 2004. **3**: p. 1183-1191.
41. Mora, L.B., et al. Constitutive activation of STAT3 in human prostate tumors and cell lines: direct inhibition of STAT3 signaling induces apoptosis of prostate cancer cells. *Cancer Research*, 2002. **62**: p. 6659-6666.
42. Watson, C.J. and W.R. Miller. Elevated levels of members of the STAT family of transcription factors in breast carcinoma nuclear extracts. *British Journal of Cancer*, 1995. **71**: p. 840-844.
43. Garcia, R., et al. Constitutive activation of STAT3 in fibroblasts transformed by diverse oncoproteins and in breast carcinoma cells. *Cell Growth & Differentiation*, 1997. **8**: p. 1267-1276.
44. Kijima, T., et al. STAT3 activation abrogates growth factor dependence and contributes to head and neck squamous cell carcinoma tumor growth *in vivo*. *Cell Growth & Differentiation*, 2002. **13**: p. 355-362.
45. Grandis, J.R., et al. Constitutive activation of STAT3 signaling abrogates apoptosis in squamous cell carcinogenesis *in vivo*. *PNAS*, 2000. **97**: p. 4227-4232.
46. Shah, N.G., et al. STAT3 expression in oral squamous cell carcinoma: association with clinicopathological parameters and survival. *International Journal of Biological Markers*, 2006. **21**: p. 175-183.
47. Gao, L.-F., et al. Inhibition of STAT3 expression by siRNA suppresses growth and induces apoptosis in laryngeal cancer cells. *Acta Pharmacologica Sinica*, 2005. **26**: p. 377-383.
48. Gao, L., et al. Down-regulation of signal transducer and activator of transcription 3 expression using vector-based small interfering RNAs suppresses growth of human prostate tumor *in vivo*. *Clinical Cancer Research*, 2005. **11**(17): p. 6333-6341.
49. Gao, L.-F., et al. Knockdown of STAT3 expression using RNAi inhibits growth of laryngeal tumors *in vivo*. *Acta Pharmacologica Sinica*, 2006. **27**: p. 347-352.
50. Nagel-Wolfrum, K., et al. The interaction of specific peptide aptamers with the DNA binding domain and the dimerization domain of the transcription factor STAT3 inhibits

- transactivation and induces apoptosis in tumor cells. *Molecular Cancer Research*, 2004. **2**: p. 170-182.
51. Turkson, J., et al. Phosphotyrosyl peptides block STAT3-mediated DNA binding activity, gene regulation, and cell transformation. *The Journal of Biological Chemistry*, 2001. **276**: p. 45443-45455.
 52. Jing, N., et al. Targeting STAT3 with G-quartet oligodeoxynucleotides in human cancer cells. *DNA and Cell Biology*, 2003. **22**(11): p. 685-696.
 53. Leong, P., et al. Targeted inhibition of STAT3 with a decoy oligonucleotide abrogates head and neck cancer cell growth. *Proceedings of the National Academy of Science*, 2003. **100**: p. 4138-43.
 54. Xi, S., W.E. Gooding, and J. Grandis. In vivo antitumor efficacy of Stat3 blockade using a transcription factor decoy approach: implications for cancer therapy. *Oncogene*, 2005. **24**: p. 970-979.
 55. Sano, S., et al. STAT3 links activated keratinocytes and immunocytes required for development of psoriasis in a novel transgenic mouse model. *Nature Medicine*, 2004. **Advanced online publication**: p. 1-7.
 56. Chan, K.S., et al. Disruption of STAT3 reveals a critical role in both the initiation and the promotion stages of epithelial carcinogenesis. *The Journal of Clinical Investigation*, 2004. **114**: p. 720-728.
 57. Coppelli, F.M. and J.R. Grandis. Oligonucleotides as anticancer agents: from the benchside to the clinic and beyond. *Current Pharmaceutical Design*, 2005. **11**: p. 2825-2840.
 58. Morishita, R., et al. A gene therapy strategy using a transcription factor decoy of the E2F binding site inhibits smooth muscle proliferation in vivo. *PNAS*, 1995. **92**: p. 5855-5859.
 59. Conte, M.S., et al. Results of PREVENT III: a multicenter, randomized trial of edifoligide for the prevention of vein graft failure in lower extremity bypass surgery. *Journal of Vascular Surgery*, 2006. **43**: p. 742-751.
 60. Gill, J.S., et al. Effects of NFkappaB decoy oligonucleotides released from biodegradable polymer microparticles on a glioblastoma cell line. *Biomaterials*, 2002. **23**: p. 2773-2781.
 61. Harimaya, K., et al. Antioxidants inhibit TNF alpha-induced motility and invasion of human osteosarcoma cells: possible involvement of NFkappaB activation. *Clinical Experimental Metastasis*, 2000. **18**: p. 121-129.
 62. Romano, M.F., et al. Enhancement of cytosine arabinoside-induced apoptosis in human myeloblastic leukemia cells by NF-kappa B/Rel A-specific decoy oligodeoxynucleotides. *Gene Therapy*, 2000. **7**: p. 1234-1237.
 63. Sumitomo, M., et al. An essential role for nuclear factor kappa B in preventing TNF-alpha-induced cell death in prostate cancer cells. *Journal of Urology*, 1999. **161**: p. 674-679.
 64. Uetsuka, H., et al. Inhibition of inducible NF-kappaB activity reduces chemoresistance to 5-fluorouracil in a human stomach cancer cell line. *Experimental Cancer Research*, 2003. **289**: p. 27-35.
 65. Kawamura, I., et al. Intratumoral injection of oligonucleotides to the NF-kappaB binding site inhibits cachexia in a mouse tumor model. *Gene Therapy*, 1999. **6**: p. 91-97.
 66. Tomita, T., et al. Suppressed severity of collagen-induced arthritis by in vivo transfection of nuclear factor kappa B decoy oligodeoxynucleotides as a gene therapy. *Arthritis and Rheumatology*, 1999. **42**: p. 2532-2542.

67. Desmet, C., et al. Selective blockade of NF- κ B activity in airway immune cells inhibits the effector phase of experimental asthma. *The Journal of Immunology*, 2004. **173**: p. 5766-5775.
68. Clinical trial: Topical NF-kappaB decoy in the treatment of atopic dermatitis. <http://clinicaltrials.gov/ct/show/NCT00125333?order=1>
69. Chae, Y.-M., et al. Sp1-decoy oligodeoxynucleotide inhibits high glucose-induced mesangial cell proliferation. *Biochemical and Biophysical Research Communications*, 2004. **319**: p. 550-555.
70. Vecchio, A.Z.S.D., et al. Inhibition of Sp1 activity by a decoy PNA-DNA chimera prevents urokinase receptor expression and migration of breast cancer cells. *Biochemical Pharmacology*, 2005. **70**: p. 1277-1287.
71. Borgatti, M., et al. Decoy molecules based on PNA-DNA chimeras and targeting Sp1 transcription factors inhibit the activity of urokinase-type plasminogen activator receptor (uPAR) promoter. *Oncology Research*, 2005. **15**: p. 373-383.
72. Ishibashi, H., et al. Sp1 decoy transfected into carcinoma cells suppresses the expression of vascular endothelial growth factor, transforming growth factor beta 1, and tissue factor and also cell growth and invasion activities. *Cancer Research*, 2000. **60**: p. 6531-6536.
73. Novak, E.M., et al. Downregulation of TNF-alpha and VEGF expression by Sp1 decoy oligodeoxynucleotides in mouse melanoma tumor cells. *Gene Therapy*, 2003. **10**: p. 1992-1997.
74. Seki, Y., et al. Construction of a novel DNA decoy that inhibits the oncogenic β -catenin/T-cell factor pathway. *Molecular Cancer Therapeutics*, 2006. **5**: p. 985-994.
75. Nakamura, H., et al. Prevention and regression of atopic dermatitis by ointment containing NF- κ B decoy oligodeoxynucleotides in NC/Nga atopic mouse model. *Gene Therapy*, 2002. **9**: p. 1221-1229.
76. Morishita, R., et al. In vivo transfection of cis element "decoy" against nuclear factor-kappaB binding site prevents myocardial infarction. *Nature Medicine*, 1997. **3**: p. 894-890.
77. Shimizu, H., et al. NF κ B decoy oligodeoxynucleotides ameliorates osteoporosis through inhibition of activation and differentiation of osteoclasts. *Gene Therapy*, 2006. **13**: p. 933-941.
78. Huckel, M., et al. Attenuation of murine antigen-induced arthritis by treatment with a decoy oligodeoxynucleotide inhibiting signal transducer and activator of transcription-1 (STAT-1). *Arthritis Research and Therapy*, 2005. **8**.
79. Wang, L.H., et al. Targeted disruption of STAT6 DNA binding activity by an oligonucleotide decoy blocks IL-4 driven T(H)2 cell response. *Blood*, 2000. **95**: p. 1249-1257.
80. Sumi, K., et al. In vivo transfection of a cis element decoy against signal transducers and activators of transcription-6 binding site ameliorates the response of contact hypersensitivity. *Gene Therapy*, 2004. **11**: p. 1763-1771.
81. Miyazaki, Y., et al. STAT-6-mediated control of P-selectin by substance P and interleukin-4 in human dermal endothelial cells. *American Journal of Pathology*, 2006. **169**: p. 697-707.
82. Yokozeki, H., et al. In vivo transfection of a cis element decoy against signal transducers and activators of transcription 6-binding site ameliorates IgE-mediated late-phase reaction in an atopic dermatitis mouse model. *Gene Therapy*, 2004. **11**: p. 1753-1762.

83. Gao, H., et al. A single decoy oligodeoxynucleotides targeting multiple oncoproteins produces strong anticancer effects. *Molecular Pharmacology*, 2006. **70**: p. 1621-1629.
84. Brown, D.A., et al. Effect of phosphorothioate modification of oligodeoxynucleotides on specific protein binding. *Journal of Biological Chemistry*, 1994. **269**: p. 26801-26805.
85. Stark, G.R., et al. How cells respond to interferons. *Annual Reviews in Biochemistry*, 1998. **67**: p. 227-264.
86. Ramana, C.V., et al. Complex roles of STAT1 in regulating gene expression. *Oncogene*, 2000. **19**: p. 2619-2627.
87. Stephanou, A. and D.S. Latchman. Opposing actions of STAT1 and STAT3. *Growth Factors*, 2005. **23**: p. 177-182.
88. Battle, T.E. and D.A. Frank. The role of STATs in apoptosis. *Current Molecular Medicine*, 2002. **2**: p. 381-392.
89. Kumar, A., et al. Defective TNF-alpha-induced apoptosis in STAT1-null cells due to low constitutive levels of caspases. *Science*, 1997. **278**: p. 1630-1632.
90. Durbin, J.E., et al. Targeted disruption of the mouse STAT1 gene results in compromised innate immunity to viral disease. *Cell*, 1996. **84**: p. 443-450.
91. Kaplan, D.H., et al. Demonstration of an interferon γ -dependent tumor surveillance system in immunocompetent mice. *Proceedings of the National Academy of Sciences*, 1998. **95**: p. 7556-7561.
92. Lin, C.J., et al. Head and neck squamous cell carcinoma cell lines: established models and rationale for selection. *Head and Neck*, 2006. **In press**.
93. Muller, M., et al. Complementation of a mutant cell line: central role of the 91 kDa polypeptide of ISGF3 in the interferon-alpha and -gamma signal transduction pathways. *The EMBO Journal*, 1993. **12**: p. 4221-4228.
94. Lee, C., et al. STAT3 is a negative regulator of granulopoiesis but is not required for G-CSF-dependent differentiation. *Immunity*, 2002. **17**: p. 63-72.
95. Teglund, S., et al. STAT5a and STAT5b proteins have essential and nonessential, or redundant roles in cytokine responses. *Cell*, 1998. **93**: p. 841-850
96. Chin, Y.E., et al. Activation of the STAT signaling pathway can cause expression of caspase 1 and apoptosis. *Molecular and Cellular Biology*, 1997. **17**: p. 5328-5337.
97. Thomas, M., et al. STAT1: modulator of chemotherapy-induced apoptosis. *Cancer Research*, 2004. **64**: p. 8357-8364.
98. Xi, S., et al. Decreased STAT1 expression by promoter methylation in squamous cell carcinoma. *Journal of the National Cancer Institute*, 2006. **98**: p. 181-189.
99. Kim, H.S. and M.-S. Lee. STAT1 as a key modulator of cell death. *Cellular Signaling*, 2006. **doi:10.1016/j.cllsi.2006.09.003**.
100. Kovacic, B., et al. STAT1 acts as a tumor promoter for leukemia development. *Cancer Cell*, 2006. **10**: p. 77-87.
101. Torrero, M.N., et al. STAT1 deficiency in the host enhances interleukin-12-mediated tumor regression. *Cancer Research*, 2006. **66**: p. 4461-4467.
102. Cho, Y.S., et al. A genomic-scale view of the cAMP-response element-enhancer decoy: a tumor target based genetic tool. *PNAS*, 2002. **99**: p. 15626-15631.
103. Gambarotta, R., et al. Ets up-regulates MET transcription. *Oncogene*, 1996. **13**: p. 1911-1917.

104. Wang, Y., et al. STAT1 as a component of tumor necrosis factor alpha receptor 1-TRADD signaling complex to inhibit NF-kappa B activation. *Molecular and Cellular Biology*, 2000. **20**: p. 4505-4512.
105. Townsend, P.A., et al. STAT1 interacts with p53 to enhance DNA damage-induced apoptosis. *Journal of Biological Chemistry*, 2004. **279**: p. 5811-5820.
106. Chung, C.D., et al. Specific inhibition of STAT3 signal transduction by PIAS3. *Science*, 1997. **278**: p. 1803-1805.
107. Nakayama, K., K.W. Kim, and A. Miyajima. A novel nuclear zinc finger protein EZ1 enhances nuclear retention and transactivation of STAT3. *Embo Journal*, 2002. **21**: p. 6174-6184.
108. Zhang, J., et al. The cell death regulator GRIM-19 is an inhibitor of signal transducer and activator of transcription 3. *PNAS*, 2003. **100**: p. 9342-9347.
109. Pomerantz, R. and J. Grandis. The epidermal growth factor receptor signaling network in head and neck carcinogenesis and implications for targeted therapy. *Seminars in Oncology*, 2004. **31**: p. 734-743.
110. Cruz, J.J., et al. Targeting receptor tyrosine kinase and their signal transduction routes in head and neck cancer. *Annals of Oncology*, 2006. **Epub Ahead of Print**.
111. Grandis, J. and D. Tweardy. Elevated levels of transforming growth factor alpha and epidermal growth factor receptor messenger RNA are early markers of carcinogenesis in head and neck cancer. *Cancer Research*, 1993. **53**: p. 3579-3584.
112. Ang, K.K., et al. Impact of epidermal growth factor receptor expression on survival and pattern of relapse in patients with advanced head and neck carcinoma. *Cancer Research*, 2002. **62**: p. 7350-7356.
113. Lynch, T.J., et al. Activating mutations in the epidermal growth factor receptor underlying responsiveness of non-small-cell lung cancer to gefitinib. *New England Journal of Medicine*, 2004. **350**(2129-2139).
114. Paez, J.G., et al. EGFR mutations in lung cancer: correlation with clinical response to gefitinib therapy. *Science*, 2004. **304**: p. 1497-1500.
115. Lee, J.W., et al. Somatic mutations of EGFR gene in squamous cell carcinoma of the head and neck. *Clinical Cancer Research*, 2005. **11**: p. 2879-2882.
116. Loeffler-Ragg, J., et al. Low incidence of mutations in EGFR kinase domain in caucasian patients with head and neck squamous cell carcinoma. *European Journal of Cancer*, 2006. **42**: p. 109-111.
117. Cohen, E.E., et al. Response of some head and neck cancers to epidermal growth factor receptor tyrosine kinase inhibitors may be linked to mutation of ERBB2 rather than EGFR. *Clinical Cancer Research*, 2005. **11**: p. 8105-8108.
118. Sok, J.C., et al. Mutant epidermal growth factor receptor (EGFRvIII) contributes to head and neck cancer growth and resistance to EGFR targeting. *Clinical Cancer Research*, 2006. **12**: p. 5064-5073.
119. Lorimer, I.A. Mutant epidermal growth factor receptors as targets for cancer therapy. *Current Cancer Drug Targets*, 2002. **2**: p. 91-102.
120. Egloff, A.M. and J.R. Grandis. Epidermal growth factor receptor-targeted molecular therapeutics for head and neck squamous cell carcinoma. *Expert Opinion in Therapeutic Targets*, 2006. **10**(5).
121. United States Food and Drug Administration. <http://www.fda.gov/bbs/topics/NEWS/2006/NEW01329.html>

122. Vermorken, J.B., et al. Cetuximab (Erbix) in recurrent/metastatic (R&M) squamous cell carcinoma of the head and neck (SCCHN), refractory to first-line platinum-based therapies. *American Society of Clinical Oncology*, 2005.
123. Kawamoto, T., et al. Growth stimulation of A431 cells by epidermal growth factor: identification of high affinity receptors for epidermal growth factor by an anti-receptor monoclonal antibody. *Proceedings of the National Academy of Sciences*, 1983. **80**: p. 1337-1341.
124. Masau, H., et al. Growth inhibition of human tumor cells in athymic mice by anti-epidermal growth factor monoclonal antibodies. *Cancer Research*, 1984. **44**: p. 1002-1007.
125. Sato, J.D., et al. Biological effects in vitro of monoclonal antibodies to human epidermal growth factor receptors. *Molecular Biological Medicine*, 1983. **1**: p. 511-529.
126. Masui, H., et al. Growth inhibition of human tumor cells in athymic mice by anti-epidermal growth factor monoclonal antibodies. *Cancer Research*, 1984. **44**: p. 1002-1007.
127. Baselga, J., et al. Antitumor effects of doxorubicin in combination with anti-epidermal growth factor receptor monoclonal antibodies. *Journal of the National Cancer Institute*, 1993. **1993**: p. 1327-1333.
128. Fan, Z., et al. Antitumor effect of anti-epidermal growth factor receptor monoclonal antibodies plus cisdiaminedichloroplatinum on well established A431 cell xenografts. *Cancer Research*, 1993. **53**: p. 4637-4642.
129. Huang, S.M., J.M. Bock, and P.M. Harari. Epidermal growth factor receptor blockade with C225 modulates proliferation, apoptosis, and radiosensitivity in squamous cell carcinomas of the head and neck. *Cancer Research*, 1999. **59**: p. 1935-1940.
130. Hoffend, J., et al. Uptake of anti-epidermal growth factor receptor antibody EMD 72000 in tumors of subjects with head and neck squamous cell carcinoma. *Proceedings of the American Association of Clinical Oncology*, 2004. **205**: p. Abstract 3043.
131. Cohenuram, M. and M.W. Saif. Panitumumab the first fully human monoclonal antibody: from the bench to the clinic. *Anti-Cancer Drugs*, 2007. **18**: p. 7-15.
132. Ganti, A.K. and A. Potti. Epidermal growth factor inhibition in solid tumors. *Expert Opinion in Biological Therapeutics*, 2005. **5**: p. 1165-1174.
133. Crombet, T., et al. Use of the humanized anti-epidermal growth factor receptor monoclonal antibody h-R3 in combination with radiotherapy in the treatment of locally advanced head and neck cancer patients. *Journal of Clinical Oncology*, 2004. **22**: p. 1646-1654.
134. Giaccone, G., et al. Gefitinib in combination with gemcitabine and cisplatin in advanced non-small cell lung cancer: a phase III trial--INTACT1. *Journal of Clinical Oncology*, 2004. **22**: p. 777-784.
135. Herbst, R.S., et al. Gefitinib in combination with paclitaxel and carboplatin in advanced non-small cell lung cancer: a phase III trial--INTACT2. *Journal of Clinical Oncology*, 2004. **22**: p. 785-794.
136. Johnson, J., et al. Approval summary for erlotinib for treatment of patients with locally advanced or metastatic non-small cell lung cancer after failure of at least one prior chemotherapy regimen. *Clinical Cancer Research*, 2005. **11**: p. 6414-6421.

137. National Cancer Institute: FDA approval for erlotinib hydrochloride. <http://www.cancer.gov/cancertopics/druginfo/fda-erlotinib-hydrochloride#Anchor-Pancreati-44285>
138. Grandis, J.R., et al. Inhibition of epidermal growth factor receptor gene expression and function decreases proliferation of head and neck squamous cell carcinoma but not normal mucosal epithelial cells. *Oncogene*, 1997. **15**: p. 409-416.
139. He, Y., et al. Inhibition of human squamous cell carcinoma growth *in vivo* by epidermal growth factor receptor antisense RNA transcribed from the U6 promoter. *Journal of the National Cancer Institute*, 1998. **90**: p. 1080-1087.
140. Lango, M.N., D.M. Shin, and J.R. Grandis. Targeting growth factor receptors: integration of novel therapeutics in the management of head and neck cancer. *Current Opinions in Oncology*, 2001. **13**: p. 168-175.
141. Niwa, H., et al. Antitumor effects of epidermal growth factor receptor antisense oligonucleotides in combination with docetaxel in squamous cell carcinoma of the head and neck. *Clinical Cancer Research*, 2003. **9**: p. 5028-5035.
142. Thomas, S., et al. Tissue distribution of liposome-mediated epidermal growth factor receptor antisense gene therapy. *Cancer Gene Therapy*, 2003. **10**: p. 518-528.
143. Azemar, M., et al. Recombinant antibody toxins specific for ErbB2 and EGF receptor inhibit the *in vitro* growth of human head and neck cancer cells and cause rapid tumor regression *in vivo*. *International Journal of Cancer*, 2000. **86**: p. 269-275.
144. Schmidt, M. and W. Wels. Targeted inhibition of tumor cell growth by a bispecific single-chain toxin containing an antibody domain and TGF- α . *British Journal of Cancer*, 1996. **74**: p. 853-862.
145. Ford, A.C. and J.R. Grandis. Targeting epidermal growth factor receptor in head and neck cancer *Head & Neck*, 2003: p. 67-73.
146. Moyer, J., et al. Induction of apoptosis and cell cycle arrest by CP-358, 774, an inhibitor of epidermal growth factor receptor tyrosine kinase. *Cancer Research*, 1997. **57**: p. 4838-4848.
147. Ciardiello, F., et al. Antitumor effect and potentiation of cytotoxic drug activity in human cancer cells by ZD-1839 (Iressa), an epidermal growth factor receptor-selective tyrosine kinase inhibitor. *Clinical Cancer Research*, 2000. **6**: p. 2053-2063.
148. Sirotnak, F.M., et al. Efficacy of cytotoxic agents against human tumor xenografts is markedly enhanced by coadministration of ZD1839 (Iressa), an inhibitor of EGFR tyrosine kinase. *Clinical Cancer Research*, 2000. **6**: p. 4885-4892.
149. Cohen, E.E., et al. Phase II trial of ZD1839 in recurrent or metastatic squamous cell carcinoma of the head and neck. *Clinical Cancer Research*, 2003. **11**: p. 8418-8424.
150. Chan, S. and V. Yu. Proteins of the Bcl-2 family in apoptosis signaling: from mechanistic insights to therapeutic opportunities. *Clinical and Experimental Pharmacology and Physiology*, 2004. **31**: p. 119-128.
151. Shangary, S. and D.E. Johnson. Peptides derived from BH3 domains of Bcl-2 family members: a comparative analysis of inhibition of Bcl-2, Bcl-XL, and Bax oligomerization, induction of cytochrome c release, and activation of cell death. *Biochemistry*, 2002. **41**: p. 9485-9495.
152. Schendel, S.L., et al. Channel formation by antiapoptotic protein Bcl-2. *Proceeding of the National Academy of Science USA*, 1997. **94**: p. 5113-5118.

153. Minn, A.J., et al. Bcl-x(L) forms an ion channel in sythetic lipid membranes. *Nature*, 1997. **385**: p. 353-357.
154. Antonsson, B., et al. Bax oligomerization is required for channel-forming activity in liposomes and to trigger cytochrome c release from mitochondria. *Biochemistry Journal*, 2000. **345**: p. 271-278.
155. O'Neill, J., et al. Promises and challenges of targeting Bcl-2 anti-apoptotic proteins for cancer therapy. *Biochimica et Biophysica Acta*, 2004. **1705**: p. 43-51.
156. Amundson, A.A., et al. An informatics approach identifying markers of chemosensitivity in human cancer cell lines. *Cancer Research*, 2000. **60**: p. 6101-6110.
157. Trask, D., et al. Expression of Bcl-2 family proteins in advanced laryngeal squamous cell carcinoma: correlation with response to chemotherapy and organ preservation. *The Laryngoscope*, 2002. **112**: p. 638-644.
158. Simoes-Wust, A.P., et al. Bcl-xl antisense treatment induces apoptosis in breast carcinoma cells. *International Journal of Cancer*, 2000. **87**: p. 582-590.
159. Guensberg, P., et al. Bcl-X_L antisense oligonucleotides chemosensitizes human glioblastoma cells. *Chemotherapy*, 2002. **48**: p. 189-195.
160. Vilenchik, M., et al. Antisense RNA downregulation of bcl-xL expression in prostate cancer cells leads to diminished rates of cellular proliferation and resistance to cytotoxic chemotherapeutic agents. *Cancer Research*, 2002. **62**: p. 2175-2183.
161. Hayward, R.L., et al. Antisense Bcl-X_L down-regulation switches the response to topoisomerase I inhibition from senescence to apoptosis in colorectal cancer cells, enhancing global cytotoxicity. *Clinical Cancer Research*, 2003. **9**: p. 28-56-2865.
162. Hopkins-Donaldson, S., et al. Induction of apoptosis and chemosensitization of mesothelioma cells by Bcl-2 and Bcl-X_L antisense treatment. *International Journal of Cancer*, 2003. **106**: p. 160-166.
163. Hayward, R.L., et al. Enhanced oxaliplatin-induced apoptosis following antisense Bcl-X_L down-regulation is p53 and Bax dependent: genetic evidence for specificity of the antisense effect. *Molecular Cancer Therapeutics*, 2004. **3**: p. 169-178.
164. Masui, T., et al. Bcl-XL antisense oligonucleotides coupled with antennapedia enhances radiation-induced apoptosis in pancreatic cancer. *Surgery*, 2006. **140**: p. 149-160.
165. Zangemeister-Wittke, U., et al. A novel bispecific antisense oligodeoxynucleotide inhibiting both bcl-2 and bcl-XL expression efficiently induces apoptosis in tumor cells. *Clinical Cancer Research*, 2000. **6**: p. 2547-2555.
166. Strasberg, R.M., U. Zangemeister-Wittke, and M. Rieber. p53-independent induction of apoptosis in human melanoma cells by a bcl-2/bcl-xL bispecific antisense oligonucleotide. *Clinical Cancer Research*, 2001. **7**: p. 1446-1451.
167. Jiang, Z., X. Zheng, and K.M. Rich. Down-regulation of Bcl-2 and Bcl-X_L expression with bispecific antisense treatment in glioblastoma cell lines induces cell death. *Journal of Neurochemistry*, 2003. **84**: p. 273-281.
168. Yamanaka, K., et al. Induction of apoptosis and enhancement of chemosensitivity in human prostate cancer LNCaP cells using bispecific antisense oligonucleotides targeting Bcl-2 and Bcl-XL genes. *BJU Int*, 2006. **97**: p. 1300-1308.
169. Lei, X.-Y., et al. Bcl-X_L small interfering RNA enhances sensitivity of Hepg2 hepatocellular carcinoma cells to 5-fluorouracil and hydroxycamptothecin. *Acta Biochimica et Biophysica Sinica*, 2006. **38**: p. 704-710.

170. Xie, Y.E., et al. Down-regulation of Bcl-XL by RNA interference suppresses cell growth and induces apoptosis in human esophageal cancer cells. *World Journal of Gastroenterology*, 2006. **12**: p. 7472-7477.
171. Lei, X.Y., et al. Silencing of Bcl-X_L expression in human MGC-803 gastric cancer cells by siRNA. *Acta Biochimica et Biophysica Sin (Shanghai)*, 2005. **37**: p. 555-560.
172. Zhu, H., et al. Bcl-XL small interfering RNA suppresses the proliferation of 5-fluorouracil-resistant human colon cancer cells. *Molecular Cancer Therapeutics*, 2005. **4**: p. 451-456.
173. Liu, F., et al. RNA interference by expression of short hairpin RNAs suppresses bcl-xl gene expression in nasopharyngeal carcinoma cells. *Acta Pharmacologica Sin*, 2005. **26**: p. 228-234.
174. Wilusz, J.E., S.C. Devanney, and M. Caputi. Chimeric peptide nucleic acid compounds modulate splicing of the bcl-x gene in vitro and in vivo. *Nucleic Acids Research*, 2005. **33**: p. 6547-6554.
175. Wang, H., et al. Preclinical pharmacology of 2-methoxyantimycin A compounds as novel antitumor agents. *Cancer Chemotherapeutic Pharmacology*, 2005. **56**: p. 291-298.
176. Tzung, S.-P., et al. Antimycin A mimics a cell-death-inducing Bcl-2 homology domain 3. *Nature Cell Biology*, 2001. **3**: p. 183-191.
177. Manion, M.K., et al. Bcl-XL mutations suppress cellular sensitivity to antimycin A. *Journal of Biological Chemistry*, 2004. **279**: p. 2159-2165.
178. Campas, C., et al. Bcl-2 inhibitors induce apoptosis in chronic lymphocytic leukemia cells. *Experimental Hematology*, 2006. **34**: p. 1663-1669.
179. Zhang, M., et al. Molecular mechanism of gossypol-induced cell growth inhibition and cell death of HT-29 human colon carcinoma cells. *Biochemical Pharmacology*, 2003. **66**: p. 93-103.
180. Dao, V., et al. Cytotoxicity of enantiomers of gossypol Schiff's bases and optical stability of gossypolone. *European Journal of Medical Chemistry*, 2004. **39**: p. 619-624.
181. Oliver, C., et al. In vitro effects of the BH3 mimetic, (-)-gossypol, on head and neck squamous cell carcinoma cells. *Clinical Cancer Research*, 2004. **10**: p. 7757-7763.
182. Bauer, J., et al. Reversal of cisplatin resistance with a BH3 mimetic, (-)-gossypol, in head and neck cancer cells: role of wild-type p53 and Bcl-X_L. *Molecular Cancer Therapeutics*, 2005. **4**(1096-1104).
183. Oliver, C., et al. (-)-Gossypol acts directly on the mitochondria to overcome Bcl-2- and Bcl-XL-mediated apoptosis resistance. *Molecular Cancer Therapeutics*, 2005. **4**: p. 23-31.
184. Wolter, K., et al. (-)-Gossypol inhibits growth and promotes apoptosis of human head and neck squamous cell carcinoma in vivo. *Neoplasia*, 2006. **8**: p. 163-172.
185. Xu, L., et al. (-)-Gossypol enhances response to radiation therapy and results in tumor regression of human prostate cancer. *Molecular Cancer Therapeutics*, 2005. **4**: p. 197-205.
186. Mohammad, R.M., et al. Preclinical studies of a nonpeptidic small-molecule inhibitor of Bcl-2 and Bcl-XL [(-)-gossypol] against diffuse large cell lymphoma. *Molecular Cancer Therapeutics*, 2005. **4**: p. 13-21.
187. Mohammad, R.M., et al. Nonpeptidic small-molecule inhibitor of Bcl-2 and Bcl-XL, (-)-gossypol, enhances biological effect of genistein against BxPC-3 human pancreatic cancer cell line. *Pancreas*, 2005. **31**: p. 317-324.

188. Liu, S., et al. The (-)-enantiomer of gossypol possesses higher anticancer potency than racemic gossypol in human breast cancer. *Anticancer Research*, 2002. **22**(1A): p. 33-38.
189. Degtarev, A., et al. Identification of small-molecule inhibitors of interaction between the BH3 domain and Bcl-X_L. *Nature Cell Biology*, 2001. **3**: p. 173-182.
190. Moreau, C., et al. Minimal BH3 peptides promote cell death by antagonizing anti-apoptotic proteins. *Journal of Biological Chemistry*, 2003. **278**: p. 19426-19435.
191. Shangary, S., et al. Sequence and helicity requirements for the proapoptotic activity of Bax BH3 peptides. *Molecular Cancer Therapeutics*, 2004. **3**: p. 1-11.
192. Chauhan, D., et al. A novel Bcl-2/Bcl-X_L/Bcl-w inhibitor ABT-737 as therapy in multiple myeloma. *Oncogene*, 2006. **E-pub ahead of press**.
193. Delft, M.F.v., et al. The BH3 mimetic ABT-737 targets selective Bcl-2 proteins and efficiently induces apoptosis via Bak/Bax if Mcl-1 is neutralized *Cancer Cell*, 2006. **10**: p. 389-390.
194. Lin, X., et al. 'Seed' analysis of off-target siRNAs reveals an essential role of Mcl-1 in resistance to the small-molecule Bcl-2/Bcl-X_L inhibitor ABT-737. *Oncogene*, 2006. **doi:10.1038/sj.onc.1210166**.
195. Konopleva, M., et al. Mechanisms of apoptosis sensitivity and resistance to the BH3 mimetic ABT-737 in acute myeloid leukemia. *Cancer Cell*, 2006. **10**: p. 375-388.
196. Del Gaizo Moore, V., et al. Chronic lymphocytic leukemia requires Bcl-1 to sequester prodeath BIM, explaining sensitivity to Bcl2 antagonist ABT-737. *Journal of Clinical Investigation*, 2007. **117**: p. 112-121.
197. Wang, G., et al. Structure-based design of potent small-molecule inhibitors of anti-apoptotic Bcl-2 proteins. *Journal of Medicinal Chemistry*, 2006. **49**: p. 6139-6142.
198. Zhang, Y.-H., et al. Chelerythrine and sanguinarine dock at distinct sites on Bcl-XL that are not the classic BH3 binding clefts. *Journal of Molecular Biology*, 2006. **364**: p. 536-549.
199. Yamanaka, K., et al. A novel antisense oligonucleotide inhibiting several antiapoptotic Bcl-2 family members induces apoptosis and enhances chemosensitivity in androgen-independent human prostate cancer PC3 cells. *Molecular Cancer Therapeutics*, 2005. **4**: p. 1689-1698.
200. Ihle, J. The Stat family in cytokine signaling. *Current Opinions in Cell Biology*, 2001. **13**: p. 211-217.
201. Diaz, J., et al. A common binding site mediates heterodimerization and homodimerization of Bcl-2 family members. *Journal of Biological Chemistry*, 1997. **272**: p. 11350-11355.
202. Otilie, S., et al. Dimerization properties of human BAD. Identification of a BH3 domain and analysis of its binding to mutant Bcl-2 and Bcl-XL proteins. *Journal of Biological Chemistry*, 1997. **272**: p. 30866-30872.
203. Oltersdorf, T., et al. An inhibitor of Bcl-2 family proteins induces regression of solid tumors. *Nature*, 2005. **435**: p. 677-681.
204. Chen, L., et al. Differential targeting of prosurvival Bcl-2 proteins by their BH3-only ligands allows complementary apoptotic function. *Molecular Cell*, 2005. **17**: p. 393-403.
205. Willis, S.N., et al. Pro-apoptotic Bak is sequestered by Mcl-1 and Bcl-XL, but not Bcl-2, until displaced by BH3-only proteins. *Genes and Development*, 2005. **19**: p. 1294-1305.
206. Coutinho, E.M. Gossypol: a contraceptive for men. *Contraception*, 2002. **65**: p. 259-263.

207. Lopez, L.M., D.A. Grimes, and K.F. Schulz. Nonhormonal drugs for contraception in men: a systematic review. *Obstetrical and Gynecological Survey*, 2005. **60**: p. 746-752.
208. Benz, C.C., et al. Biochemical correlates of the antitumor and antimitochondrial properties of gossypol enantiomers. *Molecular Pharmacology*, 1990. **37**: p. 840-847.
209. Wu, Y.W., C.L. Chik, and R.A. Knazek. An in vitro and in vivo study of antitumor effects of gossypol on human SW-13 adrenocortical carcinoma. *Cancer Research*, 1989. **49**(3754-3758).
210. Jaroszewski, J.W., O. Kaplan, and J.S. Cohen. Action of gossypol and rhodamine 123 on wild type and multidrug-resistant MCF-7 human breast cancer cells: 31P nuclear magnetic resonance and toxicity studies. *Cancer Research*, 1990. **50**: p. 6936-6943.
211. Band, V., et al. Antiproliferative effect of gossypol and its optical isomers on human reproductive cancer cell lines. *Gynecologic Oncology*, 1989. **32**: p. 273-277.
212. Poznak, C.V., et al. Oral gossypol in the treatment of patients with refractory metastatic breast cancer: a phase I/II clinical trial. *Breast Cancer Research and Treatment*, 2001. **66**: p. 239-248.
213. Flack, M.R., et al. Oral gossypol in the treatment of metastatic adrenal cancer. *Journal of Endocrinology and Metabolism*, 1993. **76**: p. 1019-1024.
214. Stein, R.C., et al. A preliminary clinical study of gossypol in advanced human cancer. *Cancer Chemotherapeutic Pharmacology*, 1992. **30**: p. 480-482.
215. Enyedy, I., et al. Discovery of small-molecule inhibitors of Bcl-2 through structure-based computer screening. *Journal of Medical Chemistry*, 2001. **44**: p. 4313-4324.
216. NIH Website: Clinical trials with AT101. <http://www.clinicaltrials.gov/ct/search?term=AT101>
217. Higgins, B., et al. Antitumor activity of erlotinib (OSI-774, Tarceva) alone or in combination in human non-small cell lung cancer tumor xenograft models. *Anti-Cancer Drugs*, 2004. **15**: p. 503-512.
218. Moyer, J., et al. Induction of apoptosis and cell cycle arrest by CP358,771, an inhibitor of epidermal growth factor receptor tyrosine kinase. *Cancer Research*, 1997. **57**: p. 4838-4848.
219. Sutter, A.P., et al. Targeting the epidermal growth factor receptor by erlotinib (Tarceva) for the treatment of esophageal cancer. *International Journal of Cancer*, 2006. **118**: p. 1814-1822.
220. Maione, P., et al. Combining targeted therapies and drugs with multiple targets in the treatment of NSCLC. *The Oncologist*, 2006. **11**: p. 274-284.
221. Tang, P., M. Tsao, and M.J. Moore. A review of erlotinib and its clinical use. *Expert Opinion in Pharmacotherapy*, 2006. **7**: p. 177-193.
222. Bai, J., et al. Predominant Bcl-X_L knockdown disables antiapoptotic mechanisms: tumor necrosis factor-related apoptosis inducing ligand-based triple chemotherapy overcomes chemoresistance in pancreatic cancer cells *in vitro*. *Cancer Research*, 2005. **65**: p. 2344-2352.
223. Dowlati, A., D. Nethery, and J.A. Kern. Combined inhibition of epidermal growth factor receptor and JAK/STAT pathways results in greater growth inhibition *in vitro* than single agent therapy. *Molecular Cancer Therapeutics*, 2004. **3**: p. 459-463.
224. Tortora, G., et al. Combination of a selective cyclooxygenase-2 inhibitor with epidermal growth factor receptor tyrosine kinase inhibitor ZD1839 and protein kinase A antisense

- causes cooperative antitumor and antiangiogenic effect. *Clinical Cancer Research*, 2003. **9**: p. 1566-1572.
225. Tortora, G., et al. The RI α subunit of protein kinase A (PKA) binds to Grb2 and allows PKA interaction with the activated EGF-receptor. *Oncogene*, 1997. **14**: p. 923-928.
 226. Turini, M.E. and R.N. DuBois. Cyclooxygenase-2: a therapeutic target. *Annual Reviews in Medicine*, 2002. **53**: p. 35-57.
 227. Kulkarni, S., et al. Cyclooxygenase-2 is overexpressed in human cervical cancer. *Clinical Cancer Research*, 2001. **7**: p. 429-434.
 228. Mirmohammadsadegh, A., et al. STAT5 phosphorylation in malignant melanoma is important for survival and is mediated through Src and JAK1 kinases. *Journal of Investigative Dermatology*, 2006. **126**: p. 2272-2280.
 229. Yamashita, H., et al. Naturally occurring dominant-negative STAT5 suppresses transcriptional activity of estrogen receptors and induces apoptosis in T47D breast cancer cells. *Oncogene*, 2003. **22**: p. 1638-1652.
 230. Li, H., et al. Activation of signal transducer and activator of transcription 5 in human prostate cancer is associated with high histological grade. *Cancer Research*, 2004. **64**: p. 4774-4782.
 231. Li, H., et al. Activation of signal transducer and activator of transcription-5 in prostate cancer predicts early recurrence. *Clinical Cancer Research*, 2005. **11**: p. 5863-5868.
 232. Xi, S., et al. Src kinases mediate STAT growth pathways in squamous cell carcinoma of the head and neck. *Journal of Biological Chemistry*, 2003. **278**: p. 31574-31583.
 233. Xi, S., et al. Constitutive activation of STAT5b contributes to carcinogenesis in vivo. *Cancer Research*, 2003. **63**: p. 6763-6771.
 234. Leong, P.L., et al. Differential function of STAT5 isoforms in head and neck cancer growth control. *Oncogene*, 2002. **21**: p. 2846-2853.
 235. Haura, E.B., J. Turkson, and R. Jove. Mechanisms of disease: insights into the emerging role of signal transducers and activators of transcription in cancer. *Nature Clinical Practice Oncology*, 2005. **2**: p. 315-324.
 236. Paukku, K. and O. Silvennoinen. STATs as critical mediators of signal transduction and transcription: lessons learned from STAT5. *Cytokine & Growth Factor Reviews*, 2004. **15**: p. 435-455.
 237. Rasche, A. and E. Lees. Chromatin acetylation and remodeling at the Cis promoter during STAT5-induced transcription. *Nucleic Acids Research*, 2003. **31**: p. 6882-2890.
 238. Brown, R.E., et al. Morphoproteomic and pharmacoproteomic rationale for mTOR effectors as therapeutic targets in head and neck squamous cell carcinoma. *Annals of Clinical & Laboratory Science*, 2006. **36**: p. 273-282.
 239. De Benedetti, A. and A.L. Harris. eIF4E expression in tumors: its possible role in progression of malignancies. *International Journal of Biochemistry and Cell Biology*, 1999. **31**: p. 59-72.
 240. Rao, R.D., et al. Disruption of parallel and converging signaling pathways contributes to the synergistic antitumor effects of simultaneous mTOR and EGFR inhibition in GBM cells. *Neoplasia*, 2005. **10**: p. 921-929.
 241. Rajan, P., et al. BMPs signal alternately through a SMAD or FRAP-STAT pathway to regulate fate choice in CNS stem cells. *Journal of Cell Biology*, 2003. **161**: p. 911-921.

242. Wieckowski, E., et al. FAP-1-mediated activation of NF- κ B induces resistance of head and neck cancer to Fas-induced apoptosis. *Journal of Cellular Biochemistry*, 2007. **100**: p. 16-28.
243. Yokogami, K., et al. Serine phosphorylation and maximal activation of STAT3 during CNTF signaling is mediated by the rapamycin target mTOR. *Current Biology*, 1999. **10**: p. 47-50.
244. Bishop, J.D., et al. Prolactin activates mammalian target-of-rapamycin through phosphatidylinositol 3-kinase and stimulates phosphorylation of p70S6K and 4E-binding protein-1 in lymphoma cells. *Journal of Endocrinology*, 2006. **190**: p. 307-312.
245. Sorrells, D.L., et al. Pattern of amplification and overexpression of the eukaryotic initiation factor 4E gene in solid tumor. *Journal of Surgical Research*, 1999. **85**: p. 37-42.
246. Nathan, C.A., et al. Molecular analysis of surgical margins in head and neck squamous cell carcinoma patients. *Laryngoscope*, 2002. **112**(2129-2140).
247. Smolewski, P. Recent developments in targeting the mammalian target of rapamycin (mTOR) kinase pathway. *Anti-Cancer Drugs*, 2006. **17**: p. 487-494.
248. Karkare, S. and D. Bhatnagar. Promising nucleic acid analogs and mimics: characteristic features and applications of PNA, LNA, and morpholino. *Applied Microbiology Biotechnology*, 2006. **71**: p. 575-586.
249. Chiarantini, L., et al. Enhanced antisense effect of modified PNAs delivered through functional PMMA microspheres. *Pharmaceutical Nanotechnology*, 2006. **324**: p. 83-91.
250. Bogatti, M., et al. Decoy molecules based on PNA-DNA chimeras and targeting Sp1 transcription factors inhibit the activity of urokinase-type plasminogen activator receptor (uPAR) promoter. *Oncology Research*, 2005. **15**: p. 373-383.
251. Fisher, L., et al. Cellular delivery of a double-stranded oligonucleotide NF κ B decoy by hybridization to complementary PNA linked to a cell-penetrating peptide. *Gene Therapy*, 2004. **11**: p. 1264-1272.